NAVAL POSTGRADUATE SCHOOL

MONTEREY, CALIFORNIA

THESIS

DEMONSTRATION OF LIGHTWEIGHT ENGINEERING SOLUTIONS FOR A LOW-COST SAFE EXPLOSIVE ORDNANCE DESTRUCT TOOL

by

Pedro J. Freitas
David M. Gerace

December 2007

Thesis Advisor:	Ronald E. Brown
Second Reader:	Jose O. Sinibaldi

Approved for public release; distribution is unlimited.

THIS PAGE INTENTIONALLY LEFT BLANK

REPORT DOCUMENTATION PAGE		Form Approved OMB No. 0704-0188

1. AGENCY USE ONLY *(Leave blank)*	2. REPORT DATE	3. REPORT TYPE AND DATES COVERED
	December 2007	Master's Thesis

4. TITLE AND SUBTITLE Demonstration of Lightweight Engineering Solutions for a Low-Cost Safe Explosive Ordnance Destruct Tool.	5. FUNDING NUMBERS OFFICE OF NAVAL RESEARCH N0001407WR20135
6. AUTHOR(S) Pedro J. Freitas and David M. Gerace	
7. PERFORMING ORGANIZATION NAME(S) AND ADDRESS(ES) Naval Postgraduate School Monterey, CA 93943-5000	8. PERFORMING ORGANIZATION REPORT NUMBER
9. SPONSORING /MONITORING AGENCY NAME(S) AND ADDRESS(ES) N/A	10. SPONSORING/MONITORING AGENCY REPORT NUMBER

11. SUPPLEMENTARY NOTES The views expressed in this thesis are those of the authors and do not reflect the official policy or position of the Department of Defense or the U.S. Government.

12a. DISTRIBUTION / AVAILABILITY STATEMENT	12b. DISTRIBUTION CODE
Approved for public release; distribution is unlimited.	A

13. ABSTRACT (maximum 200 words)

The continued development of a low-cost and safe method for neutralizing explosive threats is reported. The concept depends on the use of pure nitromethane in a totally encased lightweight plastic shaped charge, and the in situ injection of a minute quantity of diethylenetriamine just prior to employment. Penetration and impact initiation capabilities of a baseline charge, as well as function reliability were previously demonstrated.

The jet from a previously developed brass encased baseline charge is fully characterized from flash radiography, and important technical issues relative to computational prediction are resolved. A new precision 42 degree lined charge is shown to outperform the baseline by as much as 6 to 74 percent over the standoff range studied. These improvements allowed for the incorporation of a Teflon body and a bi-material Teflon/copper liner in conformance with the goal of total encasement of the nitromethane.

Relative differences in jetting characteristics and quantitative assessments of the penetration capability of the new design and small performance decrements resulting from the plastic substitutions are reported.

14. SUBJECT TERMS Explosive Ordnance Disposal, Shaped Charge, Nitromethane, Diethylenetriamine, DETA.	15. NUMBER OF PAGES 147
	16. PRICE CODE

17. SECURITY CLASSIFICATION OF REPORT	18. SECURITY CLASSIFICATION OF THIS PAGE	19. SECURITY CLASSIFICATION OF ABSTRACT	20. LIMITATION OF ABSTRACT
Unclassified	Unclassified	Unclassified	UU

NSN 7540-01-280-5500

Standard Form 298 (Rev. 2-89)
Prescribed by ANSI Std. 239-18

THIS PAGE INTENTIONALLY LEFT BLANK

Approved for public release; distribution is unlimited.

DEMONSTRATION OF LIGHTWEIGHT ENGINEERING SOLUTIONS FOR A LOW-COST SAFE EXPLOSIVE ORDNANCE DESTRUCT TOOL

Pedro J. Freitas
Lieutenant, Portuguese Navy
B.S., Portuguese Naval Academy, 1999

Submitted in partial fulfillment of the
requirements for the degree of

MASTER OF SCIENCE IN APPLIED PHYSICS

David M. Gerace
Lieutenant, United States Navy
B.S., Indiana University, 1998

Submitted in partial fulfillment of the
requirements for the degree of

MASTER OF SCIENCE IN COMBAT SYSTEMS SCIENCES AND TECHNOLOGY

from the

NAVAL POSTGRADUATE SCHOOL
December 2007

Authors: Pedro J. Freitas

David M. Gerace

Approved by: Dr. Ronald E. Brown
Thesis Advisor

Dr. Jose O. Sinibaldi
Second Reader

Dr. James Luscombe
Chairman, Department of Physics

THIS PAGE INTENTIONALLY LEFT BLANK

ABSTRACT

The continued development of a low-cost and safe method for neutralizing explosive threats is reported. The concept depends on the use of pure nitromethane in a totally encased lightweight plastic shaped charge, and the in situ injection of a minute quantity of diethylenetriamine just prior to employment. Penetration and impact initiation capabilities of a baseline charge, as well as function reliability were previously demonstrated.

The jet from a previously developed brass encased baseline charge is fully characterized from flash radiography, and important technical issues relative to computational prediction are resolved. A new precision 42 degree lined charge is shown to outperform the baseline by as much as 6 to 74 percent over the standoff range studied. These improvements allowed for the incorporation of a Teflon body and a bi-material Teflon/copper liner in conformance with the goal of total encasement of the nitromethane.

Relative differences in jetting characteristics and quantitative assessments of the penetration capability of the new design and small performance decrements resulting from the plastic substitutions are reported.

THIS PAGE INTENTIONALLY LEFT BLANK

TABLE OF CONTENTS

THIS PAGE INTENTIONALLY LEFT BLANK

LIST OF FIGURES

THIS PAGE INTENTIONALLY LEFT BLANK

LIST OF TABLES

THIS PAGE INTENTIONALLY LEFT BLANK

ACKNOWLEDGMENTS

The authors would like to extend sincere appreciation and gratitude to the Office of Naval Research (ONR) and the NPS Physics Department for their sponsorship of this graduate research program, and to the following people:

Dr. Ronald E. Brown and Dr. Jose O. Sinibaldi for their guidance, expertise, and patience.

LCDR Hung Cao, for all the help, motivation, example, and reinforcement of the concept that sometimes people need to take a break.

Mr. Bob Zoret, Mr. Jon H. Price, Engineering Manager, and Mr. Jim Varosh, General Manager, from TELEDYNE RISI, INC. for their valuable help and support during the detonation and shaped charges tests.

Dr. Ernest L. Baker (US ARMY ARDEC) for providing the Trumpet Liners required in the Shaped Charge tests, and to The Dinucci Corporation, for machining charge liners necessary for this research.

Mr. George Jaksha (NPS Staff) and Mr. Doug Learned (Intercity Manufacturing), whose efficiency and expertise was vital in manufacturing the parts required for our tests.

Mr. Eric Adint (NPS Staff) for his IT support and expertise.

There are many others who have helped us complete this thesis that have not been mentioned, but please be assured that the absence of your names does not indicate that you have been forgotten.

THIS PAGE INTENTIONALLY LEFT BLANK

I. INTRODUCTION

There are a few specially designed explosive shaped charge products that have been developed for neutralizing buried land mines and other packaged explosive threats for various military applications and humanitarian demining operations. The shaped charge is a desirable device because the kinetic energy of the jet can be accurately aimed and its energy can perforate large thicknesses of cover. These devices, however, contain high performance solid explosives, which can diminish their value for civilian application because they can present an unintended threat in the wrong hands. One of these devices, currently under development, includes a robotic mechanism for deploying a relatively large Composition C-4 shaped charge [4]. Another developed by BAE Systems for Humanitarian Demining is based on a patented design by Majerus and Brown [5]. The design technology incorporated in the latter device provides a unique mechanism possessing necessary capabilities for destroying explosive devices (including landmines) that are protected behind large covers (and/or mines that are deeply buried). In this case the liner is accurately configured to generate discrete high energy segments within the low velocity portion of the jet stream, large enough to initiate on impact most explosive threats to high-order detonation. This design innovation extends the effective length of the jet and overall penetration capability without sacrificing neutralization capability. The ARDEC Composition C-4 charge, on the other hand, is of interest because of its adaptability for robotic delivery and function.

A research program was initiated in 2005 at the Naval Postgraduate School for purposes of overcoming the principle disadvantage of using high explosive charges that could get into undesirable hands while incorporating many of the desirable features of the small shaped charge useful for surgical removal of explosive threats. The concept evolves around the use of nitromethane ("NM"), which is a low-cost commercial solvent. NM in pure form is difficult to initiate to detonation. It can become impact/shock sensitive with the addition of

physical and/or chemical impurities: for example, the addition of physical impurities composed of micron-sized silica and micro-balloons, or small concentrations of organic amines which form colloidal charge-transfer complexes can create sufficient population of hot spots to cause the build-up and sustainment of a high order detonation response in NM under certain limiting size and confinement conditions that could be incorporated into a neutralizer further limiting the probability of effective function by unintended users.

The explosive threat neutralizer concept is illustrated in Figure 1. Pure NM is housed in a shaped composite plastic container of a diameter too small to support reliable detonation. The hollow-cavity of the container is designed to match with an optimized metal-liner (or set of liners) that can produce jets of sufficient residual kinetic energy to impact initiate to high-order or rapid deflagration behind various thicknesses of cover protection: the metal liner is inserted into the body cavity just prior to neutralizer function. The composite plastic body is composed of two materials; the inner material is inert to NM and the outer casing is made of a high strength plastic. The latter is necessary for efficient energy coupling between explosive and liner. In addition to the metal liner insertion, the charge is placed on an aiming fixture and a small amount of diethylenetriamine (DETA) is injected into the NM with a detonator inserted into a well at the aft end of the charge just prior to function. It has been determined that the DETA is required for reliable initiation of the NM.

A. MOTIVATION OF RESEARCH (THE PROBLEM)

The focus of the overall program is to demonstrate an engineering solution for a low cost, robotic-compatible, precision explosive neutralizer that presents a lower unintended threat profile than similar devices containing high performance explosive. Thus far, the feasibility of using nitromethane has been confirmed based on (a) safety, (b) raw material and loading cost, (c) detonation reliability, and (d) shaped charge performance with respect to cover protection penetration

and explosive impact initiation. It is also important to note that the use of a low viscosity fluid explosive eliminates the need for sophisticated and expensive loading devices and energy-consuming materials and equipment for precision loading.

The problems addressed in this research are directed towards understanding and overcoming design and engineering issues related to the ultimate incorporation of a shaped hollow-cavity plastic body to house the nitromethane, while maintaining the necessary dynamic rigidity to assure effective shaped charge jet formation: *A family of designs rather than one unique design is ultimately desired to address the wide range of explosive threats and threat conditions.*

In order to accomplish this phase of work and to develop the necessary bases for eventual design optimizations, the finite difference techniques used within AUTODYN^{TM} must be thoroughly validated and the dynamic response of candidate structural plastics characterized.

Validation requires a thorough characterization of the jet from the baseline trumpet and a new 42-degree lined copper charge; originally derived by Dusetzina [1]. To date, the tip velocity has been estimated based on penetration time data. One can only suggest from the latter a minimum velocity of the jet tip, since the leading edge of the jet is already absorbed by the target at the time of initial sensing.

Furthermore, complete characterization will require the determination of the velocity-mass distribution along the jet from the tip to the region where penetration effectiveness is estimated to terminate. This careful analysis will provide basis for examining the effect of confinement and liner design changes on jet formation and terminal effectiveness.

Because of the size range of the charges and the degree of difficulty of the target spectrum, unique approaches will be required in order to secure the degree of zoning resolution within reasonable commitments of computational and time resources.

All of the investigations to date have been conducted with charges confined in brass. Brass was selected because it is inert to NM and there exists a large database of detonation behavior of NM contained in brass housings. This is not a reasonable material for subject application because of the cost and weight, and the hazard of fragmentation that would be imposed.

A single or composite plastic material must be selected (or developed) that is compatible with long term NM exposure and is strong enough to resist initial detonation product expansion so as to affect energy coupling efficiencies to the liner comparable to brass confinement. A single material might not comply with these requirements, at least not during the initial investigations. Thus a composite solution might have to be derived for the initial experimental studies.

As previously mentioned, the NM must be contained completely in plastic. This requires the insertion of a metal liner against a hollow cavity in the plastic containment. The contact between the plastic must be structurally rigid and conform to the spatial geometry required for jet formation. This imposes conditions for minimum plastic thickness to assure rigidity and geometric conformity and provisions for locking the metal liner in place. For the initial investigations the primary questions that must be addressed are as follows:

- To what degree of confidence can we predict the partitioning of mass between jet and slug after liner collapse?
- Are there regions along the liner (e.g. along the extreme apex and basal locations) where co-mixing of materials might not be critical to performance?
- For test cases, what solutions can be derived for the baseline trumpet and 42-degree lined charges?

A major step forward in this research demands that tentative solutions of the above material issues be experimentally demonstrated.

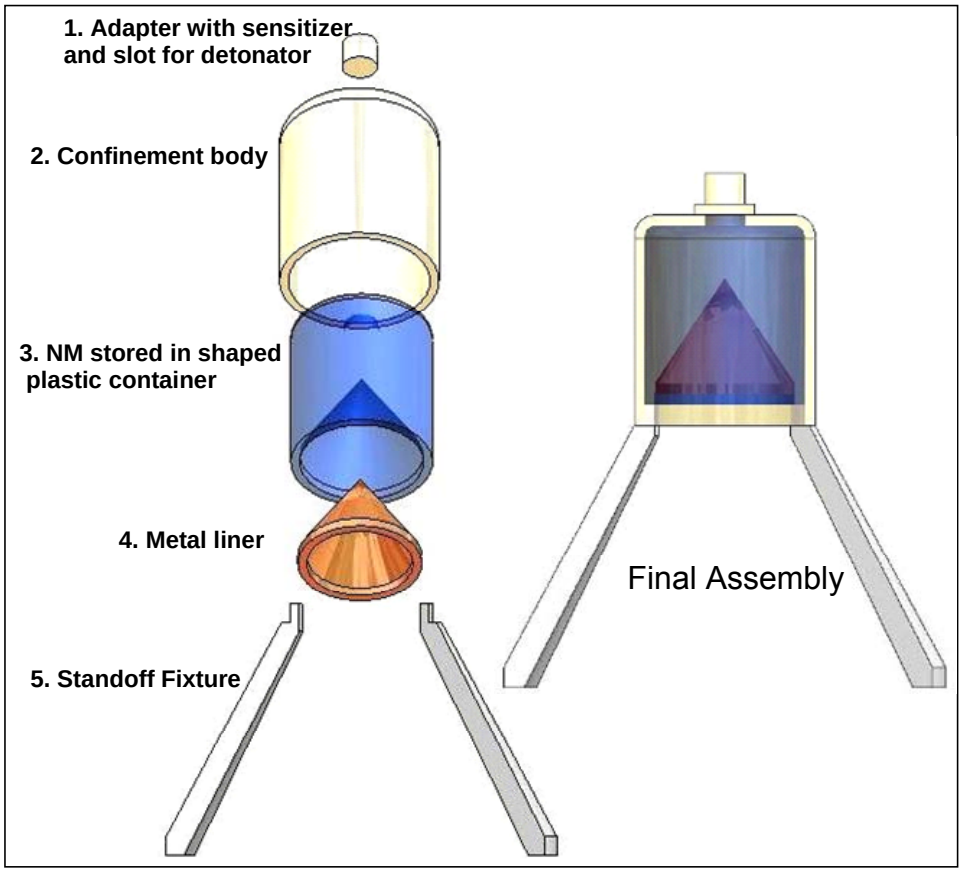

Figure 1. Low-cost Precision Explosive Ordnance Destruction Device (EDD) Concept. From [1].

B. OUTLINE OF PREVIOUS ACHIEVEMENTS

The basic feasibility of using nitromethane (NM) as the energetic material in a 25 mm shaped charge device was demonstrated by Serrano, Rigby, and E. and G. Dusetzina [1, 2, and 3]. Highlights of these studies attesting to the desired safety and reduced hazard of unintended use include the following:

- The detonability of pure NM in a polyethylene container from the output of a RP-81 (equivalent to a #8 blasting cap) is less than 10 percent. On the other hand, initiation to high order detonation is close to 100 percent with the addition of 0.1 percent reagent grade DETA.
- Based on computational analyses, a 25mm-diameter NM shaped charge contained totally in plastic will penetrate less than 24 percent of steel compared to a heavily confined copper-lined charge under the best of conditions.

From a standpoint of function and performance, function reliability of a 0.1 percent DETA solution is close to 100 percent and the measured detonation velocity of the DETA/NM mixture matches that of pure NM well within the same percentage. Dusetzina and Dusetzina [1] have also experimentally demonstrated that a 25mm charge in brass casing confinement is capable of penetrating through 184mm of aluminum (108 mm of steel) and can initiate protected Composition B to high order detonation. All of the charges used in these prior studies were encased in brass bodies.

It is important to note that numerous individuals have studied the detonation behavior of NM, the effect of using various sensitizer materials, and the shaped charge performance of NM as well as its sensitivity to hypervelocity impact. They provide the credence for our conceptual approach [1, 2, and 3]. A number of workers have successfully shown the neutralizing benefits of the shaped charge, primarily for military applications. In many cases the charges themselves are rather robust and expensive to manufacture because of the cost of the explosive content, charge components, loading, and assembly.

Brown and Majerus demonstrated means for incorporating consolidated mass elements in shaped charge jets for purposes of extending the impact initiation effectiveness of the jet, thereby providing means for reducing the charge size [5]. In doing so they were able to design charges at 30 mm caliber capable

of detonating explosive mines (irrespective of fusing) buried as deep as 200 mm in soil. They also applied the technology for humanitarian demining. The utility of the device, which contains a high performance HMX explosive, is limited in the civilian community because it poses an unintended threat. In addition, the high cost of the charge prevents its practical use in third world countries.

C. PROGRAM GOALS AND OBJECTIVES

The overall goal of this research is to demonstrate a process for robotically neutralizing explosive threats. The robotic process involves the delivery and in-situ assembly of a small shaped charge at a pre-set standoff from the threat, the connection of the charge to a “safe” firing line, and return to a firing operator. There are several combined features of the shaped charge that are unique from the standpoints of safety and cost. The explosive content (composed of NM), is an inexpensive flammable liquid which is difficult to initiate to detonation when contained in a small diameter lightly-contained housing. Even in the rare case of detonation, jet formation and fragmentation from the plastic case would present much less of a hazard than that from a high performance explosive charge. NM costs less than an order of magnitude of RDX or HMX. More importantly, the energy required to pour it into a shaped vessel is much less than that required to melt and cast TNT and TNT-based explosives, or to extrude and press-load plastic bonded explosives. The only preparations required for precision assembly are the concentricity of the shaped vessel and its cleanliness (which affects intimate interfacial attachment between the NM and the plastic wall). The criticality of DETA for function reliability adds another component of safety, since it effectively provides a safe component in addition to the final in-situ robotic placement of the detonator.

The material and geometry of conceptual housing used to store the liquid exploits the aforementioned characteristics of the NM liquid. The housing material consists of a plastic that is chemically inert to NM. The container has a

boat-tailed contour with a shaped variable angle/variable thickness inner contour that will form a jet and/or provide an interface for the placement of a jetting metal liner (see Figure 1). On the end of the plastic container is a slot for a chemical safe & arm device. This device will ultimately mate to a time-phased double trigger mechanism that upon activation injects minute quantity DETA, a liquid that forms a detonable colloidal charge-transfer complex with NM. The second trigger is a precision shock impulse from a detonator, of magnitude comparable to the output of a #8 blasting cap. This concept also exploits the ease of loading and the resultant accuracy and precision afforded by a liquid explosive.

The overall objective is to determine and hopefully define the required plastic material(s) and thicknesses sufficient to replicate brass. Once this is achieved, we will be able to specify requirements for robotic handling and handoff, DETA injection mechanisms, and dedicate attention to charge optimization.

As shown in Figure 1, the aim of the program is to develop a NM charge that is totally encased in a lightweight structural plastic container. This means that the selected plastic must have sufficient dynamic hoop strength for energy coupling and must be thin enough in the lined cavity to eliminate the flow of plastic into the portion of the jet stream that contributes to penetration and impact initiation. For experimental purposes, we have selected Teflon charge bodies (due to its machinability and compatibility with NM) and Ultem 1000 plastic (detailed physical characteristics of Ultem are listed in Appendix J), which is an unfilled polyetherimide machined into a completely removable sleeve fitting around the charge body.

Thus there are three crucial objectives:

- The jet characteristics of the baseline trumpet charge predicted by finite difference (AUTODYN^{TM}) have only been qualitatively confirmed by inference from observed penetration-times at selected standoffs. While the data appears to correlate well with predicted jet tip (only), *direct*

measurements of not only the jet tip but the entire velocity-mass distribution of the jet is necessary for assessing the effect of the types of charge modifications ultimately required.

- *Plastic materials must be selected and their effect assessed in order to reach conclusive suggestions for confinement structure and effect on potential robotic requirements.*
- *The maximum thickness of the inert plastic component must be established in order to progress to final designs.* This will require confidence in computer modeling and as such good correlation with experiment. Impediments to resolving the flow of liner material, particularly about the apex region that affect jet tip must be overcome.

D. BRIEF STATEMENT OF RESULTS AND IMPLICATIONS

This research accomplished a number of objectives related to the improvement of nitromethane shaped charges in various configurations. Initially using the brass confinement studied in previous research, flash radiography obtained from the Ernst-Mach Institute (EMI) in Germany effectively characterized jet formation and performance, providing a baseline from which to continue further study. One of the primary factors in the development of an autonomous delivery mechanism for a shaped charge is weight, creating a need for an effective charge constructed of lightweight material such as a compatible plastic. The simulated and experimental findings closely replicated the results obtained in previous experiments using brass by substituting a charge body completely constructed of Teflon, which greatly minimizes operational hazards through significant reduction in the weight of the charge and increased safety of transport. At a standoff of two charge diameters (2CD), the difference in penetration performance between a brass body and a Teflon body was

negligible. In the case of the trumpet-lined charges, the simulations and experiments performed remained consistent with radiographic results throughout this research.

An important part of our predecessors' research was to begin the evaluation of the performance of a 42 degree liner contained in the shaped charge. It was found in their simulations that this configuration performed extremely well using AUTODYN™ [1]. Results from this study confirm the prior predictions made by Dusetzina. The 42 degree charge has a greater penetration capability at all standoffs studied to date (i.e., between 2 and 5 CD). It has been estimated that this charge produces a faster jet based on measured penetration rates and observed holes sizes, which are significantly larger than those made by the trumpet. Larger and more massive jetting might also contribute to the differences in holes sizes.

II. TECHNICAL ISSUES

A. PENETRATION PERFORMANCE OF BASELINE CHARGE

1. Optimum Stand-off Distance

Serrano and Rigby [2 and 3] determined the maximum penetration of the baseline shaped charge at a single standoff distance (3.1 CD). Dusetzina and Dusetzina [1] further characterized the optimum standoff distance, performing experiments with standoff distances between 2 and 5 CD. It was determined that each of our Teflon and brass experiments would be performed at standoff distances between 2 and 4 CD.

2. Quantitative Characterization of Shaped Charge Jet

In order to accurately assess the effectiveness and performance of the shaped charge, a combination of computational and experimental results must be analyzed. While jet velocity can be determined through correlation of computational simulations and experimental data, jet diameter can only be measured experimentally by flash radiography (work at EMI has involved flash radiography studies, discussed in further detail in the Technical Approach section).

B. ESTIMATE DESIGN DIRECTION FOR IMPROVEMENT

1. Alignment Accuracy

Previous experiments performed by Dusetzina and Dusetzina [1] used a charge confinement consisting of two cylindrical pieces attached with epoxy. In order to further optimize the accuracy of the alignment, our Teflon and brass charge confinements were machined and extruded as a single continuous piece.

2. Optimization of Performance

Using a point initiation, initial experiments involved a trumpet shaped liner in a Teflon charge body, both with and without an Ultem 1000 plastic sleeve encasing the charge. Teflon was selected as a substitution for brass for the first set of tests due to its compatibility with NM and its machinability. Contained in the first series of experiments are several tests utilizing Ultem plastic in an effort to assess its effectiveness as a supplement for an all-Teflon charge design. The performance of the baseline shaped charge with a 42 degree conical liner was initially determined in computational simulations by Dusetzina and Dusetzina [1]. After the 42 degree conical liner design was completed and machined, the second set of experiments involved the use of the 42 degree conical liner encased in brass.

III. TECHNICAL APPROACH

A. LITERATURE REVIEW

The concepts of shaped charge initiation and jet impact must be understood in order to achieve success in developing effective new variations on existing shaped charge technology. There are a number of factors which influence the performance of a particular shaped charge concept.

A number of important shaped charge concepts are relevant in understanding the improvements discussed in Section II:

1. Shaped charge concept

a. Nomenclature

Like any specialized community, those familiar with shaped charges use a common nomenclature. This is illustrated in Figure 2, where a basic shaped charge containing a detonator, booster, secondary high explosive (HE), and conical liner is shown. Common references when discussing shaped charge explosives are as follows [7]:

- Liner diameter (LD) – Outer diameter of the conical liner. As depicted in Figure 2, the LD is the smallest of the measured diameters.
- Charge diameter (CD) – This refers to the inner diameter of the cylindrical case surrounding the explosive and is not to be confused with cone diameter. Standoff distances are measured in CD's.
- Warhead diameter (WD) – This is the outer diameter of the confinement case containing the shaped charge.
- Charge length (L) – Overall length of the shaped charge device.

- Head height – Length between the apex of the conical liner and the booster.
- Standoff distance (more commonly referred to as simply standoff) – Distance between the charge base and the intended target.
- Effective (or Virtual) standoff – Distance from the virtual origin (point at which the jet of the shaped charge can be assumed to originate) to the target.

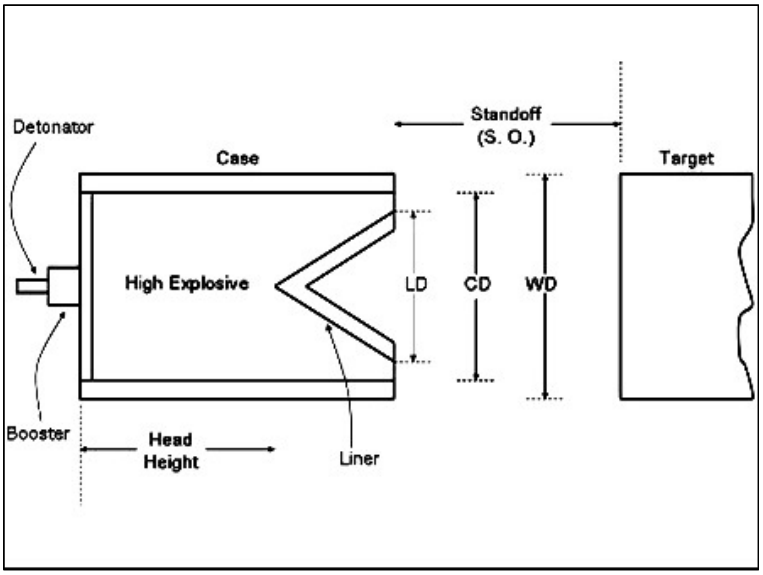

Figure 2. Shaped charge configuration nomenclature illustrated. From [7].

b. Shaped Charge Generalities

A number of variables and parameters affect the performance of shaped charges, and all must be considered in the development and improvement of new technology:

- ***Liner Geometry:*** The most significant element of shaped charge design is the liner. An important variable in this design is the LD. Generally a bigger liner results in a longer jet, which increases target penetration. Wall thickness (typically between 1 and 4 percent of the CD) is another

critical design variable, and is dependent on liner geometry, materials, and intended jet properties. The liner apex angle also plays an important role in charge design. For a conical liner, smaller apex angles result in a faster jet tip velocity and smaller jet mass. For larger apex angles, the opposite effect will be produced [7].

- ***Liner material:*** The type of material used in the charge liner is critical. Properties of a good jet material will include a higher melting temperature, high density (this enhances penetration), high bulk speed of sound for jet cohesiveness and high dynamic strength in order to withstand severe pressure and high strain rate conditions [7].
- ***Charge diameter:*** In general, explosive must be located near the base of the liner to enable adequate liner collapse and facilitate penetration. The required sub-calibration ratio is dependent on the liner and confinement geometry and materials as well as the type of explosive used [7].
- ***Charge length:*** Explosive charge length must be sufficient in order to provide the explosive energy necessary to facilitate liner collapse. In the case of point initiated charges, head height must be large enough to result in a uniform detonation wave to interact with the liner. In the case of insufficient head height, a spherical wave will cause a non-uniform collapse of the liner. In order to minimize the bulk and weight of the charge, the minimum head height necessary to achieve satisfactory results must be determined [7].
- ***Initiation Mode:*** Point initiation is the most common mode used in detonating shaped charges. Typically a detonator-booster combination is attached at a single point on the centerline of a cylindrical explosive charge [7]. The point initiation mode is used exclusively in this research.

c. Jet Formation

High velocity metal jets generated by shaped charges are widely used in the render-safe (detonation or deflagration) of conventional or improvised explosive ordnance [18]. Formation of the jet is initiated when a hollow cavity at one end of the charge cylinder is lined with a thin layer of any solid and is detonated at the opposite end of the cylinder. This phenomenon, known as the Munroe effect in United States and United Kingdom and the von Foerster or Neumann effect throughout Europe, accounts for the focusing of detonation products caused by the hollow cavity. Upon initiation of a hollow lined charge, the resulting high pressure shock wave travels outward from the point of initiation at an extremely high velocity. This wave surrounds the lined cavity and the liner material is accelerated under the detonation pressure [7]. The acceleration of the liner causes it to behave like a fluid and collapses on the centerline of the shaped charge. Once the liner reaches the centerline, the inner layer of the liner material forms a high velocity jet containing approximately 15-20 percent of the liner mass. The remainder of the liner mass forms a low velocity slug [8]. Figure 3 illustrates the formation of the jet and slug in a shaped charge detonation.

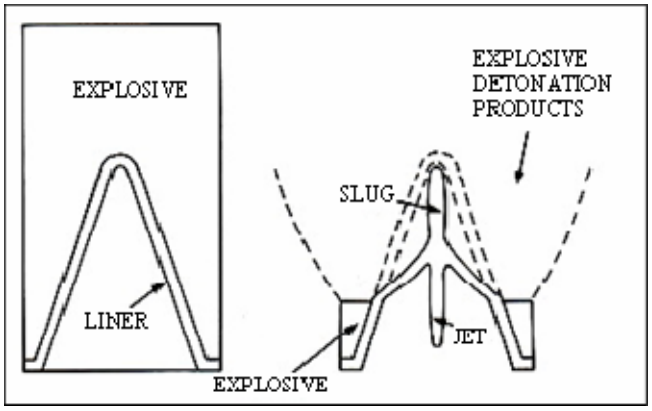

Figure 3. Illustration of liner collapse and formation of jet and slug. From [8].

Due to the velocity gradient (the result of explosive/liner mass ratio variation along the liner), the jet continues to lengthen as it forms. Jet velocities

typically range between 7 to 10 km/s at the tip (for HE charges) and 1 to 2 km/s at the tail. During the lengthening process, the jet eventually breaks apart and reduces penetration effectiveness [8]. In Figure 4, a flash radiograph of a 75 mm shaped charge illustrates the breaking up of the jet.

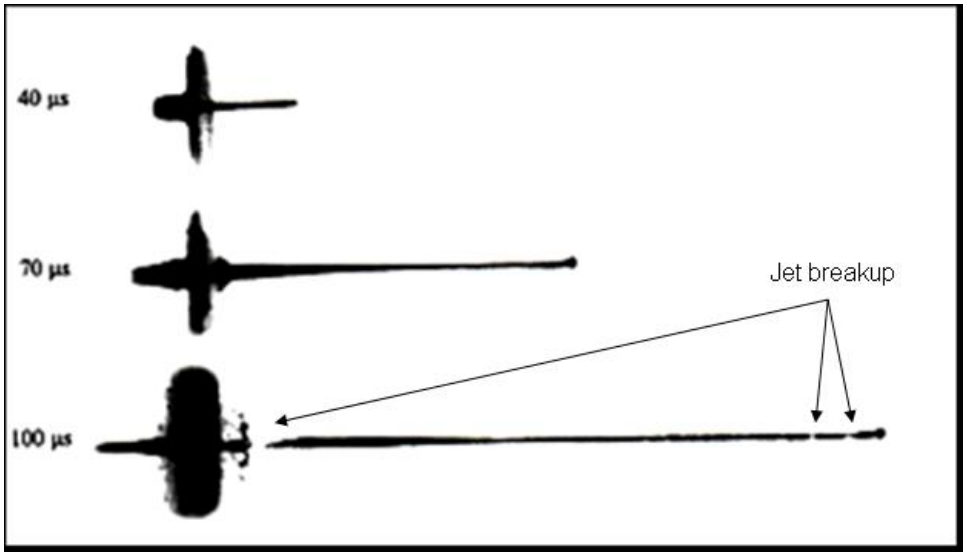

Figure 4. 75mm diameter shaped charge jet flash radiograph. From [8].

Conical shaped charge jet formation theory was introduced by Birkhoff et. al. assuming both steady state conditions and a constant collapse velocity of the liner. While this work failed to calculate the elongation of the jet, modifications by Pugh, Eichelberger, and Rostoker (often referred to as PER) in 1952 included varying collapse velocities of the liner, explaining jet elongation [7]. In Figure 5, the collapse process for the liner is shown. With decreasing jet velocity, collapse angle β is increased and the liner portion entering the jet is increased. The ultimate collapse angle is comprised of the liner angle α and the turning angle δ. The liner angle is determined by geometry, while the turning angle depends on the interaction with the detonation front and the liner.

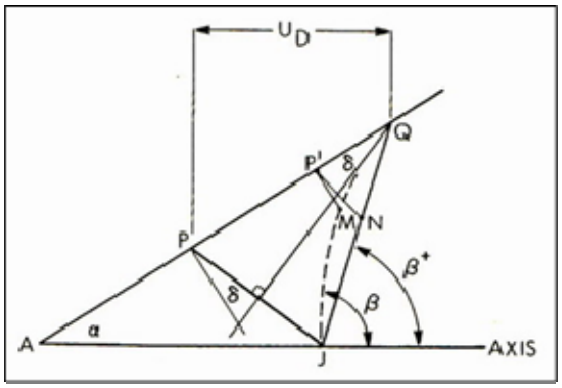

Figure 5. Collapse process for a variable collapse velocity liner. From [7].

d. Effect of Standoff

The optimum amount of standoff distance must be determined in order to produce the maximum target penetration. In Figure 6, the relationship between standoff distance and penetration is depicted. Shorter standoffs result in reduced penetration due to lack of time to lengthen, while longer standoffs will result in the jet breaking apart, producing this same effect [20]. The steady decrease in penetration is important to note once the jet begins to break up [7].

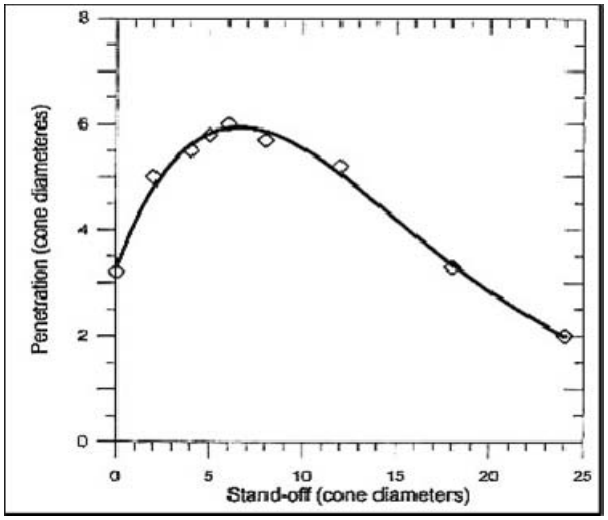

Figure 6. Effect of standoff on penetration. From [20].

e. Jet Penetration

The penetration of a shaped charge jet into a target can be compared to the manner in which a high speed water jet (such as from a hose) will penetrate into the soil. The material of the target displaces radially at a high velocity as depicted in Figure 7.

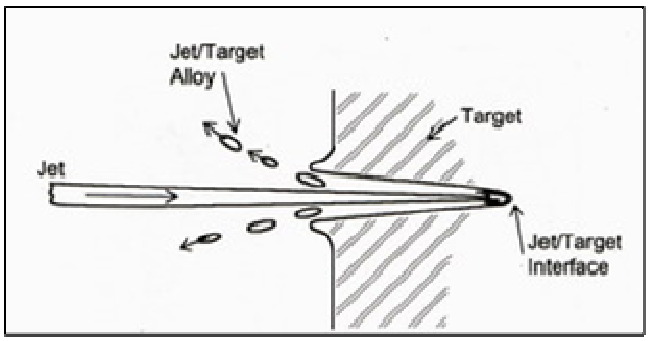

Figure 7. Target penetration illustrated. From [20].

The jet at high velocity produces a pressure exceeding the yield point of most materials, resulting in a consistent rate and depth of penetration regardless of the target material strength. Penetration rate and depth can be explained with hydrodynamics to the first approximation due to the negligible strength and viscosity of the target materials [11].

Considering a shaped charge jet with length l, density ρ_j, and velocity V penetrating a semi-infinite and monolithic target with density ρ_t (with penetration velocity U), the simple penetration is shown in Figure 8.

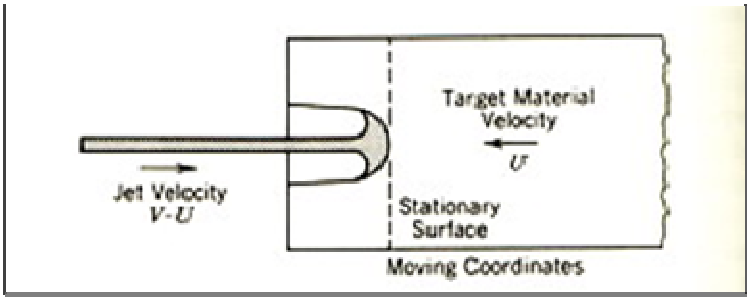

Figure 8. Target penetration at penetration velocity U. From [6].

It can be seen that the jet moves to the right with a velocity of (V-U) with the target moving left at velocity U. Identical pressure is present on both sides of the jet/target interface. With stationary coordinates, Bernoulli's theorem can therefore be applied:

$$\frac{1}{2}\rho_j(V-U)^2 = \frac{1}{2}\rho_t U^2 \quad (3.1)$$

In Figure 7, jet erosion is depicted during the penetration of the target. Assuming instantaneous transition to steady state and final penetration when the last jet particle strikes the target, total penetration P is defined by:

$$P = Ut_f = \frac{Ul}{(V-U)} = l\left(\frac{\rho_j}{\rho_t}\right)^{\frac{1}{2}} \quad (3.2)$$

With t_f representing the time elapsed during penetration and l is the length of the jet.

Equation 3.2 indicates that the penetration depth is dependent on only density and length of the jet and target, independent of jet velocity. The rate at which the jet erodes (and ultimately the final jet length) is dependent on jet velocity through the l term [7]. While the equation is true for jets with constant properties throughout the penetration, actual shaped charges require more complex computation.

The U velocity in equation 3.1 also holds true for steady state conditions. To counteract the case of variable jets, velocity measurements made over short distances with slight variances can be approximated [9].

$$U = \frac{V}{(1+\gamma^{\frac{1}{2}})} \quad (3.3)$$

where $\gamma = \frac{\rho_t}{\rho_j}$ (3.4)

B. EXPERIMENTAL APPROACH

The technical issues described in section II were addressed and resolved with the following experimental approach guidelines. The NM/DETA mixture used with proper cautious preparation and safe handling resulted in a successful initiation of our shaped charge. A simple modification to the previous shaped charge design makes the design more easily to handle and assemble, improving accuracy and capabilities. Sensors to determine the jet time of arrival were constructed and used as in previous experiments [1, 2].

1. Handling and Preparation of NM/DETA mixture

Appendices A and B describe procedures for storage, handling, and preparation of the NM/DETA mixture. It is important to have a fresh batch of the mixture (in the last set of experiments a new batch was prepared every two tests) to ensure no degradation or thermal and photo-induced decomposition.

2. Electric-Bridge Wire Detonator

For the penetration potential experiments the Teledyne RISI RP-81 EBW detonator was used. The RP-81 detonator has the equivalent output of a #8 blasting cap. Additional specifications of the detonator are featured in the RISI website [11].

3. Firing Tank

The firing tank used at Teledyne RISI is shown on Figure 4. It was used for all penetration tests. The tank volume is approximately 4 cubic feet. More information can also be found on the RISI website [11].

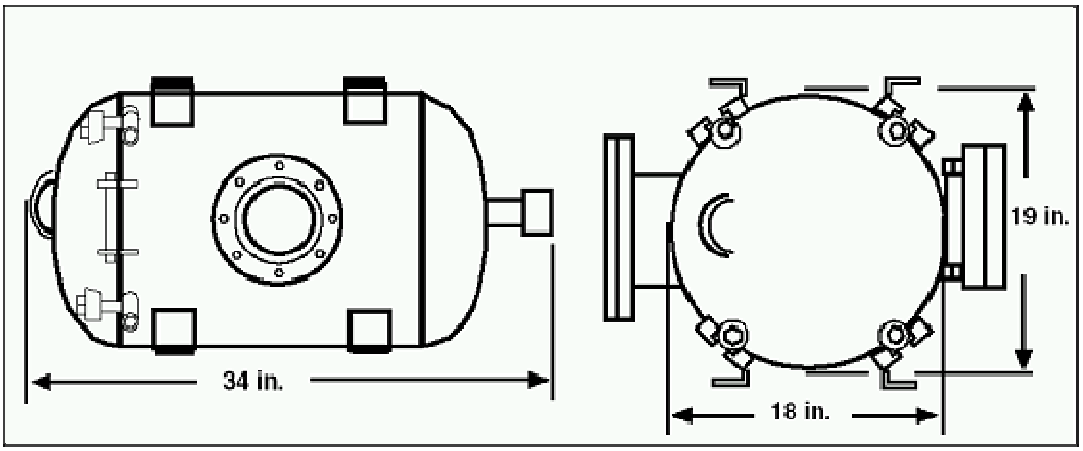

Figure 9. Firing Tank. From [11].

4. Liners

a. Trumpet Liner

The trumpet liners were used mainly in the initial series of RISI tests and at EMI in Germany because they have been successfully used in previous research and produced consistent results. Specific details of the liner are on Appendix C.

b. 42 Degree Conical Liner

The 42 degree conical liners were used in the second test series; it has been observed that charges with cone shaped liners with an angle of around 42 degrees achieve excellent penetration, as mentioned previously. The Dinucci Company in Concord, CA manufactured these liners using OFHC copper and also a bi-material liner made of Teflon and OFHC copper. Specific details of these liners can be found on Appendix D.

5. Shaped Charge Design

The same shaped charge design (Appendix E) was used for every type of liner previously described and is an improvement of older research designs. Our

design was fabricated in brass and also in Teflon, as both materials are chemically compatible with NM.

6. Ultem Confinement

For the Teflon charge design, Ultem 1000 plastic was chosen as an additional confinement component due to its machinability and favorable dynamic hoop strength [10]. The Ultem plastic was precision machined into sleeves of three different outer diameters and made to slide neatly around the Teflon charge, effectively increasing the existing containment.

7. Target Assembly and Penetration Velocity Sensors

a. Target Assembly

Target Plates: Target plates measuring 50mm x 50mm used during the penetration experiments at Teledyne RISI were constructed separately with 6061 Aluminum and 1018 Carbon Steel (Appendix F). The plates were cut into different thicknesses, at 6.35 mm and 25.4 mm for the steel plates and 3.17mm, 6.35 mm, and 25.4 mm for the aluminum plates

Brackets: As in previous research tests, brackets were used to hold target plates tightly during all testing. A pair of brackets (top and bottom) holds the entire target assembly, as shown in figure 10. These brackets measure 150mm x 150mm and are constructed of 1018 steel (Appendix H). For functional purposes the top bracket had a centered hole to accommodate a pipe flange in order to hold the shaped charge standoff. Both top and bottom brackets have aligned holes in each of the corners, with threaded bottom bracket holes to facilitate the attachment of bolts and nuts to secure the assembly. The usual setup is assembled by placing target plates and sensors on top of the lower bracket, followed by the pipe flange. The top bracket is then placed on top and

four threaded rods are fed through the top holes, fastened into the threaded holes on the bottom bracket, and secured with washers and tightened nuts on the top.

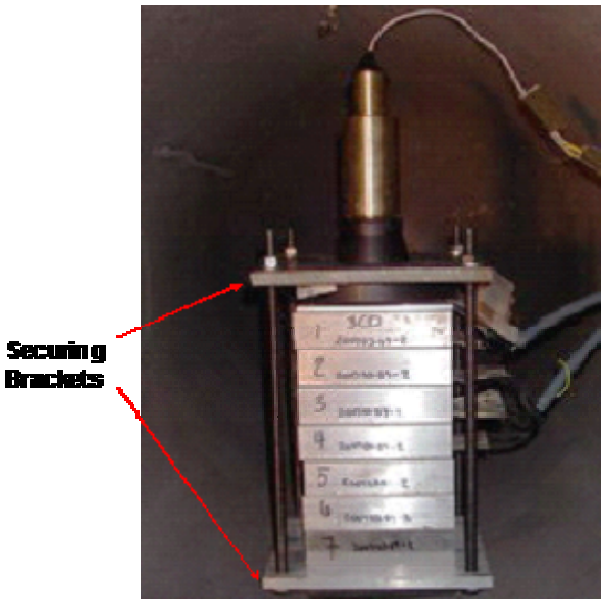

Figure 10. Target assembly. From [1].

b. Sensors

Sensors were built for detection of jet arrival and penetration velocity (see Appendix H for details on sensor construction) and placed between the target plates. Only six sensors were used for each test due to the number of connections available with the two oscilloscopes. Using measurements from the six sensors, we obtained five time measurements, providing sufficient data to calculate the penetration velocity of the jet. On figure 11 we can see the basics of our make/break switch that works when the two electric isolated aluminum foils with packing tape complete the circuit by the jet penetrating the sensor, thus sending a signal to the oscilloscope.

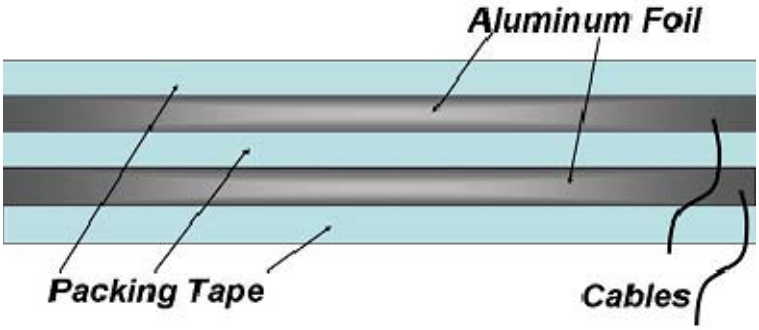

Figure 11. Make/break switch. From [2].

C. COMPUTATIONAL APPROACH

1. AUTODYN ™ Solvers (Euler)

AUTODYN™ is an analysis software package created by Century Dynamics and is capable of fully modeling the nonlinear dynamics of interactions between solids, liquids, and gases. It contains a hydrodynamic code (or hydrocode), which can be used to simulate a variety of applications, including the mechanics of penetration, blast effects, and armor/anti-armor design and optimization [14]. For use at NPS, this hydrocode has been experimentally validated with observation for explosive detonation, shaped charge jetting, and penetration data.

For shaped charge simulation, AUTODYN™ contains many different settings and options which can be set in order to maximize the results pertinent to shaped charge performance. The full Eulerian approach is most effective in tracking the motions of the shaped charge liner. This solver employs a fixed numerical mesh, with free surfaces and material interfaces given the ability to flow through. All material motions can be tracked using complex numerical techniques included in the software. Due to its fixed grid, AUTODYN™ easily handles large material deformations [14].

Using the Eulerian approach, a number of grid cells or zones (typically a minimum of three) must be placed in the thickness of the liner in order to model liner behavior throughout the detonation [15]. This approach has been validated and utilized by several previous researchers and continues to be used in this research.

2. Shaped Charge Modeling Approaches

Section III.1. Shaped charge mechanics discussed the significant role of the liner in the performance of a shaped charge. This research includes analysis of shaped charge performance with three different liners (trumpet, 42 degree cone, and 42 degree bi-material cone) and two different charge body materials (brass and Teflon) through examination of the jet characteristics using AUTODYN^{TM} computations. These computations will help to provide information necessary to gauge the performance of the various configurations used in the experimental process. Appendix I includes detailed procedures involved in setting up our various shaped charge simulations.

- *Zoning:* This refers to the actual number of grid cells per millimeter in AUTODYN^{TM}. A large amount of computational time and memory is required with an increased level of zoning. Initially, a comparison between the performances of different zoning levels was completed, which included the results of past research simulation and experimental data (see Figure 20). Because of the close correlation between predicted and observed penetration histories of the trumpet charge in the work by Dusetzina and Dusetzina, it was concluded that zoning at 10 to 14 cells/mm would be accurate. In this research it was found that this zoning was insufficient since the predicted jet tip velocity of 5.3 km/s is much slower than that observed from a set of flash radiographic experiments performed by the Ernst Mach Institute in support of this research. Because of the increase in time required to complete simulations with the increased zoning, it was determined that several techniques found in references 12 and 14 greatly

reduced the time necessary to complete the simulations [1]. For the trumpet lined simulations performed in this research, an improved variable zoning procedure was devised using a 16 cell/mm zoning near the centerline (containing the jet) with a gradual reduction of zoning up the y axis of the simulation. For all simulations involving the 42 degree conical liner, 10 cells/mm was determined to be sufficient for simulation.

- *Jet Velocity vs. Cumulative Mass:* One relationship useful in exploring the performance of a shaped charge is that of the jet velocity versus the cumulative mass of the jet. In Section IIIA1c Jet Formation, according to PER theory an increased collapse angle will result in a more massive jet with a reduced velocity. To maximize performance, a jet with high velocity and reasonable mass is desired.

THIS PAGE INTENTIONALLY LEFT BLANK

IV. RESULTS

This section reports the experimental and computational results of all investigations. This work was directed towards completing both a quantitative assessment of the trumpet shaped charge (previously studied by Serrano, Rigby, and Dusetzina and Dusetzina) and the 42-degree charge recommended by the latter. In addition the study of the effect of plastic substitutions that might form the bases for future engineering solutions is explored.

The Ernst Mach Institute (EMI) in Germany conducted a series of flash x-radiography tests for purposes of characterizing the jet from the trumpet shaped charge. The results showed that the zoning used by the previously mentioned former researchers was likely insufficient. The predicted jet velocities of 5.3 km/s were found to be substantially less than those determined from the radiographic results. These results led to a study of zoning effects, keeping in mind that eventually charge optimization will be dependent on accurate computational prediction. A series of computations were also performed to design a Teflon/copper bi-material liner.

Two series of tests were performed. In the first series, the effect of substituting plastic for the brass body was investigated. The trumpet shaped charge was used exclusively in these tests. It was originally planned to add various thicknesses of Ultem plastic over 7.6mm thick Teflon encased charges. It was found, however, in the first test that the Ultem addition does not appear to have an effect on penetration. The remaining tests were then dedicated to determining the difference between brass and Teflon.

The second test series was dedicated to evaluating the 42-degree charge. Penetration standoff data for the brass-confined charge was obtained. Additional tests were performed to determine the effect of partially replacing the copper liner with Teflon, and a single test was performed using a Teflon/copper lined charge

in a Teflon body. The final test in this series was performed to assess the potential threat of an all-plastic lined shaped charge.

Make-break switches were used in most of the penetration tests to detect jet time-of-arrival. These data were used to estimate the average penetration velocities of jet through the target. By differentiation we were able to also estimate the velocities of the tip portions of the jets.

A. FLASH X-RAY RADIOGRAPHY EXPERIMENTS

Seven tests were completed at EMI with a trumpet liner encased in a brass body shaped charge. X-Ray flash times were set to capture the jet prior to breakup for purposes of estimating mass and the flash times for a second set of tests were set at longer delay times for purposes of determining jet break up time. Average jet tip velocity was estimated simply from the translation of the leading edge of the jet stream between flash times.

Some of the tests yielded wavy and/or bifurcated jets. It was revealed that the standoff tubes were sawed off after liner installation, which likely dislodged the liner in two of these tests. The causes of the imperfections might have also resulted from asymmetries in the fixtures used to hold and position the charges; a description of the test fixture is shown in Figure 12. The set-up for the tests is shown in Figure 13.

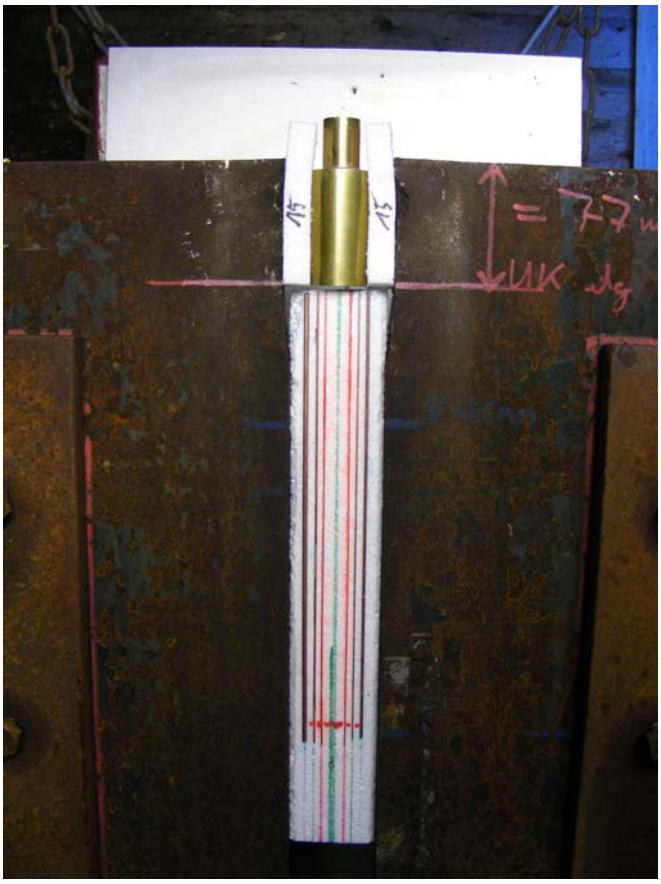

Figure 12. Brass body shaped charge ready for Flash X-Ray Photographs.

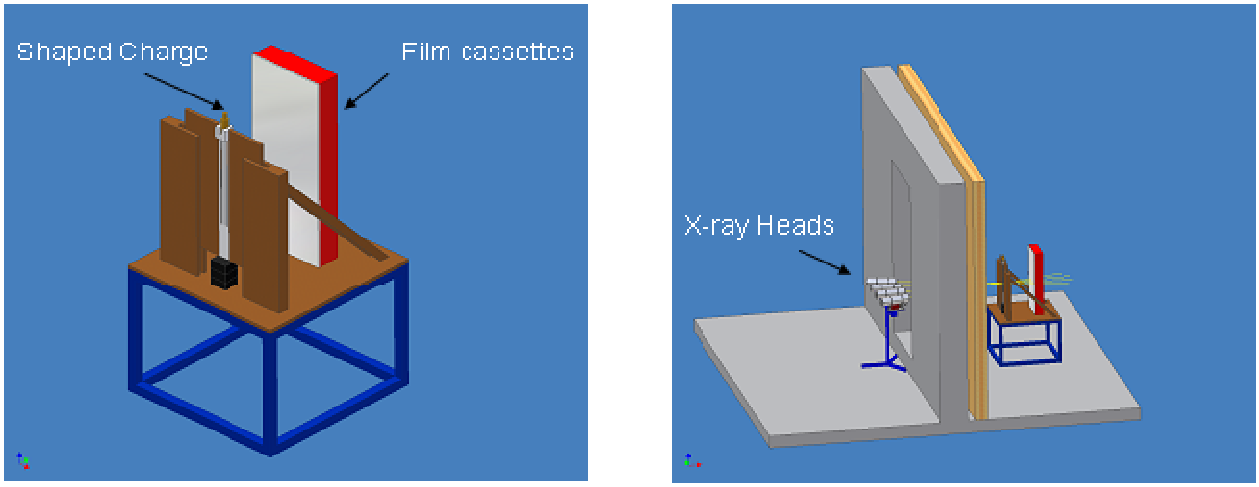

Figure 13. Flash X-Ray Test Set-Up.

1. Test No. 1

Shown in Figure 14 is the set of radiographs for this test. The jet was mostly straight and continuous, with a prominent tip velocity of 5.7 km/s. The exposure times are 24.7 μs, 29.5 μs, 34.7 μs and 39.6 μs.

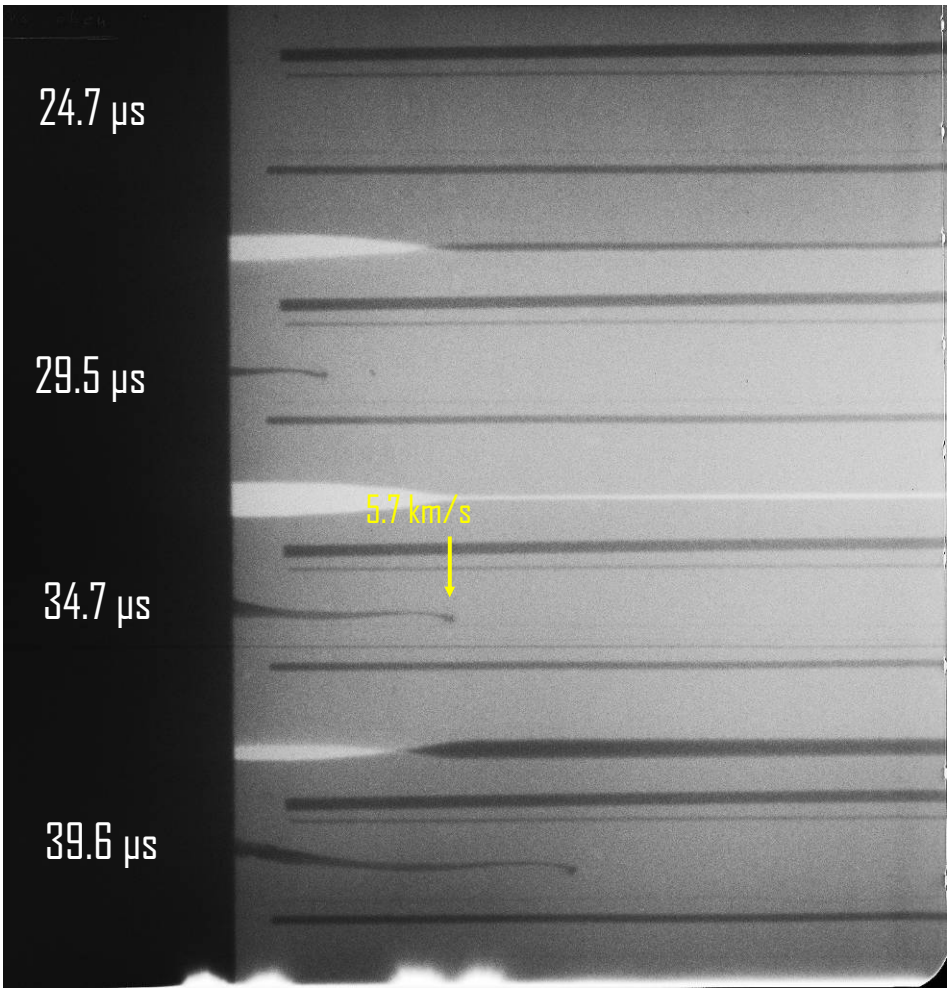

Figure 14. Early time radiographs of the jet from the brass encased trumpet shaped charge from Test No. 1.

2. Test No. 2

In this test the resulting jet was wavy and divergent. The highest velocity was 5.7 km/s. The exposure times are 49.7 μs, 59.7 μs, 69.8 μs and 79.6 μs.

3. Test No. 3

Shown on Figure 15 is the set of radiographs for test no. 3. The jet was particulated. The jet tip velocity was 6.3 km/s. The exposures times are 49.7 μs, 59.6 μs, 69.8 μs and 79.8 μs.

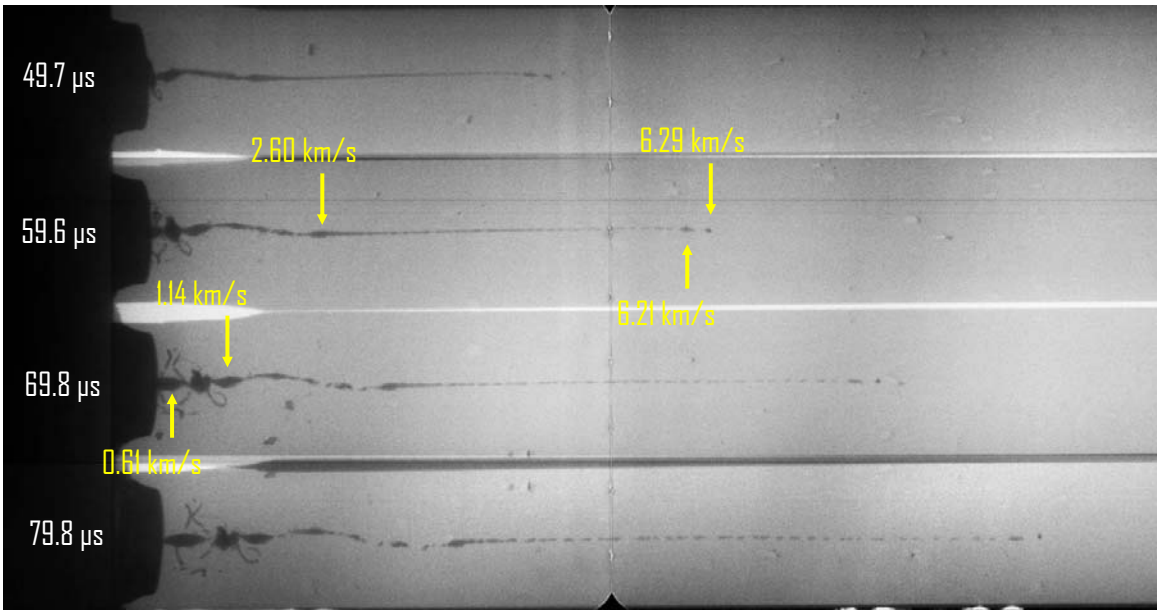

Figure 15. Flash X-Ray Test No. 3.

4. Test No. 4

For test four the jet was divergent and the jet tip could not be determined. The exposure times are 32.7 μs, 37.4 μs, 42.7 μs and 47.5 μs.

5. Test No. 5

Shown in Figure 16 is the set of radiographs for test five. The jet was also divergent and the jet tip velocity was estimated at approximately 6.02 km/s, as it was difficult to determine. The exposure times are 32.8 μs, 37.5 μs, 42.8 μs and 47.7 μs.

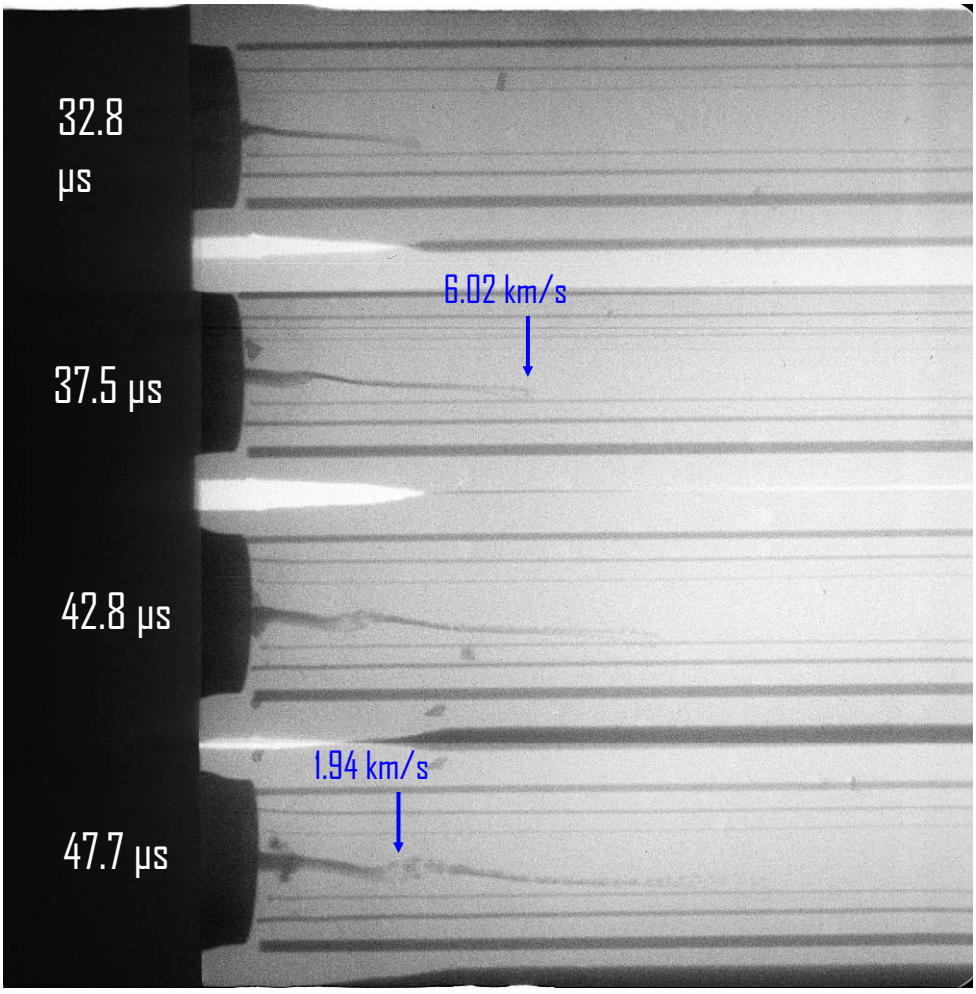

Figure 16. Flash X-Ray Test No. 5

6. Test No. 6

For test No. 6 the jet was divergent and the jet tip velocity and other characteristics were once again unable to be determined. The exposure times are 37.9 μs, 41.7 μs, 45.5 μs and 49.6 μs.

7. Test No. 7

Shown in Figure 17 is the set of radiographs for this test. The jet remained continuous with a jet tip velocity of 6.0 km/s. The exposure times are 37.7 μs, 41.5 μs, 45.8 μs and 49.5 μs.

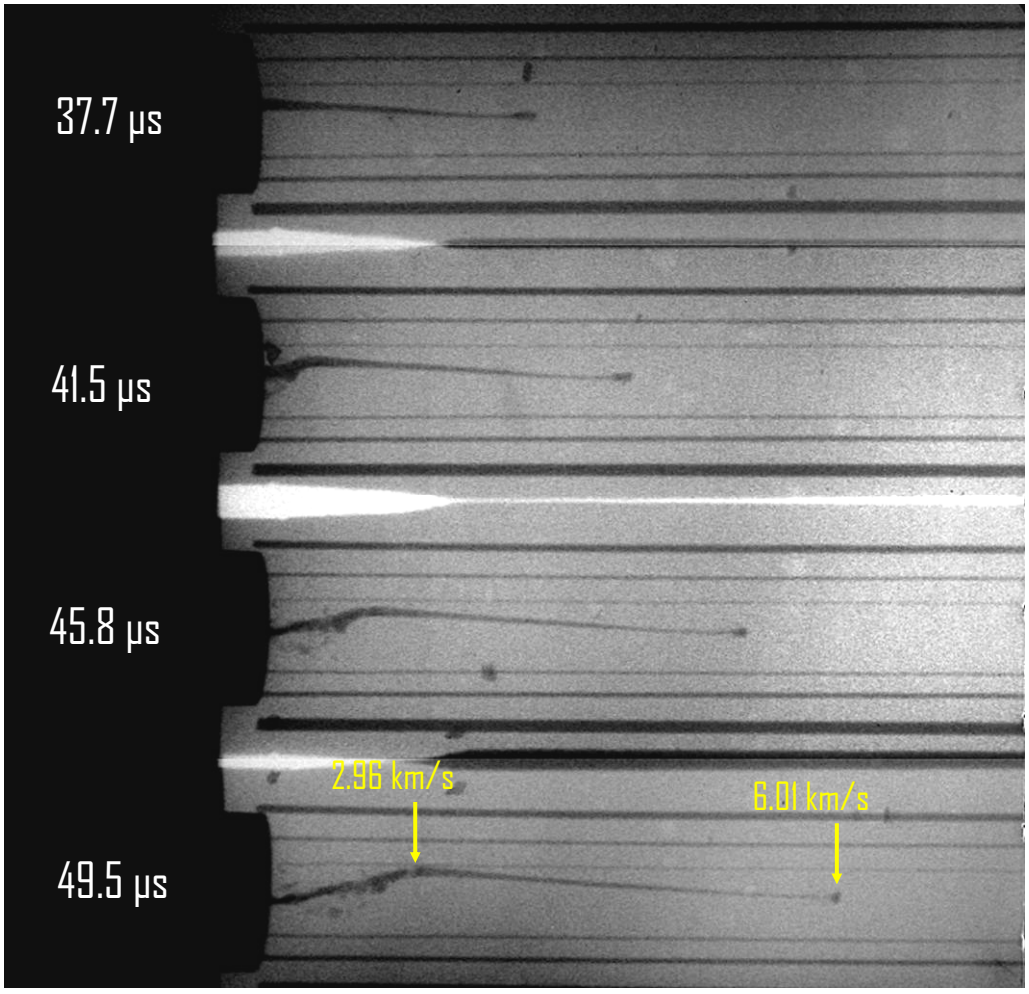

Figure 17. Flash X-Ray Test No. 7.

Shown in Figure 18 is a typical display of fragments from the brass body collected from the detonation– the rulers are dimensioned in centimeters (cm).

A summary of the estimated jet tip velocities from these tests, excluding those containing imperfections, is reported in Table 1. Figure 19 shows a graph of velocity vs. cumulative mass.

Figure 18. Example of the fragments formed from the brass casing of the baseline trumpet shaped Nitromethane shaped charge: From EMI No. 7.

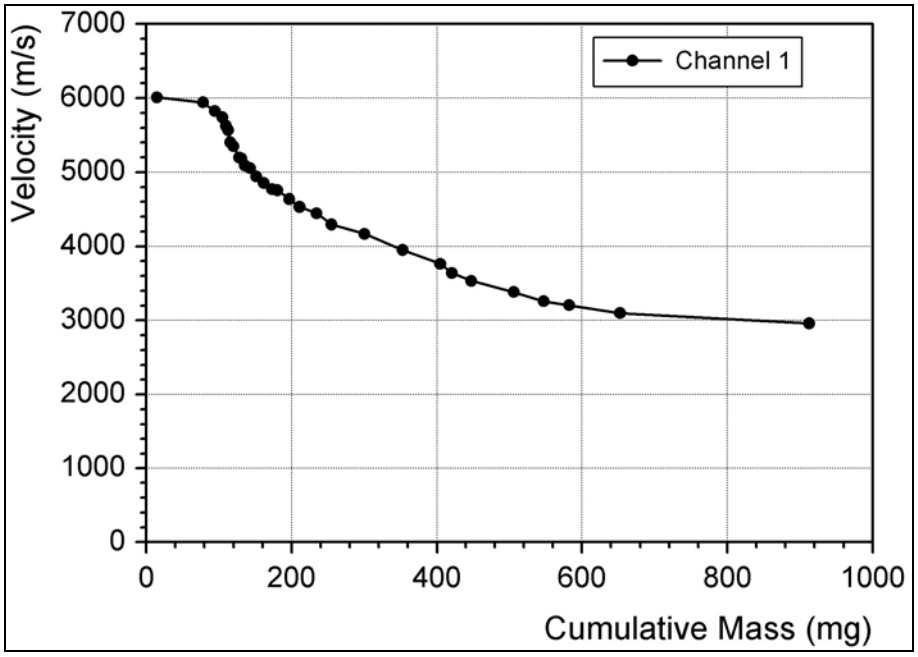

Figure 19. Estimated jet velocity-cumulative mass distribution from the baseline trumpet charge (based on jet radiography).

Table 1. Table of average jet tip velocities from the EMI radiographs

TEST	Jet tip velocity (km/s)	Type of Jet
3	6.29	Particulated
5	6.02	Divergent
7	6.01	Continuous

B. COMPUTATIONS

Simulations were used to determine the jet characteristics in order to facilitate comparison to experimental data obtained from the jet penetration experiments and to achieve the following objectives:

- Evaluate the performance of shaped charges with three different liners (trumpet, 42 degree cone, and 42 degree cone bi-material).
- Determine a plastic composition and thickness for the trumpet liner sufficient to replicate existing brass results.
- Predict the partitioning of mass between jet and slug after liner collapse.

Prior to receiving data from EMI, estimates of jet velocity and mass from the trumpet and 42 degree lined charges were estimated from moderately zoned AUTODYN^{TM} computations, and experimental penetration-time data. In the latter case, best-fit quadratic equations derived from penetration time-of-arrival gauges were differentiated and the penetration velocity of the leading portion of each jet estimated from the *dP/dt* intercept. The velocity of the leading portion of each respective jet was than estimated using hydrodynamic theory, assuming strength-less behavior (see Equation 3.3). The velocities from the trumpet shaped charge estimated in this manner were found to be much lower than those from the experimental radiographic data: The AUTODYN^{TM} predicted values obtained by Dusetzina and those early in this research were at 5.3 km/sec, which is approximately 15 percent lower than observation. Because of these noted

differences and the importance of establishing a well-founded baseline from which future design changes could be based, additional computations were performed for purposes of resolving the differences.

Initial recalculations were performed for purposes of determining the effect of zoning for predicting jet penetration dynamics, since this was the original approach for estimating jet tip velocity. A more direct approach directed towards estimating jet tip directly was ultimately employed and completed by Cao [16].

1. Trumpet Liner Shaped Charge Jet Characterizations

It is important to examine the effects of zoning on computational analysis. As previously mentioned in Section IIIc2, the goal is to obtain maximum accuracy in calculated results while minimizing the increased time required in order to perform simulations with a high level of zoning.

A series of increasingly fine-zoned jetting-penetration computations were performed, as indicated above, for purposes of comparing with penetration-time-of-arrival data. The target position in these simulations is at a 2 CD standoff: These computations were performed prior to the EMI tests. Differences between experimental data reported by Dusetzina and AUTODYN^{TM} prediction were found to decrease with computational cell size decrease. The best fit to experiment was found from variable zoned computations, in which 16 cells per millimeter were mapped about the centerline out to a radius of 2 mm (see Figure 20). While this variable method compared favorably to prior research, it was found that simulated baseline jet tip velocity was still considerably lower than that found in the EMI radiographic experiments shown in Figure 19: This computational set up was still insufficient since the predicted jet tip velocity was only 5.3 km/s.

Another computation at 3CD standoff and comparison with experimental time of arrival data is shown in Figure 21.

A computation was then started at a cell size of 25/mm by Cao [16]. Stationary tracers were placed along and radially off-set from the axis of

symmetry of the charge, and moving tracers within the liner were used to detect the velocity of the jet, which at this point was known to be of the order of only milligrams. The velocities from these tracers were found to be close to the experimental results. A plot of the fixed tracers is shown in Figure 22. The lead velocity of the jet from this computation correlates well with the estimated value derived from the radiographic data.

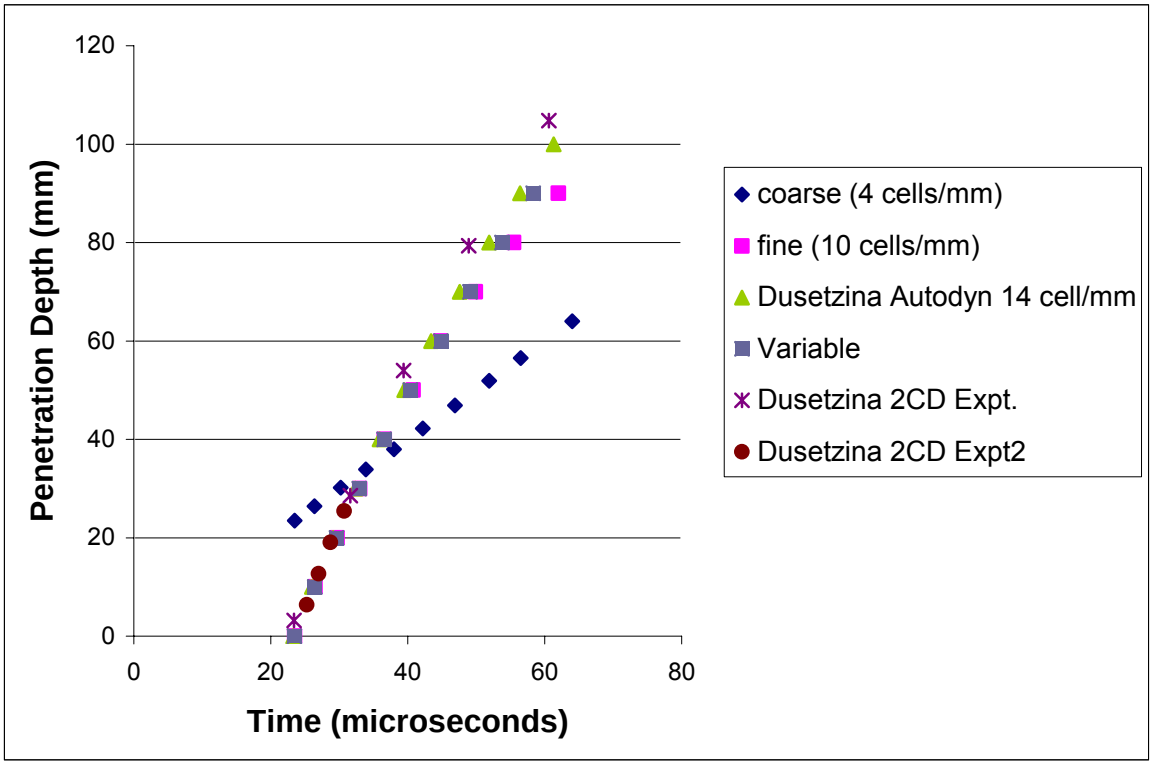

Figure 20. Effects of different zoning on 2 CD penetration simulations and previous experiments.

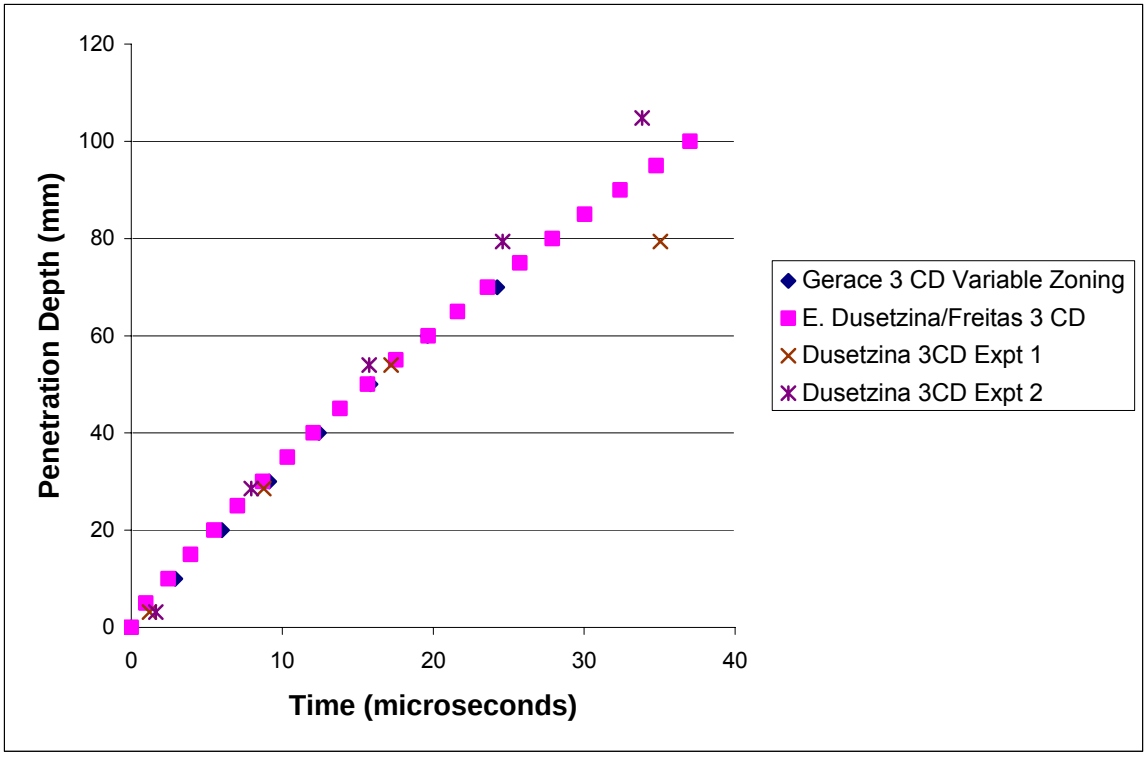

Figure 21. Comparison between experimentally determined penetration time-of-arrival data and a variable zoned AUTODYN™ prediction at 3CD standoff.

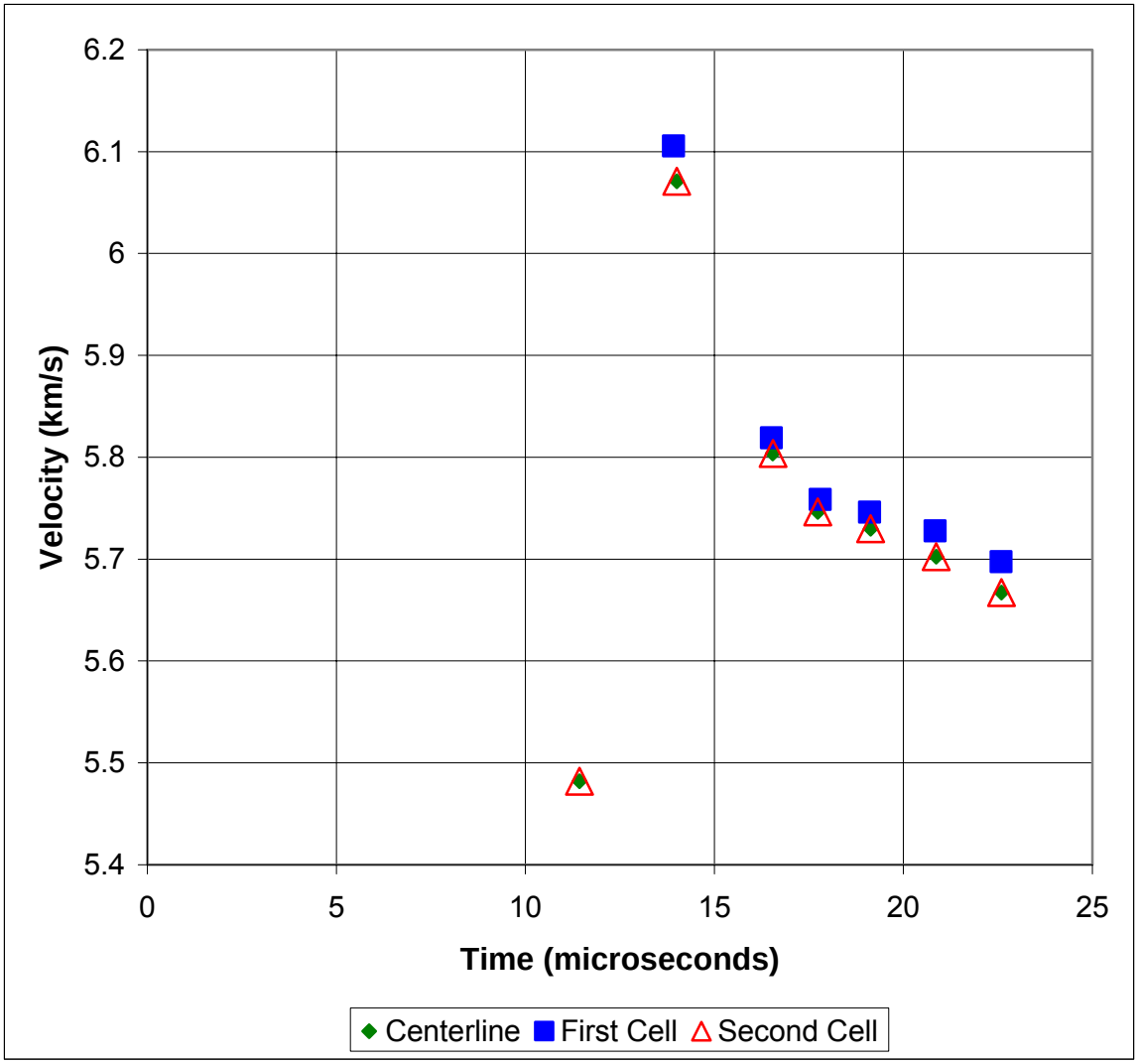

Figure 22. Predicted velocities of the jet stream rushing through a fixed computational tracer at 11.5 mm from the base of the trumpet-lined charge, and at 0.04 and 0.08 mm above the centerline. From [16].

2. Predicted Effects of Plastic Substitutions

Prior to receiving the quantitative characterization of the jet from the baseline trumpet-shaped charge, a study was performed for purposes of determining the effect of plastic substitution in the charge body and liner. This primary objective of work focuses on the ultimate intent of designing a lightweight

plastic (or composite plastic) shaped body that is chemically inert with nitromethane, and to which a copper (or other metal) liner can be attached just prior to employment.

A series of computations was performed in which Teflon was substituted for the brass body at identical thickness, and varying thicknesses of Ultem, a high strength plastic material. Another set of computations was performed for purposes of determining the maximum thickness of Teflon that could be mass substituted in the liner without affecting copper jet formation. In the first case, it was assumed that a variable zoning resolution starting at 16 cells/mm and in the second case a uniform zoning of 10 cells/mm would be sufficient, even though in hindsight it was found that this zoning is insufficient to resolve the exact velocity and mass distribution in the lead portion of the jet. These analyses, nevertheless, provided sufficient guidance to construct two fruitful series of tests.

To begin the analysis of Teflon use in a shaped charge body, the first simulation was planned as an evaluation of jet tip velocity and diameter. The initial simulation using a Teflon body was conducted using an identical setup to that of a brass simulation, substituting Teflon for brass and leaving all parameters intact. Figure 23 shows the jet just prior to a potential target impact. The jet tip velocity and diameter were predicted to be at 4.67 km/s and 1.8 mm, respectively. This represented a slight reduction from previous experiments conducted using brass, which produced a jet tip with a velocity of 5.3 km/s at 2.6 mm diameter [1]. It can be seen that the Teflon confinement is displaced much more rapidly than its brass counterpart which will result in a reduced jet mass, faster jet breakup and ultimately a more limited penetration value.

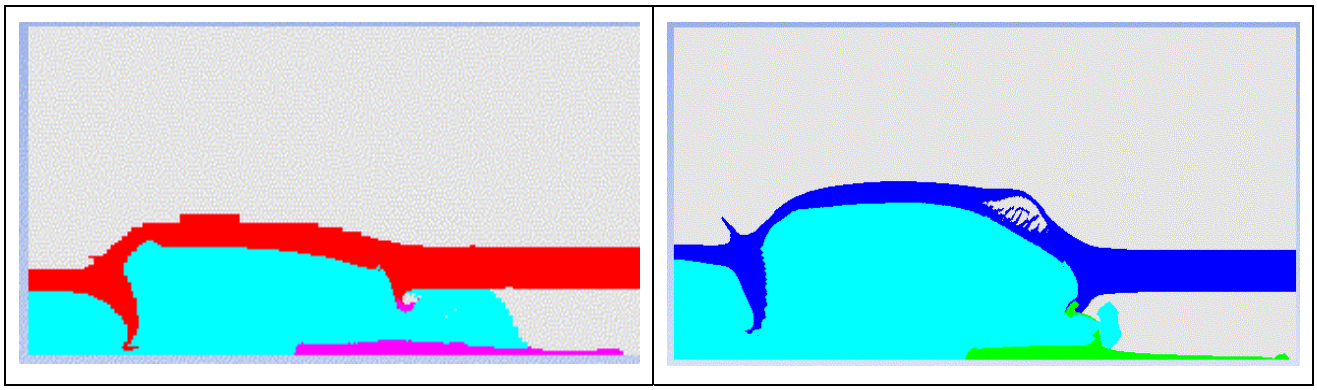

Figure 23. Comparative expansion of a Brass (left) and Teflon body of identical thickness 24.3 microseconds after initiation.

After determining the jet characteristics using a Teflon charge body, the next simulation was run to determine the effect of Teflon substitution on jet penetration into an aluminum target. Figure 24 shows the depth of jet penetration versus time for both a brass and a Teflon body (identical dimensions, leaving all other parameters constant) with a 2 CD standoff at an identical time following detonation.

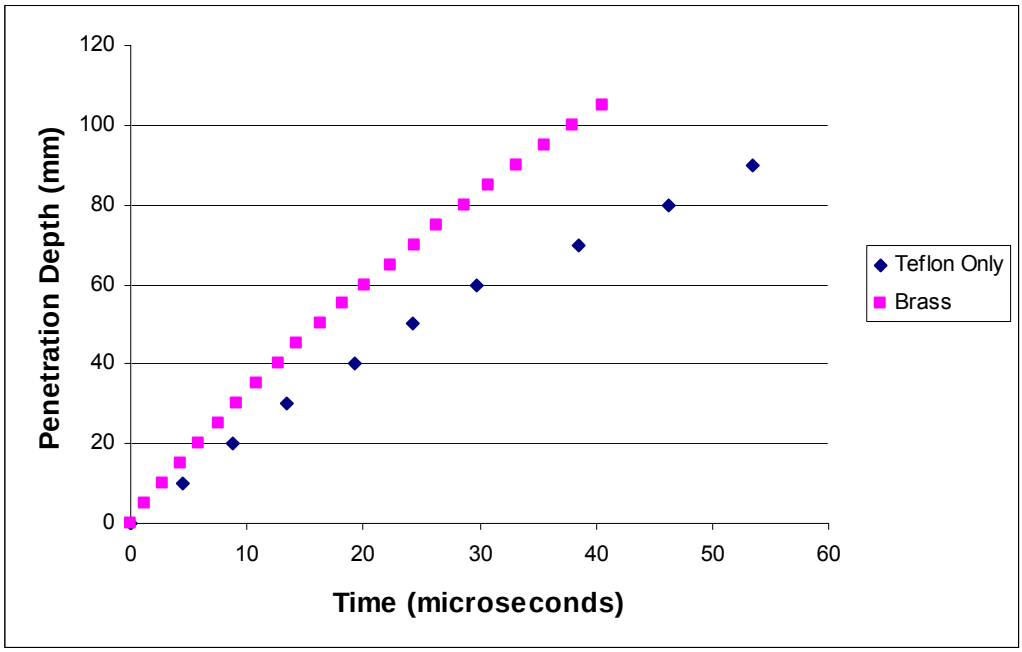

Figure 24. Comparison between the early-time penetration of jets from brass and Teflon encased charges at 2CD standoff.

For the final trumpet lined Teflon simulation, the addition of Ultem plastic sleeve was simulated by increasing the thickness of Teflon. It was assumed that the addition of this plastic would increase effective confinement.

Since Ultem plastic is not included in the AUTODYN^{TM} material library, a Teflon thickness equal to the greatest Ultem diameter was substituted at an outer diameter of 3 in (76.2 mm). In Figure 25, the penetration depth vs. time for the charge in the "increased thickness" (28.4 mm) Teflon body is predicted. Predicted penetration velocities are shown in Figure 27 and tabulated in Table 2.

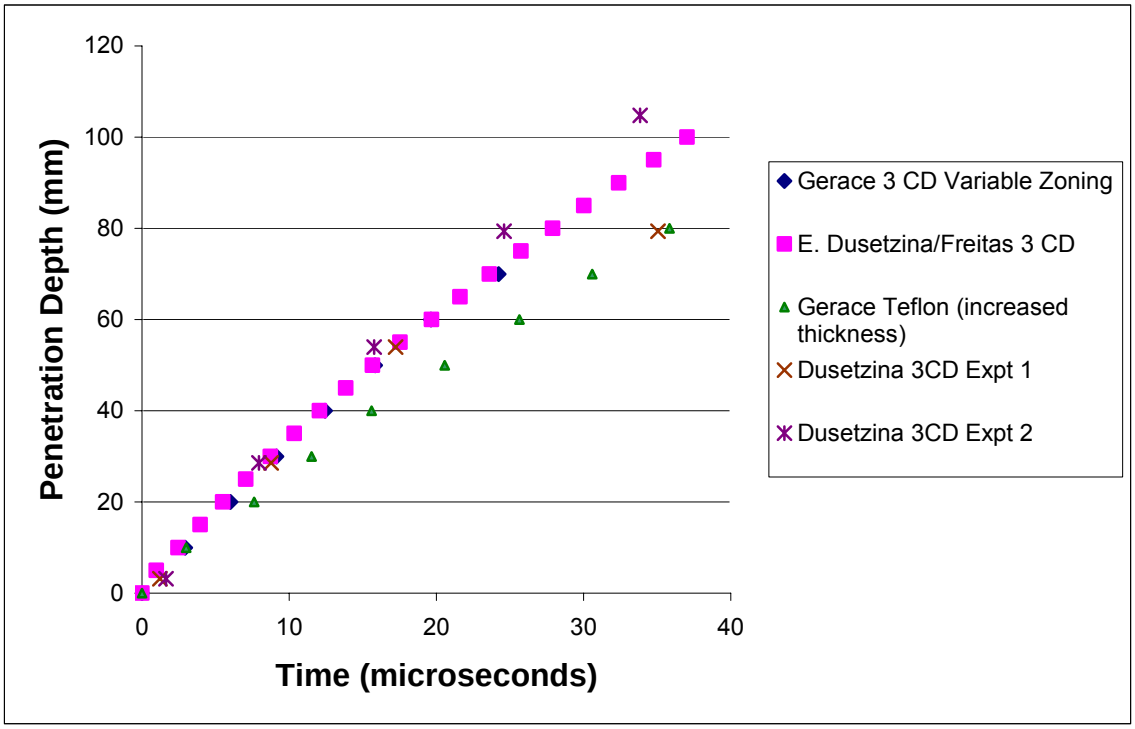

Figure 25. Penetration depth vs. Time for increased thickness (28.4 mm) Teflon at a 3 CD standoff.

In Figure 26, the jet is depicted as it penetrates into an aluminum target. Gauges are set at fixed points (every 10 mm in this case) in order to track the penetration depth as a function of time. This information can easily be used to calculate the penetration velocity for a given depth.

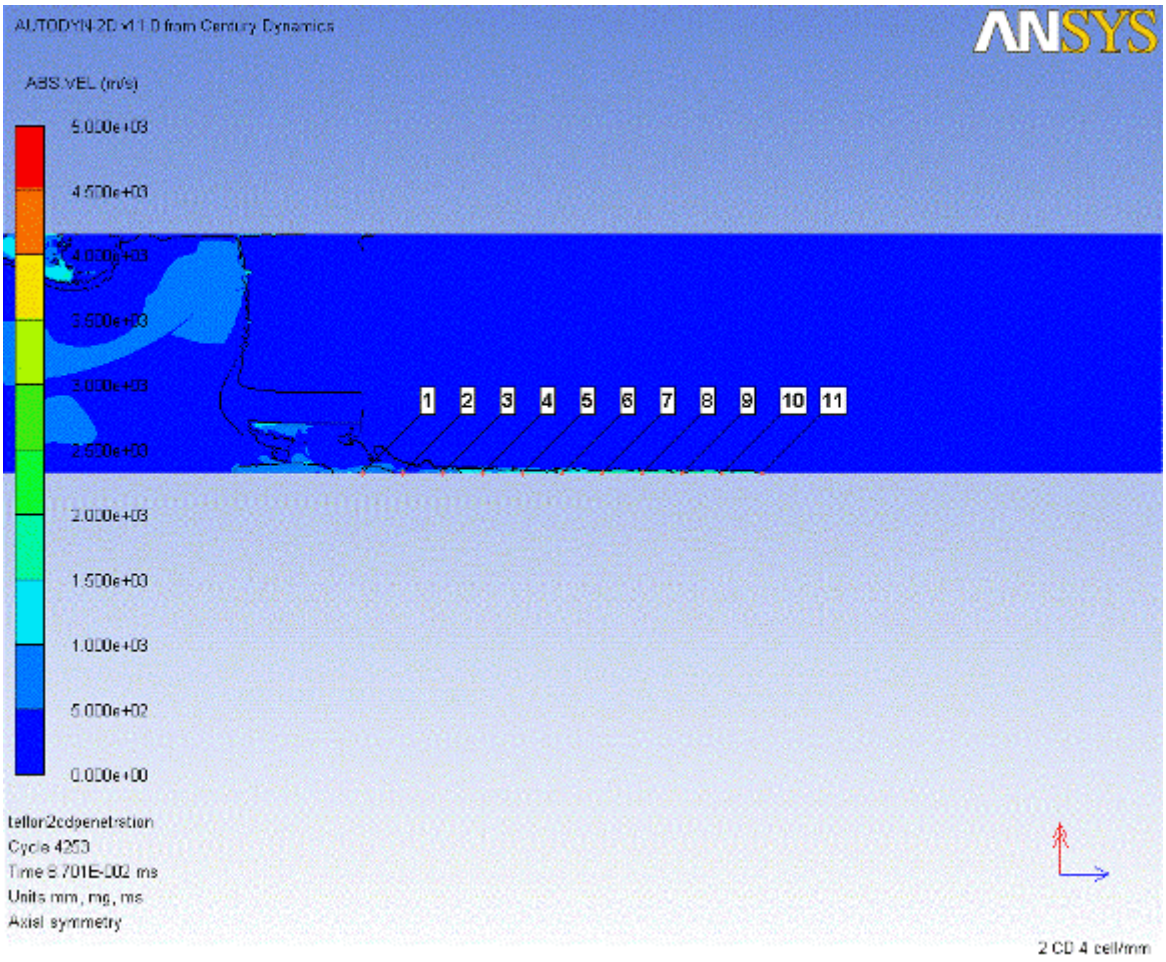

Figure 26. Copper jet from the 7.6 mm thick Teflon-encased charge penetrating through aluminum at 2CD standoff 87.0 microseconds after initiation.

A plot of Teflon penetration velocity as a function of depth is shown on Figure 27. Using a regression line, we can derive an analytical expression to determine the jet velocity at the onset of detonation using Equation 3.3. The various penetration and jet velocities and the corresponding depths can be found in Table 2. As expected, the initial velocity for the Teflon encased charge is predicted to be lower than the values achieved using a brass charge.

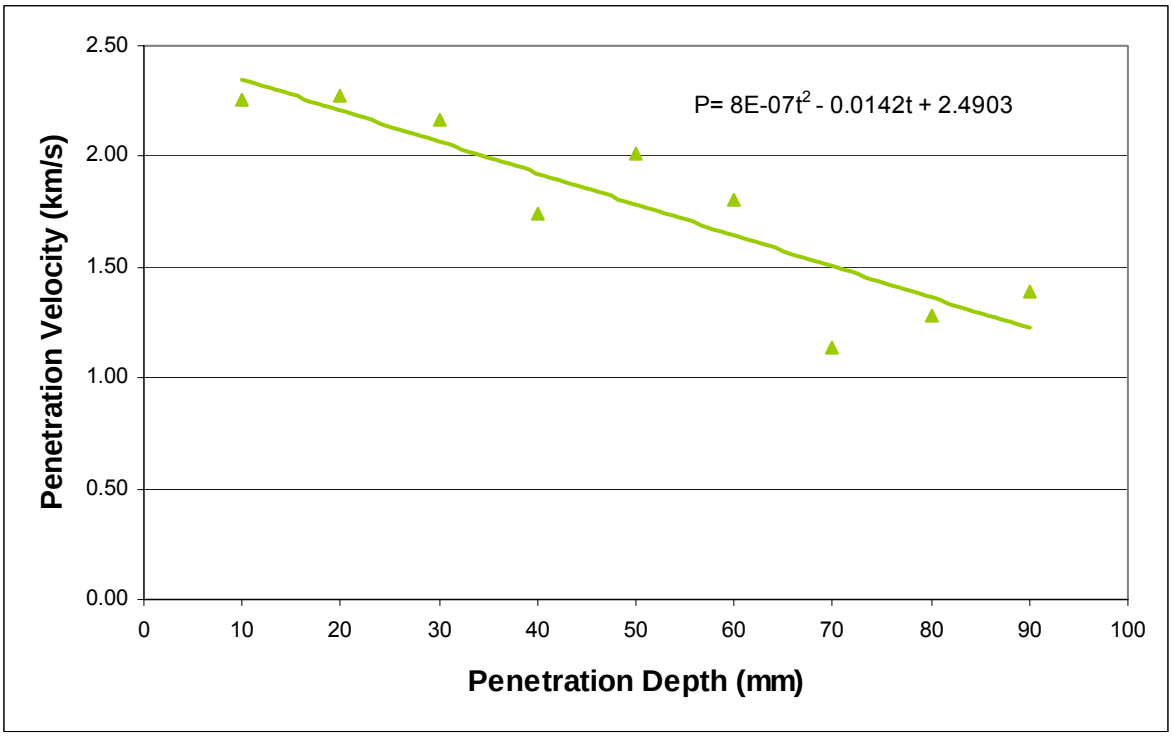

Figure 27. Penetration velocities of the jet from the trumpet shaped charge encased in Teflon vs. depth at 2 CD

Table 2. Estimated jet velocities at 2CD standoff from penetration velocity data reported in Figure 27

Penetration Depth (mm)	Penetration Velocity (mm/µs)	Jet Velocity (mm/µs)
0	2.49	3.88
10	2.26	3.51
20	2.28	3.55
30	2.16	3.37
40	1.74	2.72
50	2.01	3.13
60	1.81	2.81
70	1.14	1.77
80	1.28	2.00
90	1.39	2.16

3. 42-Degree Liner Shaped Charge Jet Characterizations

The initial simulation using a 42 degree conical liner with a brass body was conducted using an identical setup to that of a trumpet liner simulation, substituting the trumpet liner for a 42 degree conical liner, leaving all remaining parameters intact. Figure 28 shows the jet forming at a 2CD standoff distance and Table 3 compares the maximum predicted velocity and tip diameter with the trumpet liner/brass body: It is important to note again, that the zoning used in these computations is not sufficient enough to predict the velocity and mass characteristics of the lead portion of the jet. The values reported have only relative importance, and as such it appears that the 42-degree liner should produce a faster and more massive jet than that from the trumpet baseline charge.

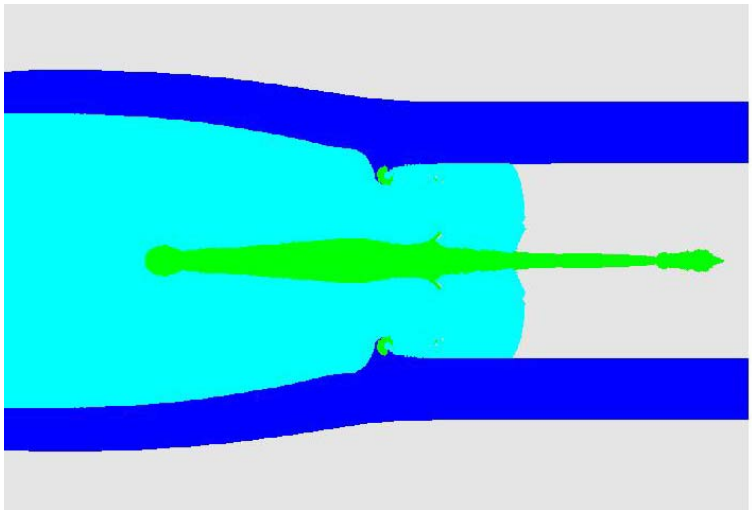

Figure 28. Lead portion of the jet predicted to be produced by the 42 degree lined nitromethane shaped charge at 19.4 microseconds.

Table 3. Maximum velocity and tip diameter.

Shaped Charge	Velocity (km/s)	Diameter (mm)	Cumulative Mass (mg)
Trumpet Liner	5.3	2.6	800
42 Degree Liner	6.11	3.1	850

In the case of the 42 degree copper conical liner, the jet diameter was measured at approximately 3.1 mm from a 2 CD standoff distance.

The previous simulation was also run to determine the portion of liner that forms the jet and the slug, as part of the bi-material liner study. The next series of simulations were run with different percentages of copper and Teflon (from 50% Cu, 50% Teflon to 80% Cu, 20% Teflon), but maintaining the original mass of the liner. Table 4 outlines maximum velocity and cumulative mass, taken at the same jet tail velocity of 3km/s.

Table 4. Velocity and Cumulative mass data for the three SC designs

Shaped Charge	Velocity (m/s)	Cumulative Mass (mg)
Trumpet	5.25	800
42 degree 100% Cu	6.10	850
42 degree 80% Cu	5.96	960
42 degree 60% Cu	5.97	880

Figure 29 illustrates the jet penetration through an aluminum target at a 2CD distance for the case of the 42 degree conical liner. The target is embedded with gauges to track the penetration depth of the jet as a function of time. As expected, the penetration potential of the 42 degree lined charge is predicted to be greater than that of the trumpet lined charge.

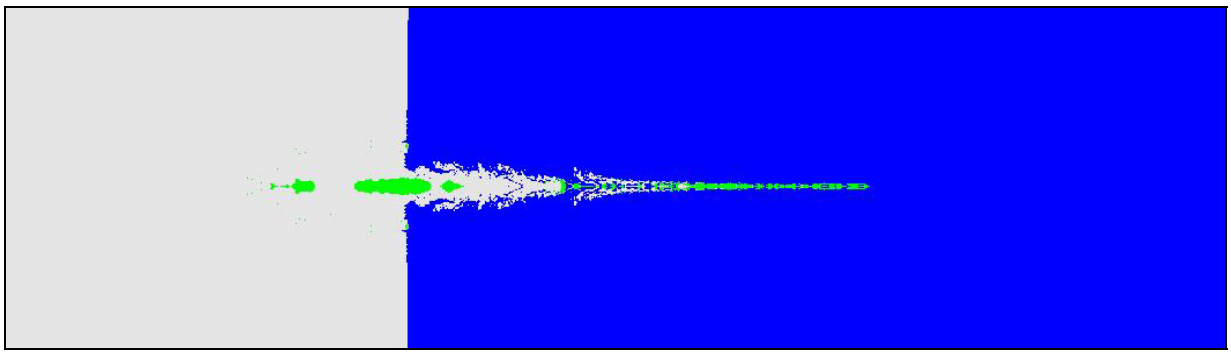

Figure 29. Jet from the 42 degree lined charge penetrating through aluminum target positioned at 2CD from the charge base. The time is 98.1 microseconds.

Figures 30, 31, and 32 show the penetration depth as a function of time to determine the penetration velocities at various penetration depths for the 42 degree conical liner (copper and bi-material) at different standoff distances. As expected, replacing 20% of the copper liner with Teflon is predicted to have minimal impact on the penetration potential of the 42 degree lined charge.

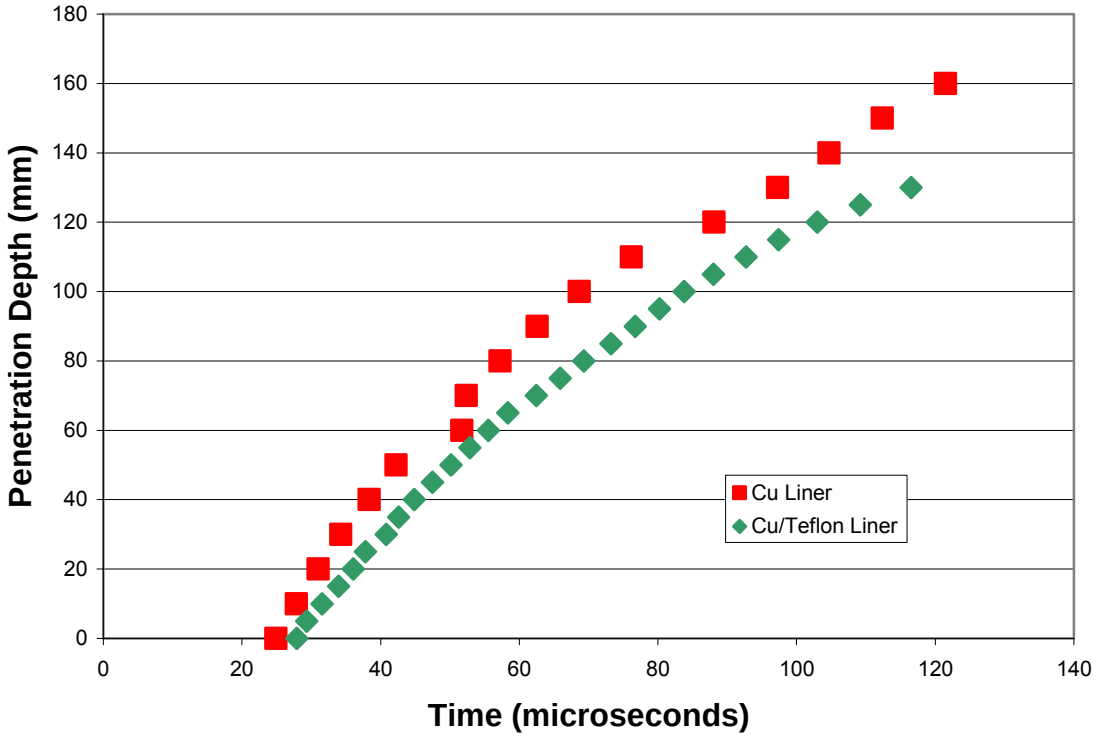

Figure 30. Predicted differences in the early time penetration of the copper jets from the 42 degree charge into an aluminum target at 2CD affected by Teflon body and partial liner substitution

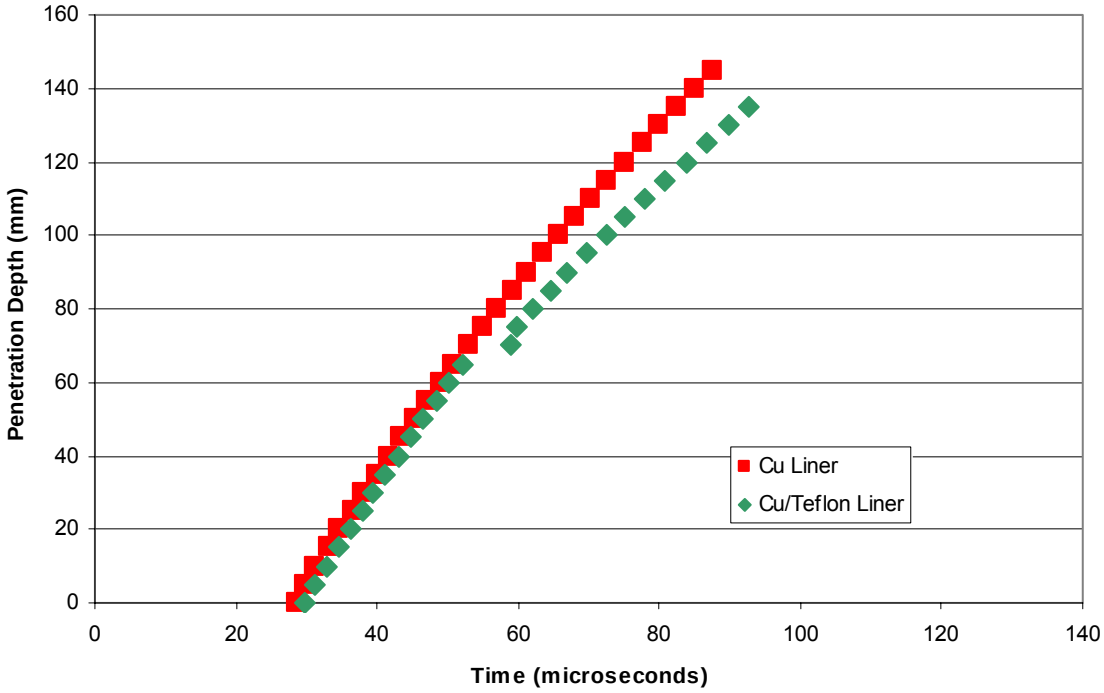

Figure 31. Predicted differences in the early time penetration of the copper jets from the 42 degree charge into an aluminum target at 3CD affected by Teflon body and partial liner substitution.

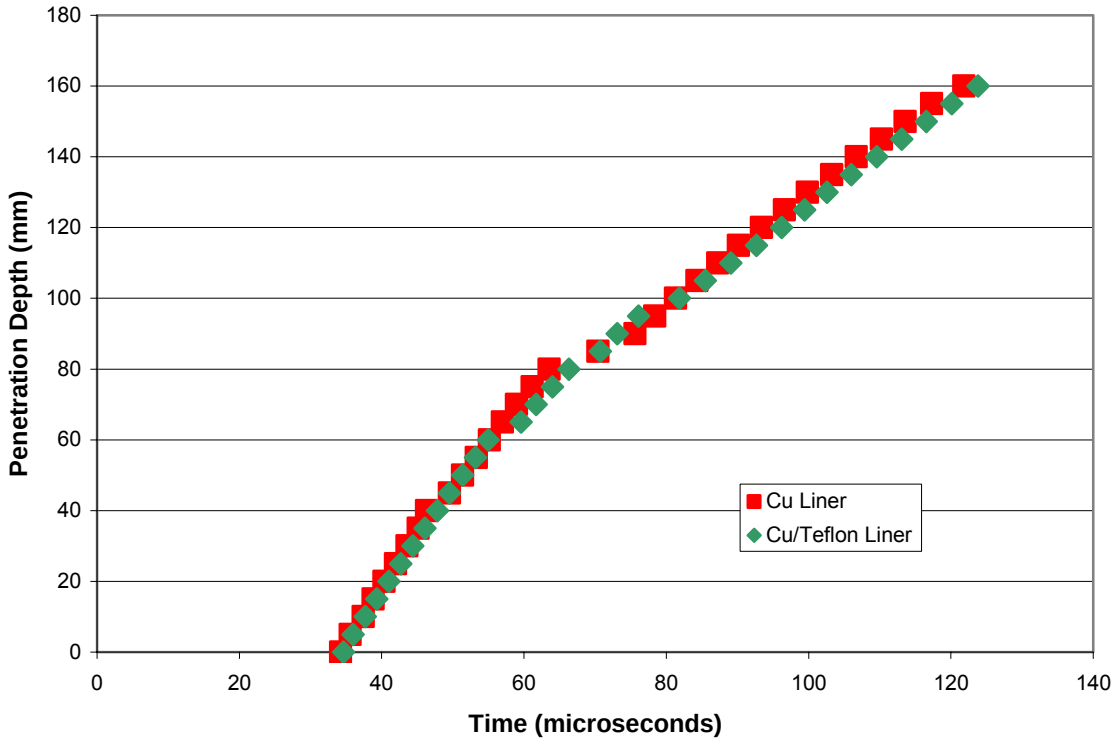

Figure 32. Predicted differences in the early time penetration of the copper jets from the 42 degree charge into an aluminum target at 4CD affected by Teflon body and partial liner substitution

4. Summary of Computational Investigations

In the trumpet lined charge simulations, zoning agreement issues with EMI radiography results were resolved by increasing the zoning level to 25 cells/mm, as performed by Cao [16]. Jet tip velocity predictions correlate with EMI radiography results.

As expected, the substitution of Teflon for brass resulted in a slightly decreased prediction of jet tip velocity and penetration potential. In addition, Ultem Plastic was simulated through an increased thickness of Teflon with minimal change to the aforementioned Teflon results.

The 42 degree liner simulations resulted in higher velocities and more massive jets, as expected. This anticipates higher values of penetration and impact initiation potentials for this liner design. Replacement of 20% of the copper liner with Teflon was shown to be possible without any reduction in performance.

C. PENETRATION POTENTIAL EXPERIMENTS (TEST SERIES 1): EFFECT OF PLASTIC CONFINEMENT

The objectives of the first test series were to complete the determination of penetration-standoff for the trumpet-lined charge and to assess the effect of substituting plastic for the brass body. A secondary objective was to use the data to estimate any differences in the average velocity of the jets entering the first portion of target.

Experimental work was conducted in the explosive chamber at Teledyne RISI facility in Tracy, CA shown in Figure 33. The setup of these tests and the procedures followed are similar to those reported by Serrano and Rigby, and Dusetzina and Dusetzina [1, 2, and 3].

The shaped charge components (Teflon bodies and copper liners) were rinsed with acetone and assembled several days prior to the testing date.

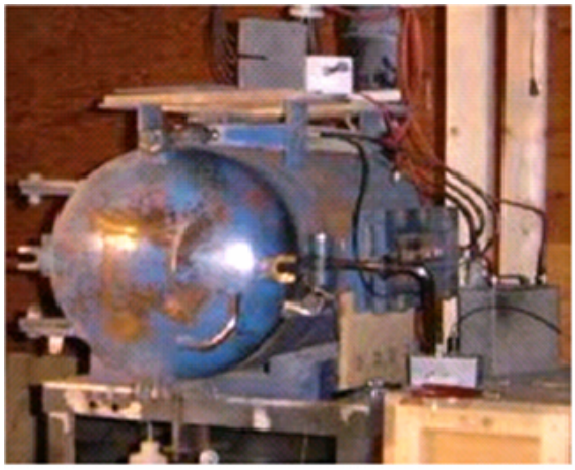

Figure 33. Teledyne RISI Explosive Chamber. From [13].

Aluminum foil switches were fabricated and used for the first series of experiments. All target plates were assembled prior to the test date, and the placement of the switches was made just prior to the shots. Following this arrangement, a mixture of the two chemicals, nitromethane (NM) and diethylenetriamine (DETA) was prepared, loaded into the shaped charge and placed into the explosive chamber as shown in Figure 34.

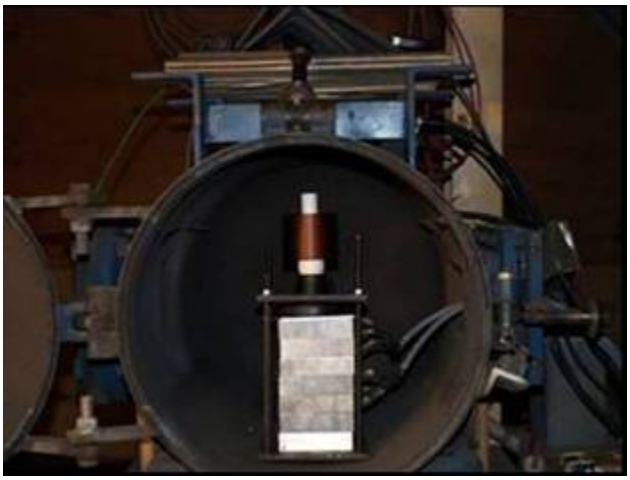

Figure 34. 3CD Shaped charge inside explosive chamber.

Six tests were completed during this session. Target assemblies consisted of eight aluminum plates. Thickness of the top plate was 3.18 mm (1/8 in) and that of the other plates was 25.4 mm (1 in).

1. Shaped Charge Test 1-1

The initial test employed a shaped charge encased in a composite body composed of Teflon and Ultem. A description of the charge is shown in Appendix E. The test was performed at a 3 CD standoff against one of our target assemblies (180.98 mm of aluminum plates). Six aluminum foil switches were placed in the assembly, beginning with the top plate and in between the following

plates. The jet penetrated through 129 mm of aluminum. Figure 35 shows that the hole produced by the jet penetration is centered and symmetric, indicating a good jet and proper liner alignment.

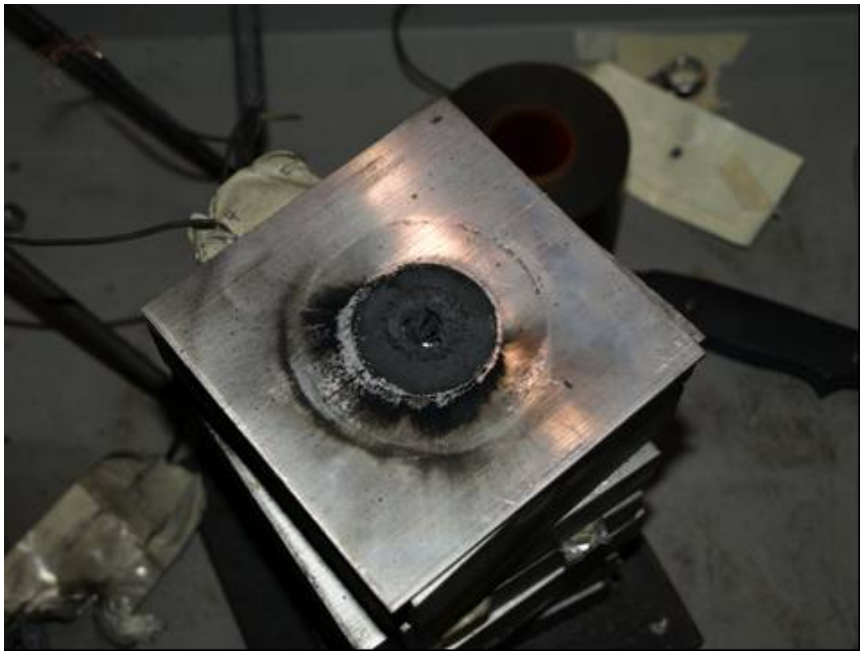

Figure 35. Damage to top target plate: Test 1-1.

Just four out of the six make/break switches provided readings of jet arrival time during penetration. Time of arrival data is outlined on Table 5. Penetration velocity was approximated as 3.48 km/s from the linear regression of penetration depth as a function of time as shown in Figure 36. Estimated jet tip velocity was determined from Equation 3.3. Calculated average jet tip velocity was 4.94 km/s.

Table 5. Time of Arrival Data of Jet through Aluminum: Test 1-1.

Penetration Depth (mm)	Time (μs)
3.175	0
28.575	8.268
53.975	17.612
79.375	28.305

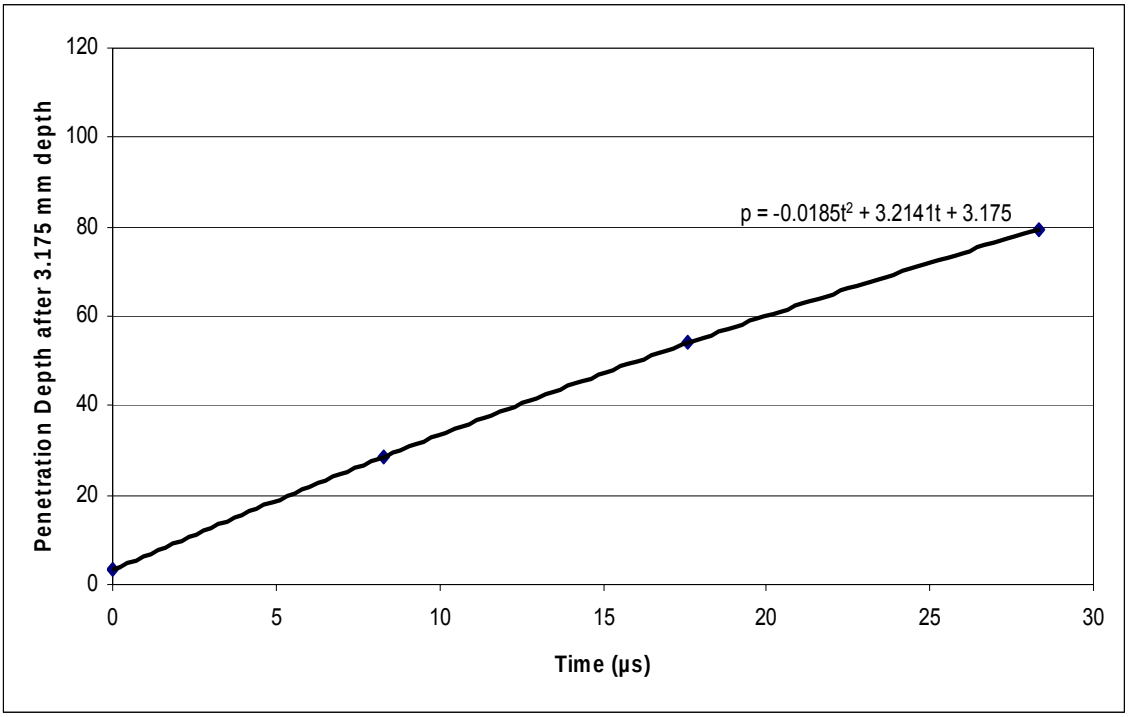

Figure 36. Penetration Depth vs. Time: Test 1-1.

2. Shaped Charge Test 1-2

The second test in this series was fired at a 2 CD standoff. The charge was identical to that used in Test 1-1. Six aluminum foil switches were placed in the assembly, beginning with the top plate and in between the following plates.

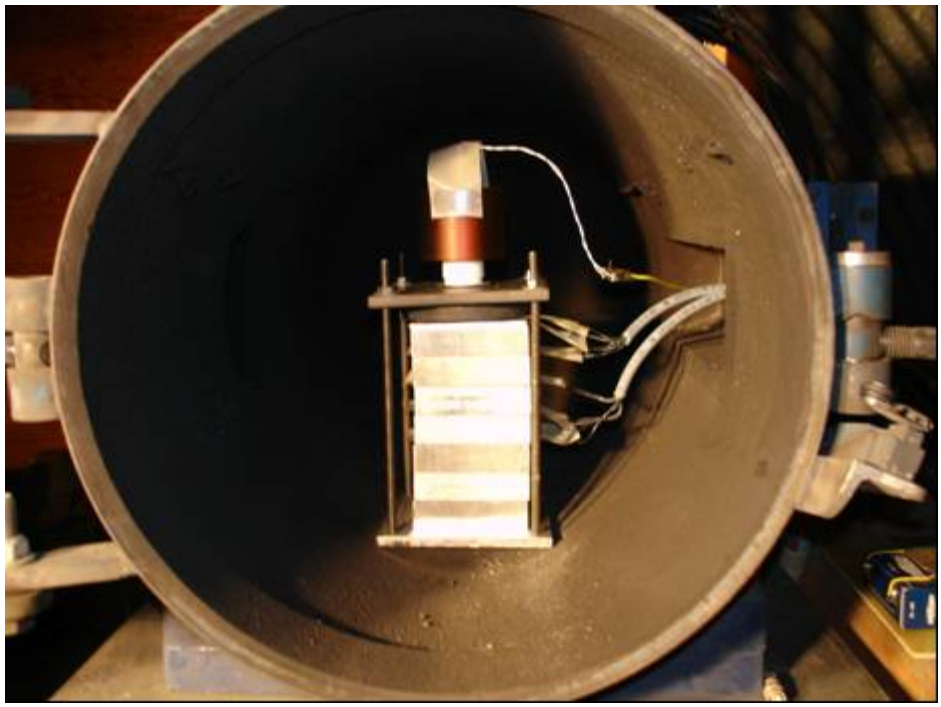

Figure 37. 2CD Shaped Charge inside Explosive Chamber: Test 1-2.

The jet penetrated through 112 mm of aluminum plate. Figure 38 shows that the hole produced by the jet penetration is irregular in top plate, which is indicative of a crooked jet.

Figure 38. Damage to top target plate: Test 1-2.

The penetration velocity was unable to be determined since only the first switch provided a reading.

3. Shaped Charge Test 1-3

Since the hole produced by the jet from Test 1-2 implied a misaligned liner in the plastic vessel, another test was necessary to verify the result. This target assembly was identical to Test 1-2 as shown in Figure 37.

Unexpectedly, the nitromethane mixture failed to detonate. There are several reasons why the detonation might have failed, such as a low concentration of DETA, an air bubble trapped inside the charge during the loading process, exposure of the mixture (it was prepared three hours before this test and could have incurred thermal and photo-induced decomposition), or contamination of the DETA prior to these tests.

4. Shaped Charge Test 1-4

Since Test 1-3 failed, a new batch of mixture was prepared and the percentage of DETA was increased to 0.6%. The charge was encased only in Teflon. The standoff was at a 2 CD standoff from a semi-infinite aluminum target. The jet penetrated 145 mm into the target. The first target plate is shown in Figure 39. The round hole in top plate and entrapped slug are indicative of a straight jet. Time-of-arrival aluminum foil switches did not function.

Figure 39. Entrapped slug: Test 1-4.

5. Shaped Charge Test 1-5

Since Test 1-4 indicated excellent penetration results, we used a new batch of NM/DETA mixture encased in a Teflon charge body, with a trumpet-lined shaped charge at a 3 CD standoff distance from our semi-infinite aluminum target. The jet penetrated 114 mm into the target. The first target plate is shown in Figure 40. The keyhole shape in the top plate is indicative of a crooked jet. In the event of a straight jet, we would have likely achieved much greater penetration. Data from time-of-arrival aluminum foil switches is outlined on Table

6 (this data is likely influenced by the curvature of the jet). Penetration depth as a function of time is shown in Figure 41. The estimated lead portion of jet from the penetration-time data is 3.44 km/s.

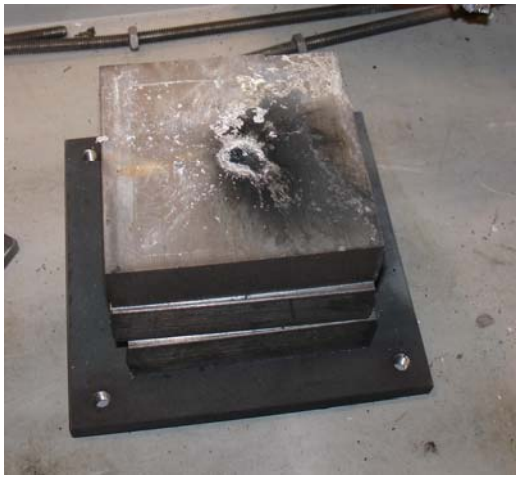

Figure 40. Key-hole in target plate: Test 1-5.

Table 6. Time of Arrival Data of Jet through Aluminum: Test 1-5.

Penetration Depth (mm)	Time (μs)
0	0
3.175	1.262
28.575	9.646
53.975	18.746
79.375	29.852
104.775	61.920

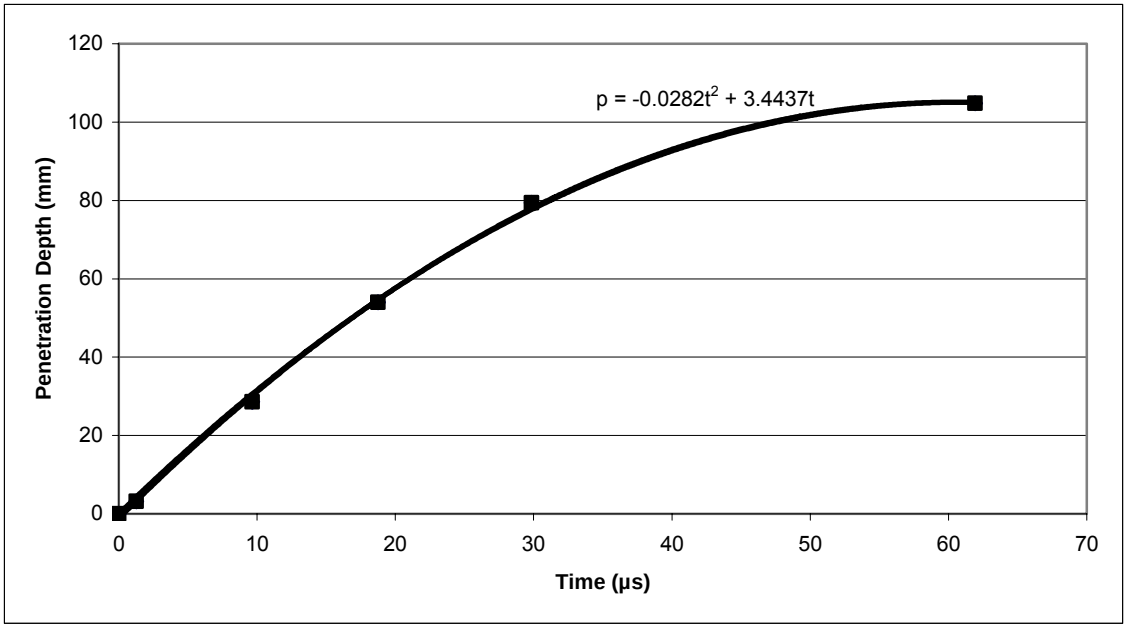

Figure 41. Penetration Depth vs. Time: Test 1-5.

6. Shaped Charge Test 1-6

A charge encased in Teflon/Ultem, of the same dimensions as used in Test 1-1 was tested at 2 CD standoff against semi-infinite aluminum. The DETA concentration was once again prepared at 0.6%. Six aluminum foil switches were placed in the assembly, beginning with the top plate and in between the following plates.

The jet penetrated 131 mm into the target. The first target plate presents a round hole and entrapped slug, indicative of a straight jet, as shown in Figure 42.

Figure 42. Entrapped slug: Test 1-6.

Data obtained from time-of-arrival aluminum foil switches is outlined in Table 7. Penetration velocity was approximated as 2.99 km/s from the linear regression of penetration depth as a function of time as shown in Figure 43. Calculated average jet tip velocity is 4.66 km/s.

Table 7. Time of Arrival Data of Jet through Aluminum: Test 1-6.

Penetration Depth (mm)	Time (μs)
0	0
3.175	0.854
28.575	9.816
53.975	19.686
79.375	30.522
104.775	42.562

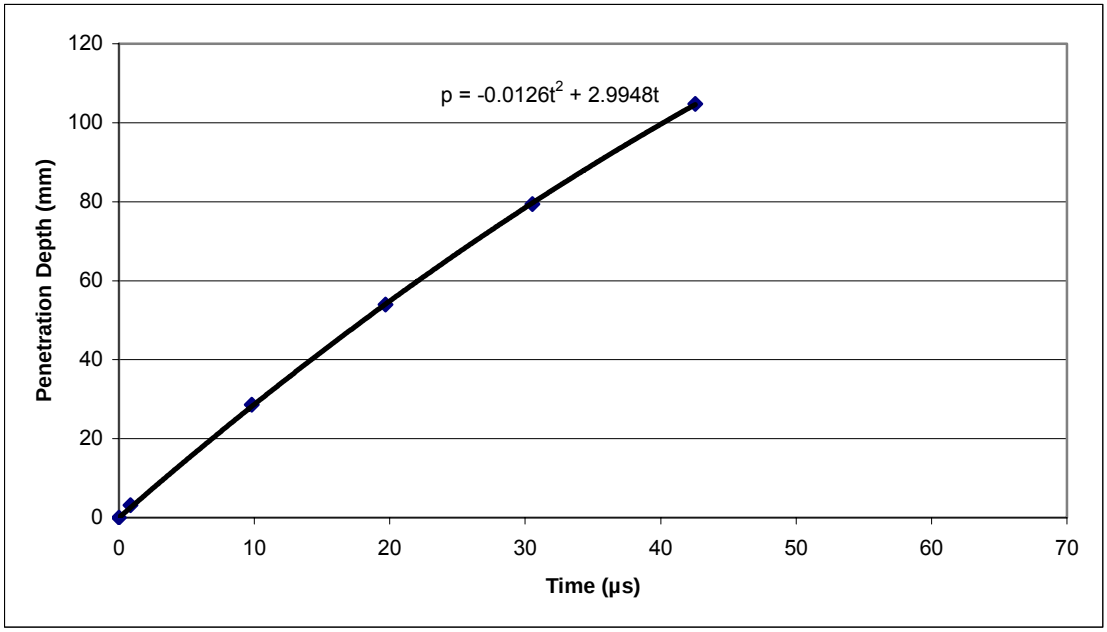

Figure 43. Penetration Depth vs. Time: Test 1-6.

7. Summary of Test Series 1

As stated above, the objective of this test series is to determine the effect of substituting plastic for brass. The following results were observed:

- Figure 44 shows the total penetration depth as function of the standoff distance, comparing the types of confinement. Teflon alone was determined to be superior to a charge with an Ultem addition at 2 CD. The optimum standoff for both types of confinement is 2 CD, with a maximum penetration through semi-infinite aluminum of 145 mm for Teflon only confinement. Using a composite confinement, the maximum penetration is 131 mm (just a 2 mm difference at 3 CD).
- As expected, a brass charge resulted in superior results over Teflon, however the penetration difference at 2 CD standoff was only 7%, as shown in Table 8.

Table 8. Charge confinement comparison for total penetration value in mm.

Standoff (CD)	Brass	Teflon
2	156	145
3	184	129
4	168	-

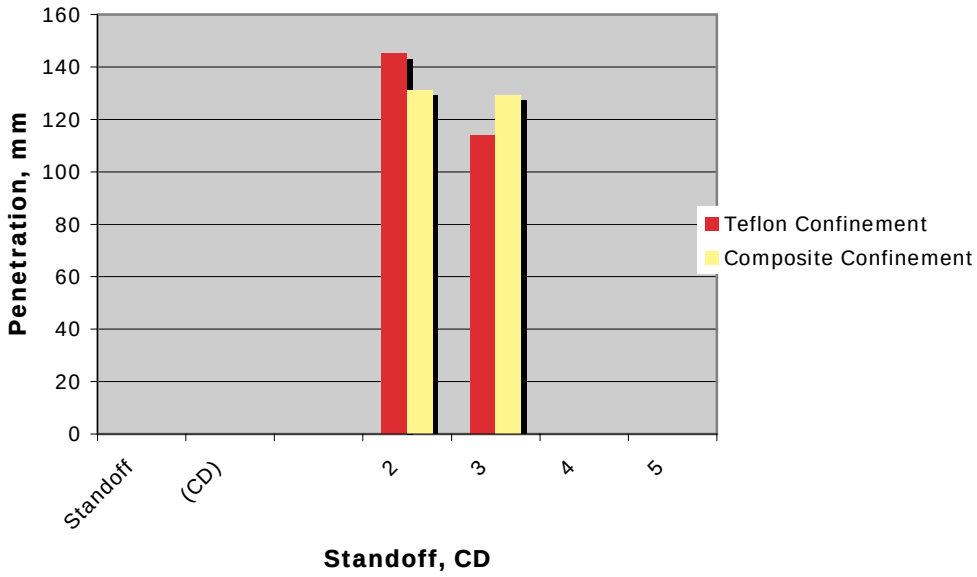

Figure 44. Total penetration for the trumpet lined charge with Teflon and Teflon/Ultem confinement, at 2 CD and 3 CD standoff.

- The penetration velocities at 2 and 3 CD standoff distances are 2.99 km/s and 3.48 km/s, respectively.
- At the onset of detonation, the jet velocities of the shaped charge at 2 CD and 3 CD standoff distances are 4.66 km/s and 4.94 km/s, respectively, compared to 5.6 km/s for the brass encased charge at 2 and 3 CD. This indicates that the jet must be traveling at velocities greater than the estimates, which is consistent with the radiographic results.

D. PENETRATION POTENTIAL EXPERIMENTS (TEST SERIES 2): EVALUATION OF 42 DEGREE COPPER AND BI-MATERIAL LINER PERFORMANCE

The primary objective of this series of tests was to assess the penetration performance of the 42 degree copper and copper/Teflon lined charges. Because of the successes experienced during the testing, Teflon bodies were included in some of the tests. Eleven tests were completed during this session. All sensors, shaped charges, and mixtures were all prepared as in the previous test series.

1. Shaped Charge Test 2-1

The initial test used a brass body shaped charge with a 42 degree copper conical liner and a 2 CD standoff against a target assembly made of one thin aluminum top plate (3.18 mm), six aluminum plates, and one steel plate (thicknesses are 25.4 mm). Six aluminum foil switches were placed in the assembly, beginning with the top plate and in between the following plates.

The jet penetrated through 159 mm of aluminum. Figure 45 shows the damage to the top target plate.

Figure 45. Damage to top target plate: Test 2-1.

Data from time-of-arrival aluminum foil switches is outlined in Table 8. Penetration velocity was approximated at 4.17 km/s from the linear regression of penetration depth as a function of time as shown in Figure 59 (test series 2 summary). Calculated average jet tip velocity is 6.47 km/s.

Table 9. Time of Arrival Data of Jet through Aluminum: Test 2-1.

Penetration Depth (mm)	Time (μs)
0	0
3.175	0.782
28.575	7.124
53.975	14.318
79.375	22.277
104.775	31.687

2. Shaped Charge Test 2-2

Test 2-2 was the lone exception to the conical test series and was a repeat of test 1-5 due to the crooked jet obtained in the initial test (this originally produced a total penetration of only 114 mm). This used a Teflon body shaped charge with trumpet liner and a 3 CD standoff from our semi-infinite aluminum target (as described in test series 1). Six aluminum foil switches were placed in the assembly, beginning with the top plate and in between the following plates.

The jet penetrated through 129 mm of aluminum. Based on the appearance of the target in Test 1-5, which indicated a crooked jet, the result of this test is used as a basis of comparison. Data from time-of-arrival aluminum foil switches is outlined in Table 10. Penetration depth as a function of time is shown in Figure 46. The estimated average velocity of the leading portion of jet penetrating through the first 3.175mm layer of target in this test is 5.13 km/sec.

Table 10. Time of Arrival Data of Jet from the trumpet lined charge encased in a Teflon body through aluminum at 3 CD standoff: Test 2-2.

Penetration Depth (mm)	Time (µs)
0	0
3.175	1.306
28.575	9.534
53.975	19.085
79.375	29.942
104.775	47.697

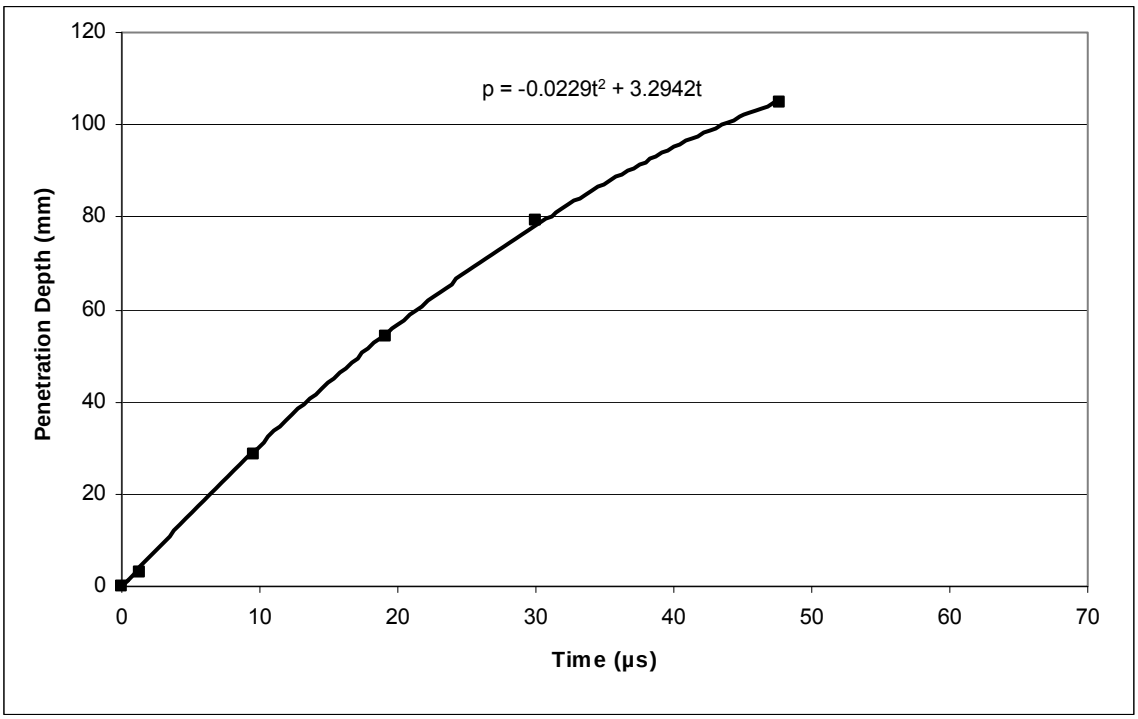

Figure 46. Penetration Depth vs. Time: Test 2-2.

3. Shaped Charge Test 2-3

Test 2-3 used a brass encased shaped charge with a 42 degree copper conical liner and a 3 CD standoff against a target assembly equal to that used in

test 2-1. Six aluminum foil switches were placed in the assembly, beginning with the top plate and in between the following plates.

The jet penetrated 161 mm of aluminum. Figure 47 shows the damage to the top target plate, which is quite larger in diameter than holes resulting from the impact of jets from the trumpet-lined charge.

Figure 47. Damage to top target plate: Test 2-3.

Data from time-of-arrival aluminum foil switches is outlined on Table 11 (sensor #3 did not register). Penetration velocity was approximated as 4.19 km/s from the linear regression of penetration depth as a function of time as shown in Figure 59 (test series 2 summary). Calculated average jet tip velocity is 6.50 km/s.

Table 11. Time of Arrival Data of Jet through Aluminum: Test 2-3.

Penetration Depth (mm)	Time (μs)
0	0
3.175	0.616
28.575	7.236
79.375	22.139
104.775	31.707

4. Shaped Charge Test 2-4

The fourth test repeated test 2-1 with the target assembly entirely composed of aluminum plates (180.98 mm total). As aluminum is preferred due to its lower density, increased measurement sensitivity is evident due to the depth of the holes produced. Six aluminum foil switches were placed in the assembly, beginning with the top plate and in between the following plates.

The jet penetrated through 166 mm of aluminum. Figure 48 shows the damage to the top target plate.

Figure 48. Damage to top target plate: Test 2-4.

Data from time-of-arrival aluminum foil switches is outlined in Table 12 (the first two sensors did not register). Penetration velocity was approximated at 4.12 km/s from the linear regression of penetration depth as a function of time as shown in Figure 58 (test series 2 summary). Calculated average jet tip velocity is 6.38 km/s.

Table 12. Time of Arrival Data of Jet through Aluminum: Test 2-4.

Penetration Depth (mm)	Time (μs)
0	0
53.975	14.428
79.375	22.526
104.775	31.975

5. Shaped Charge Test 2-5

The conditions of Test 2-3 were repeated in this test. Six aluminum foil switches were placed in the assembly, beginning with the top plate and in between the following plates.

The jet penetrated through 171 mm of aluminum; slightly greater than the 161mm achieved in Test 2-3. Figure 49 shows the damage to the top two target plates.

Figure 49. Jet penetration through first and second target plates: Test 2-5.

Data from time-of-arrival aluminum foil switches is outlined in Table 13 (the first two sensors did not register). Penetration velocity was approximated at 4.10 km/s from the linear regression of penetration depth as a function of time as shown in Figure 59 (test series 2 summary). Calculated average jet tip velocity is 6.36 km/s, which is slightly lower than the result from Test 2-3 of 6.50 km/s.

Table 13. Time of Arrival Data of Jet through Aluminum: Test 2-5.

Penetration Depth (mm)	Time (μs)
0	0
3.175	0.546
28.575	7.454
53.975	14.297
79.375	22.428
104.775	31.674

6. Shaped Charge Test 2-6

The sixth test marked the first use of the 42 degree bi-material (copper/Teflon) conical liner with a brass body shaped charge and a 3 CD standoff against an aluminum target assembly. Six aluminum foil switches were placed in the assembly, starting with the top plate and in between the following plates.

The jet penetrated through 172 mm of aluminum. Figure 50 shows the damage to the top and bottom target plate. This charge penetrated into aluminum to practically the same depth as the all-copper lined charge (see results from Tests 2-3 and 2-5). The hole in this target was also found to be very similar in size to those from the jet from the all copper lined charge fired in Test 2-3 and 2-5.

Figure 50. Jet penetration through first and last target plates: Test 2-6.

Data from time-of-arrival aluminum foil switches is outlined in Table 14. Penetration velocity was approximated at 3.99 km/s from the linear regression of penetration depth as a function of time as shown in Figure 59 (test series 2 summary). The calculated average jet tip velocity is 6.20 km/s.

Table 14. Time of Arrival Data of Jet through Aluminum: Test 2-6.

Penetration Depth (mm)	Time (μs)
0	0
3.175	0.588
28.575	7.56
53.975	14.611
79.375	22.411
104.775	31.417

7. Shaped Charge Test 2-7

Test 2-7 included a brass body shaped charge with a 42 degree copper conical liner and a 4 CD standoff against a target assembly made of two thin aluminum top plates (3.18 mm each), plus five steel plates (thickness 25.4 mm

each). Six aluminum foil switches were placed in the assembly, starting with the top plate and between the following plates.

In order to calculate the total penetration, the steel plates were converted to aluminum thickness through density calculation. Thus, the jet penetrated through the equivalent of 201.5 mm of aluminum. Figure 51 shows the damage to the top two target plates.

Figure 51. Jet penetration through first and second target plates: Test 2-7.

Data from time-of-arrival aluminum foil switches is outlined on Table 15. Penetration velocity was approximated as 4.20 km/s from the linear regression of penetration depth as a function of time. Calculated average jet tip velocity is 6.50 km/s.

Table 15. Time of Arrival Data of Jet through Aluminum: Test 2-7.

Penetration Depth (mm)	Time (μs)
0	0
3.175	0.868
6.350	1.354
54.206	9.751
97.571	20.202
140.936	39.107

8. Shaped Charge Test 2-8

Displayed in Figure 52 is the setup for test 2-8, where a Teflon shaped charge body was configured with a 42 degree bi-material copper/Teflon conical liner and a 3 CD standoff against a target assembly made of one thin aluminum top plate (3.18 mm), plus seven additional aluminum plates (thickness 25.4 mm each). Six aluminum foil switches were placed in the assembly, beginning with the top plate and in between the following plates.

The jet penetrated through 127 mm of aluminum. Figure 53 shows the damage to the top target plate.

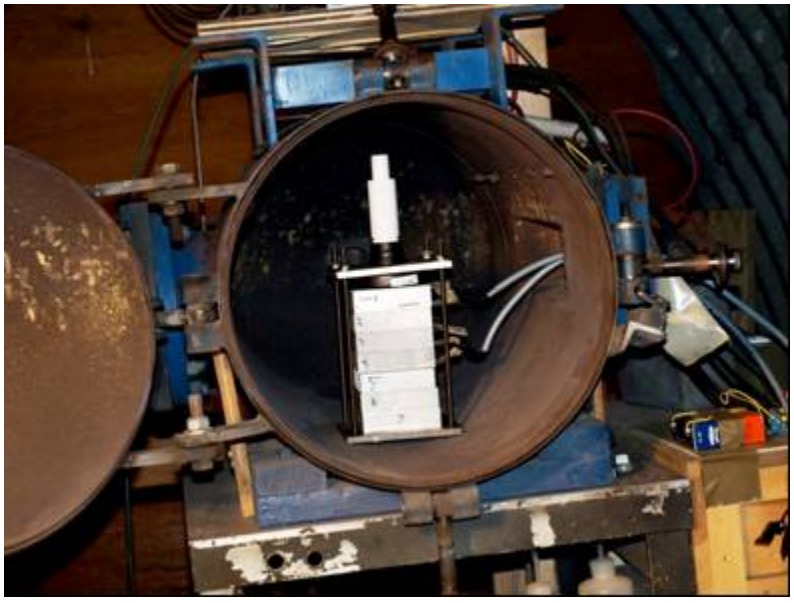

Figure 52. 3CD Teflon encased Shaped Charge inside Explosive Chamber: Test 2-8

Figure 53. Damage to top target plate: Test 2-8

Data from time-of-arrival aluminum foil switches is outlined in Table 16. Penetration velocity was approximated at 3.27 km/s from the linear regression of penetration depth as a function of time as shown of Figure 59 (test series 2 summary). Calculated average jet tip velocity is 5.07 km/s.

Table 16. Time of Arrival Data of Jet through Aluminum: Test 2-8

Penetration Depth (mm)	Time (µs)
0	0
3.175	1.15
28.575	9.208
53.975	18.419
79.375	29.005
104.775	42.077

9. Shaped Charge Test 2-9

Test 2-9 included a Teflon body shaped charge with a 42 degree bi-material copper/Teflon conical liner and a 2 CD standoff against the same target type as in the previous test. The jet penetrated through 67 mm of aluminum. Figure 54 shows the damage to the top target plate. The keyhole shape in the top plate is consistent with that of a crooked jet, indicating that the total penetration could have been much greater. As a result, only two sensors were activated.

Figure 54. Damage to top target plate: Test 2-9

Data from time-of-arrival aluminum foil switches is outlined in Table 17. Penetration velocity was approximated as 1.25 km/s from the linear regression of penetration depth as a function of time as shown in Figure 58 (test series 2 summary). Calculated average jet tip velocity is 1.94 km/s.

The results from this test are excluded in the final analysis of this work because the jet was not well formed and not straight, based on the appearance of the hole, and the unusually smaller amount of penetration and slower penetration velocities

Table 17. Time of Arrival Data of Jet through Aluminum: Test 2-9

Penetration Depth (mm)	Time (μs)
0	0
3.175	1.404
53.975	43.130

10. Shaped Charge Test 2-10

The tenth test in this series employed a brass body shaped charge with a 42 degree copper conical liner and a 5 CD standoff against a target assembly composed of a thin aluminum top plate (3.18 mm), plus four thick steel plates (25.4 mm each) and four 6.35 mm steel plates (with two bottom brackets installed to ensure protection of the chamber) as shown in Figure 55. Six aluminum foil switches were placed in the assembly, starting with the top plate and in between the following plates.

Figure 55. Target assembly after the shot: Test 2-10.

In order to calculate the total penetration, the steel plates were converted to aluminum thickness through density calculation. Thus, the jet penetrated through the equivalent of 198.3 mm of aluminum. Data from time-of-arrival aluminum foil switches is outlined on Table 18. Penetration velocity was approximated at 4.10 km/s from the linear regression of penetration depth as a function of time. Calculated average jet tip velocity is 6.36 km/s.

Table 18. Time of Arrival Data of Jet through Aluminum: Test 2-10.

Penetration Depth (mm)	Time (μs)
0	0
3.175	0.586
48.786	9.002
92.151	19.038
135.516	32.223
178.881	50.885

11. Shaped Charge Test 2-11

Test 2-11 was set up to evaluate the amount of penetration that could be obtained from the detonation of nitromethane in a shaped Teflon body. This would be representative of a stored and fielded device prior to metal liner insertion and should represent the degree of directed line-of-sight hazard.

This charge consisted of a Teflon body shaped charge at 2 CD with a 42 degree conical liner consisting solely of Teflon. The target assembly was constructed of only aluminum plates as shown in Figure 56, with no switches installed.

Figure 56. 2CD Teflon Shaped Charge with Teflon Liner: Test 2-11.

The jet penetrated through 22 mm of aluminum. Figure 57 shows the damage to the top target plate.

Figure 57. Damage to top target plate: Test 2-11.

12. Summary of Test Series 2

- Figure 58 shows penetration depth as a function of time for all tests at a 2 CD standoff. The result from Test 2-9 is probably not an accurate gauge of performance potential for the reasons stated above.

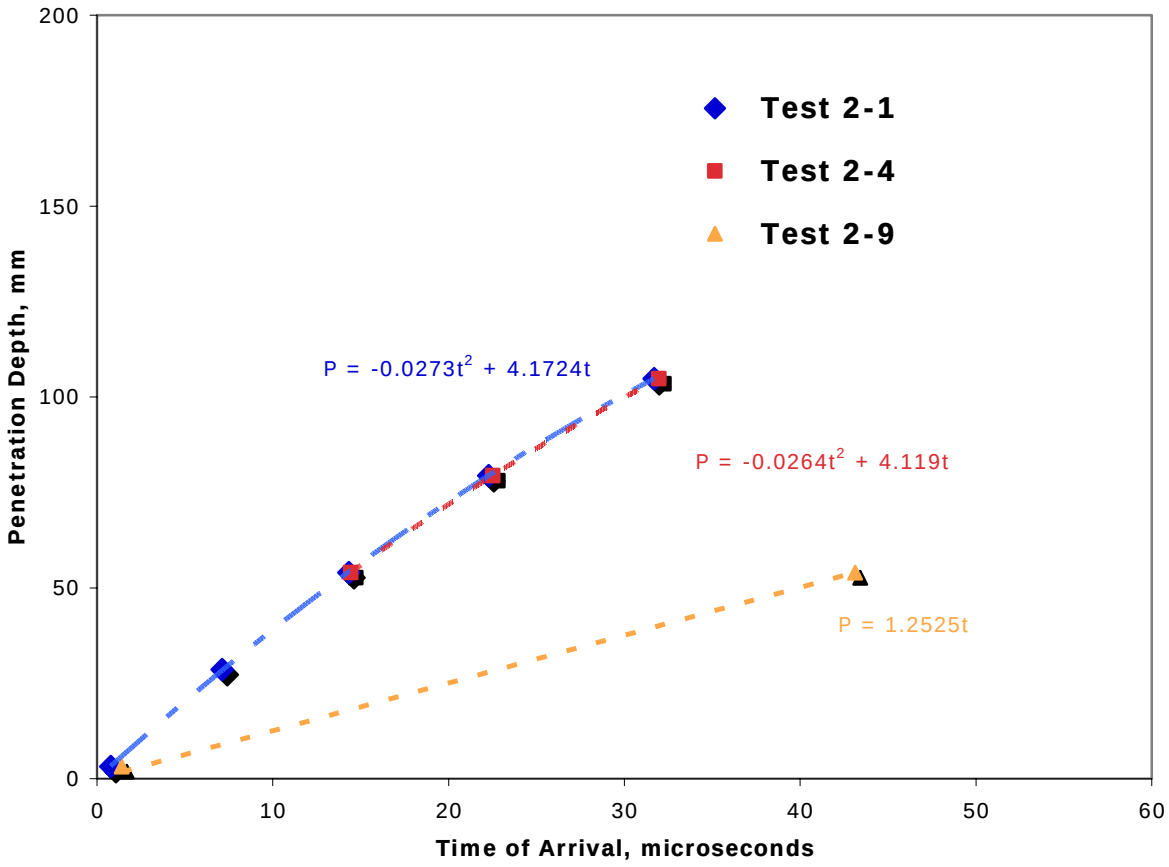

Figure 58. Penetration Depth vs. Time for Charges with 42 Degree Liner: Test Series 2 at 2CD Standoff.

- Figure 59 shows penetration depth as a function of time for all tests at 3CD Standoff.

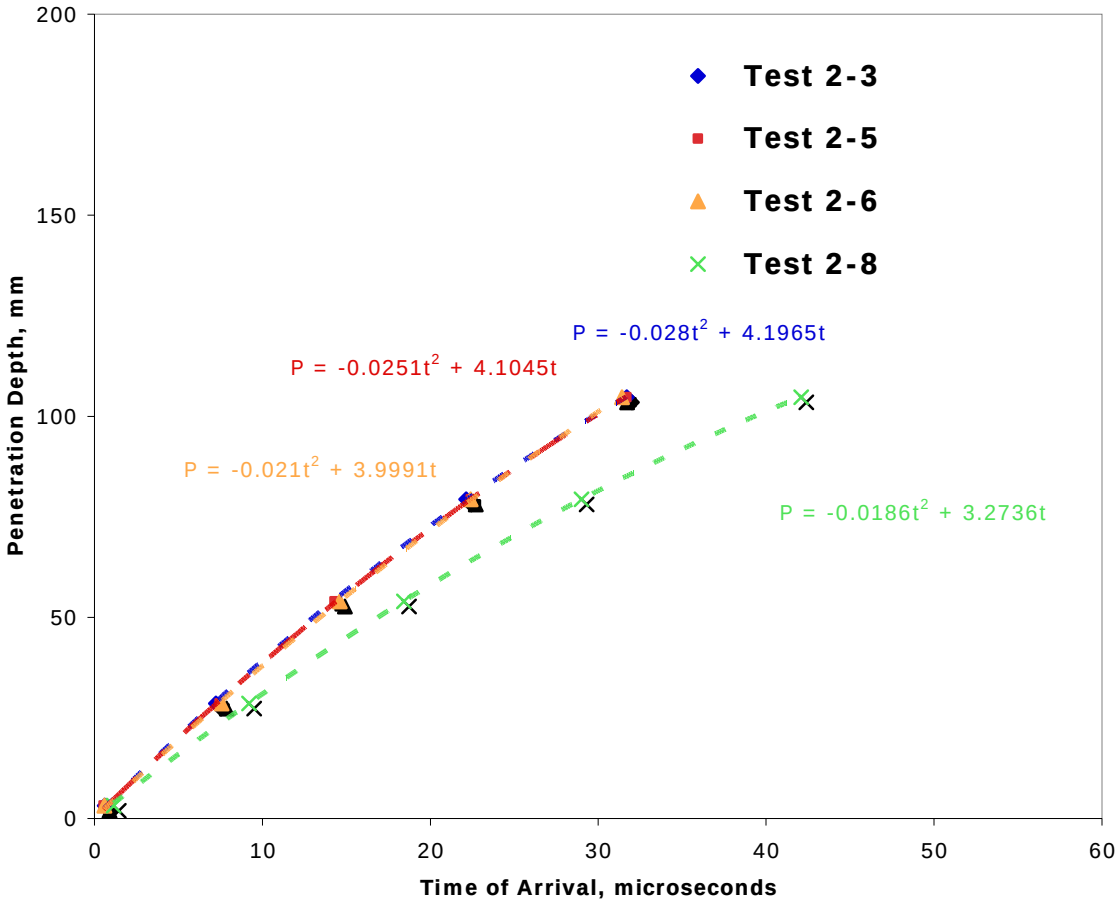

Figure 59. Penetration Depth vs. Time for Charges with 42 Degree Liner: Test Series 2 at 3CD Standoff.

- Table 19 shows total penetration depth for brass and Teflon shaped charges with 42 degree copper and bi-material liners. The optimum standoff distance for brass body shaped charges with 42 degree copper liners is 4 CD, with a maximum penetration through semi-infinite aluminum of 201.5 mm.

SO (CD)	Type SC	Penetration Depth (mm) Aluminum	Penetration Depth (mm) Steel	Penetration Depth (mm) Soil
2	BB 42 Cu	159	93	185
2	BB 42 Cu	166	97	192
2	TB 42 Tf	22	13	26
3	BB 42 Cu	161	94	187
3	BB 42 Cu	171	100	198
3	BB 42 Cu/Tf	172	100	199
3	TB 42 Cu/Tf	127	74	147
4	BB 42 Cu	202	118	234
5	BB 42 Cu	198	116	230

Table 19. Total Penetration Depth at various standoffs distances: Test Series 2

- Table 20 shows calculated average jet tip velocities for brass and Teflon shaped charges with 42 degree copper and bi-material liners.

Table 20. Average Jet Velocity at various standoff distances: Test Series 2.

SO (CD)	Type SC	Average Jet Velocity (km/s)
2	BB 42 Cu	6.45
3	BB 42 Cu	6.45
3	BB 42 Cu/Tf	6.20
3	TB 42 Cu/Tf	5.10
4	BB 42 Cu	6.50
5	BB 42 Cu	6.40

V. DISCUSSION OF RESULTS

A. BASELINE SHAPED CHARGE

1. Jet Characterization of the Brass Encased Trumpet-Shaped Charge

The jet from the baseline trumpet shaped nitromethane charge has been completely characterized, based on analyses of flash radiography performed by the Ernst Mach Institute. The tip velocity of jets from the brass encased charge is between 6.0 and 6.3 km/s. The total mass of the jet between the tip and 3.0 km/s is 950 mg.

Initial velocity-mass predictions by Dusetzina and from computations during this research were not able to accurately resolve the rather small amount of mass in the tip region of the jet, where there was found from the radiography approximately 50 milligrams of mass. A computation performed with the assistance of Cao at 25 cells/mm did yield velocities close to the experimental values; thus it is concluded that grid fineness at least at this level will be required for subsequent design studies.

Lower limits of jet tip velocity are also obtained from penetration time of arrival data. That is, the leading edge of the jet, which includes the tip and preceding jet (at slightly slower velocity) contributes to initial jet entry. In this case the velocity of the average portion of jet from the brass encased copper-lined trumpet nitromethane charge is between 5.78 and 5.60 km/s based on tests at 2 and 3CD, respectively. These estimates are, on average, 15 percent less than the observed tip velocity.

2. Effect of Teflon Body Substitution

The replacement of the brass casing with Teflon results in a decrease in overall penetration rates and total penetration, as would be expected based on

differences in strength and density between the two. The penetration decreases with greater target standoff, as shown in Figures 58-59, and Table 21. The rates of penetration at initial jet entry into aluminum appear to be similar irrespective of confinement, however. The average initial rates estimated from the charge encased in brass (from Dusetzina results) and those from this study are summarized in Table 22. The average penetration rate at target entry and the estimated velocity of the jet absorbed during initial entry is 3.65 km/s and 3.48 km/s, respectively from the brass and Teflon encased charges.

The decrease in penetration rate of the jet from the Teflon encased charge falls off at a faster rate. As a result the total penetration by the Teflon encased charge is less in all cases studied. The decrease, however, appears to be the least at short standoff. As shown in the table below, the decrease at 2CD standoff is only 7 percent.

Table 21. Effect of confinement on penetration performance for the trumpet shaped charges.

SO (CD)	**Penetration (mm)**	
	Brass	**Teflon**
2	156	145
3	184	129

Table 22. Effect of confinement on jet entry velocities for the trumpet shaped charges.

SO (CD)	Jet Entry Velocity (km/s)	
	Brass	Teflon
2	5.60	4.66
3	5.60	4.94

It was found from the experiments that the addition of Ultem does not improve penetration.

3. Assessment of the 42 Degree Charge

Based on rates of penetration between the baseline trumpet and the 42 degree shaped charge, it appears that the jet from the 42 degree charge is approximately 15 percent faster than that from the trumpet, as shown by the data summarized in Table 23.

These jet entry velocities are estimated, as before, on the initial penetration rate and hydrodynamic theory (see Table 24). These results are qualitatively consistent with Dusetzina's original predictions. If we assume that zoning used in their computational prediction contains the same degree of error than the actual jet tip should be close to 7 km/s.

Table 23. Jet Entry Velocity comparison for Brass Encased Shaped Charges (km/s).

SO (CD)	Trumpet Liner	42 Degree Liner
2	5.6	6.45
3	5.6	6.45
4	5.8	6.50
5	---	6.40

Table 24. Penetration and Average Jet Entry Velocities at various standoff distances for the 42 Degree Lined Charge.

SO (CD)	Penetration Velocity (km/s)	Average Jet Entry Velocity (km/s)
2	4.17	6.45
3	4.20	6.45
4	4.20	6.50
5	4.10	6.40

It is interesting to note that the initial penetration velocity of the jet from the bi-material 80/20 copper/Teflon lined 42 degree charge is close to those from the all-copper liners (3.99 km/s versus an average of 4.17 km/s for the latter). This indicates that this bi-material design approach satisfactorily prevented the intrusion of Teflon in the effective portion of the jet.

The increased total penetration capability of the 42 degree charge relative to the baseline trumpet is consistent with code prediction. While the 184mm penetration of the trumpet charge peaks at 3CD, the penetration of the 42 degree charge peaks in the vicinity of 4-5 CD; the penetration at 4 CD is 202mm. The

magnitude of difference and the location of the peak indicate that is consistent with faster and more robust jetting. Penetration data is summarized in Table 25.

Table 25. Improvement in Penetration achieved with the 42 Degree Liner (in mm).

SO (CD)	Trumpet Liner	42 Degree Liner	% Difference
2	156	166	+6 %
3	184	171	-7 %
4	168	202	+20 %
5	114	198	+74 %

The fact that the jets from the copper and copper/Teflon 42 degree charges were found to have the same penetration capability validates the design approach and more importantly points to another aspect of concept feasibility. Additional work will be required to properly evaluate the capability of the Teflon encased bi-material lined charge: The penetration capability of this charge at 2 CD should be much greater than that found at 3 CD (i.e., 127mm).

B. RELIABILITY DATA

As of the time of the work of Dusetzina and Dusetzina [1], successful detonation had been observed in 36 out of 39 experiments for a 92 percent reliability rate. In this research, high order detonation was observed in 16 out of 17 tests, improving the reliability for this sample to 93 percent.

The single detonation failure experienced in the course of this research (Experiment 1-3) may have been caused by one or more factors. Though Serrano and Rigby [2 and 3] concluded that 0.1 percent DETA is required for

reliable high order detonation, the solution was increased to 0.6 percent for the remainder of the tests in this research. High order detonation was observed in each of the remaining 14 experiments. It can be inferred that slightly increasing the DETA concentration in the NM mixture may raise the overall reliability of detonation, but further examination is required to validate this idea.

C. HAZARD REDUCTION

It has been proven that the bi-material 42 degree liner has been successfully employed with virtually the same results as a similar liner consisting of only copper. Using a plastic casing coupled with the bi-material liner maximizes the safety in storage, transport, and delivery of the charge. Employing the copper portion of the bi-material liner just prior to detonation further enhances safety factors; in the unlikely event of detonation, it has been shown that the plastic portion of the liner will penetrate only 22 mm of Aluminum 6061.

VI. CONCLUSION

Key questions pertaining to possible engineering issues were treated in this research. The concept is primarily based on the use of nitromethane because (i) it presents limited hazard to unintended use (ii) it is relatively inexpensive, and (iii) the energy required to load it is cost-effective, and other attributes that might affect performance are equally as important, specifically the use of lightweight inert plastic confinement and the inclusion of the same plastic in the liner. The results of work conducted show that the inclusion of an all plastic shaped vessel is possible with minimal detriment to performance potential.

This research builds upon the established results of Dusetzina and Dusetzina and has greatly improved upon the baseline nitromethane shaped charge. Computational simulations correlated with experimental results and hydrodynamic theory. Improvements made upon existing designs were accurately assessed in several key areas. Not only has performance been increased using both a copper and bi-material 42 degree liner, but a Teflon-encased charge has been proven as a feasible alternative with excellent results.

Of the two basic shaped charge variations tested, the 42 degree charge represents a significant performance increase. The jet from this charge has been proven to contain more kinetic energy than the baseline trumpet, contributing to a maximum penetration 10% higher than that of its trumpet-lined counterpart. Using a simulation technique to estimate the partitioning of a bi-material copper/Teflon 42 degree liner, it has been determined that a liner mass composed of 80 percent copper and 20 percent Teflon is capable of achieving equal penetration results when compared to that of a 42 degree liner constructed of copper. Experimentally, the maximum aluminum penetration achieved with a copper 42 degree liner was 201.5 mm at a 4 CD standoff. Based on the kinetic

energy and perforation size produced by the 42 degree jet, this shaped charge design should have substantial impact initiation potential.

The Teflon charge body substitution represents a significant reduction in the total weight of the charge, increasing its versatility in transport and automated delivery. Additionally, the enhanced safety provided by a plastic inert nitromethane confinement further improved the value of Teflon as an alternative charge body material. Experimentally, the performance of charges with a Teflon body proved its feasibility; the jet penetration results at 2 CD were only 7 percent less than the established brass penetration data obtained by previous research.

In conclusion, introductions of both the 42 degree conical liner and the Teflon charge body have proven to be significant improvements in nitromethane shaped charge design, increasing its effectiveness in explosive ordnance disposal.

VII. RECOMMENDATIONS

The conception of nitromethane based shaped charges employing various configurations of a completely plastic charge body construction and a 42 degree copper and bi-material liner has been proven to be extremely feasible through computational and experimental studies. Due to time constraints, this research was not able to fully explore the potential of these different shaped charge configurations. A summary of recommendations for the continuation of this research follows:

- Assessments should be made in order to evaluate the neutralization potential of the new liner design, including the 42 degree copper liner and the 42 degree bi-material liner.
- The design of alternative liners should be explored. The optimal liner configuration must be determined for shaped charges used in various capacities, including those intending to initiate detonation or deflagration of explosive ordnance.
- Continuing research should be devoted to automated remote delivery of this shaped charge technology. Work within the department has resulted in marked progress in the development of a robotic arm capable of delivering a lightweight charge.
- For remote delivery of shaped charges, a practical encapsulated shaped charge design should be devised. In addition, an automated DETA addition mechanism must be installed in order to facilitate the NM/DETA mixture immediately prior to detonation.

THIS PAGE INTENTIONALLY LEFT BLANK

LIST OF REFERENCES

[1]. E. Dusetzina and G. Dusetzina., “Development of an Effective Low-Cost Safe Explosive Ordnance Destruct Tool,” M.S. Thesis, Naval Postgraduate School, Monterey, California, 2007.

[2]. G. Serrano., “Potential Utility of Nitromethane for Explosive Ordnance Disposal,” M.S. Thesis, Naval Postgraduate School, Monterey, California, 2005.

[3]. J. P. Rigby., “Potential Utility of Nitromethane for Explosive Ordnance Disposal,” M.S. Thesis, Naval Postgraduate School, Monterey, California, 2006.

[4] D. Fisher, E. Baker, I. Wu, A. Richwald and G. Miller., “The Design and Development of a Robotically Emplaced Hand Packed Shaped Charge.”

[5] M.E. Majerus and R.E. Brown., “Shaped Charge Device with Progressive Inward Collapsing Jet,” U.S. Patent 5,614,612, Mar. 1997.

[6]. C.J. Anderson, M.E. Pinco, and S.B. Murray, “Sensitivity Study of Nitroparaffin-Based Blends,” in *Tenth International Symposium on Detonation*, 1993, p. 294.

[7]. W.P. Walters and J.A. Zukas, *Fundamentals of Shaped Charges*, Baltimore: CMC Press, 1989.

[8]. W.P. Walters and J.A. Zukas, *Explosive Effect and Applications*, New York: Springer, 1998.

[9]. G. Birkhoff, D.P. MacDougall, E.M. Pugh, and G. Taylor, “Explosive with Lined Cavities,” *Journal of Applied Physics*, vol 19, pp. 563-582, September 1948.

[10]. R.E. Brown (private communication), 2007.

[11]. TELEDYNE RISI, INC., November 2007. http://www.teledynerisi.com/.

[12]. Century Dynamics, Inc., *AUTODYN ™ Theory Manual Version 6.0*, Century Dynamics, Inc. 2006.

[13]. Century Dynamics, Inc., *Euler Shaped Charge Calculations: AUTODYN ™ Technical Note*, Century Dynamics, Inc., 2006.

[14]. M.H. Kulawiak, “Strong Detonation Effects on Shaped Charge Jetting,” M.S. Thesis, Naval Postgraduate School, Monterey, California, 2006.

[15]. Sigma Aldrich, Nitromethane: Material Safety Data Sheet No.75-52-5, Sigma-Aldrich Corp., St. Louis, MO, USA.

[16]. LCDR Hung Cao (private communication), November 2007.

[17]. Commercial Solvents Corporation, *Storage and Handling of NITROMETHANE*, NP Series, TDS No. 2, 1961.

[18]. McMASTER-CARR, November 2007, http://www.mcmaster.com.

[19]. M.C. Chick, I.B. McIntyre, and R.B. Frey, “The Jet Initiation of Solid Explosives,” in *Eight International Symposium on Detonation*, 1985, pp. 318-329.

[20]. P.W. Cooper, *Explosives Engineering*. New York: Wiley-VCH, 1996.

[21]. *Ultem 1000 Technical Property Data*, November 2007, http://www.k-mac-plastics.net.

APPENDIX A. HAZARD SUMMARIES OF CHEMICALS

A. HAZARD SUMMARY FOR NM

- May cause skin irritation and harmful if absorbed through skin.
- May cause eye irritation.
- May be irritating to mucous membranes and upper respiratory tract and may be harmful if inhaled.
- Harmful if swallowed.
- Handle as a CARCINOGEN with extreme caution.
- NM is a HIGHLY FLAMMABLE and REACTIVE chemical and a DANGEROUS FIRE and EXPLOSION HAZARD.

B. HAZARD SUMMARY FOR DETA

- DETA is a CORROSIVE CHEMICAL and contact can severely irritate and burn the skin and eyes with possible eye damage.
- Harmful if inhaled and extremely destructive to tissue of mucous membranes and upper respiratory tract. Inhalation may result in spasm.
- Harmful if swallowed.
- May cause allergic respiratory and skin reactions.
- Symptoms of exposure include burning sensation, wheezing, shortness of breath, headache, nausea, and vomiting.

Summary of hazards obtained from Sigma Aldrich Material Safety Data Sheets (MSDS). From [15].

THIS PAGE INTENTIONALLY LEFT BLANK

APPENDIX B. RECOMMENDATIONS FOR STORAGE, HANDLING AND USE OF NITROMETHANE

- Store in original drums as received in a cool place away from hazardous conditions or transfer to an underground or barricaded storage tank.

- Protect storage and processing vessels from high-energy objects by a suitable barricade.

- Ordinary steel, aluminum, or stainless steel are satisfactory materials of construction. Formulations employing NM should not be exposed to brass, bronze, or copper unless tests have shown them to be inert. Lead, such as terne plate, is not satisfactory with NM.

- NM is combustible. Its fires can be extinguished with CO_2 or water.

- Do not expose NM to dry caustic.

- Do not sell empty NM drums to reconditioners unless they have first been well rinsed with water.

- Do not allow solutions of NM and bases to become dry.

- Certain mixtures of NM and amines are sensitive to a No. 8 cap, so if such mixtures are required in a process, they should be diluted with an inert material or should be protected from severe shock.

- Some ternary mixtures of NM, amines, and heavy metal oxides can be very hazardous.

- Like other organic compounds, NM may form a sensitive explosive mixture with strong oxidizing agents such as nitrogen tetroxide.

- Liquid NM should not be processed or handled in high pressure equipment which would permit elevated pressures and temperatures.

- NM should be protected from all possible sources of adiabatic compression.

- Detonation traps should be installed at each end of lines of ½ - inch diameter or more from storage processing.

Recommendations obtained from Reference. From [17].

THIS PAGE INTENTIONALLY LEFT BLANK

APPENDIX C. SHAPED CHARGE TRUMPET LINER

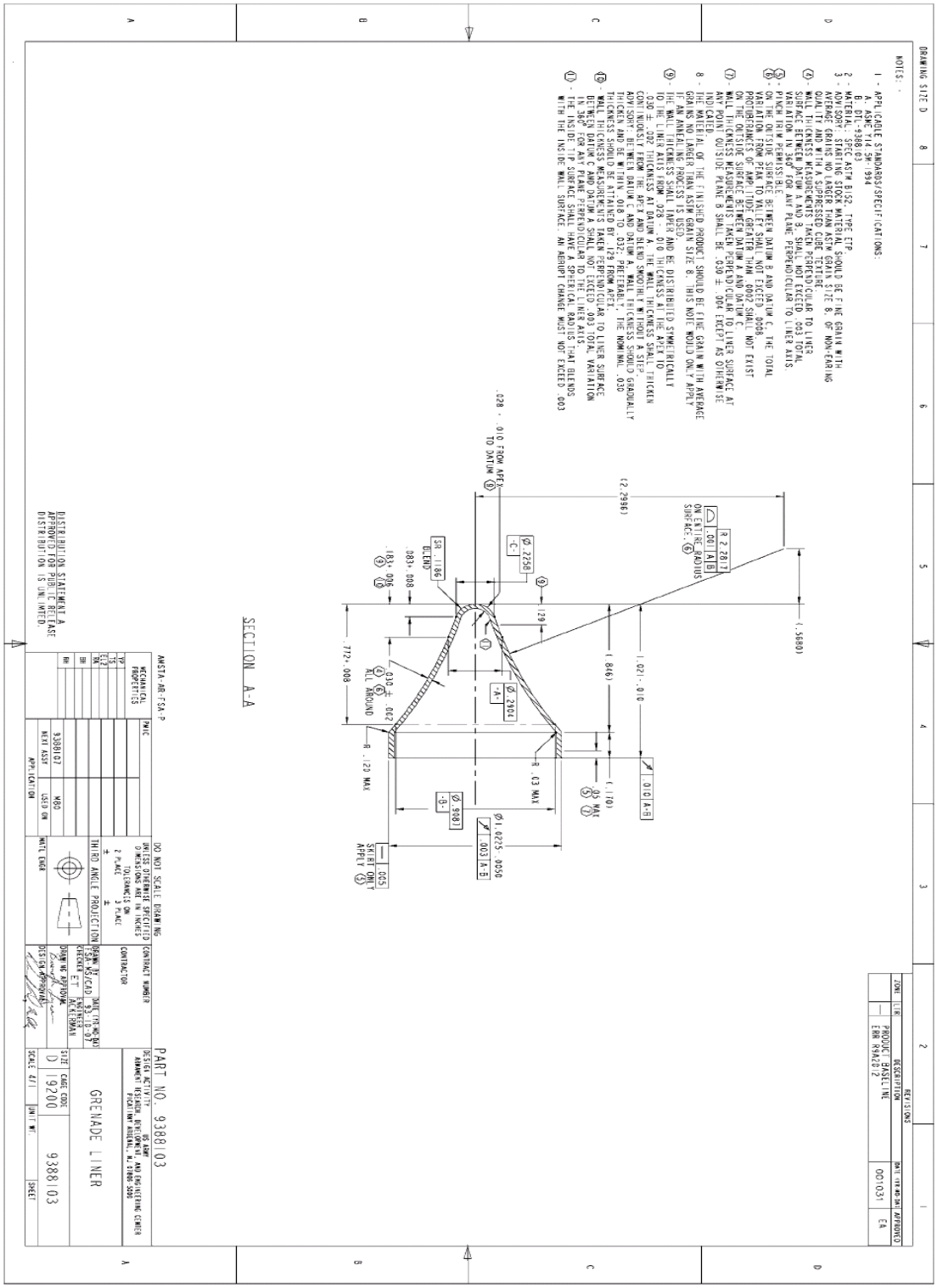

THIS PAGE INTENTIONALLY LEFT BLANK

APPENDIX D: SHAPED CHARGE 42 DEGREE LINER

A. 42 DEGREE LINER OF HC COPPER

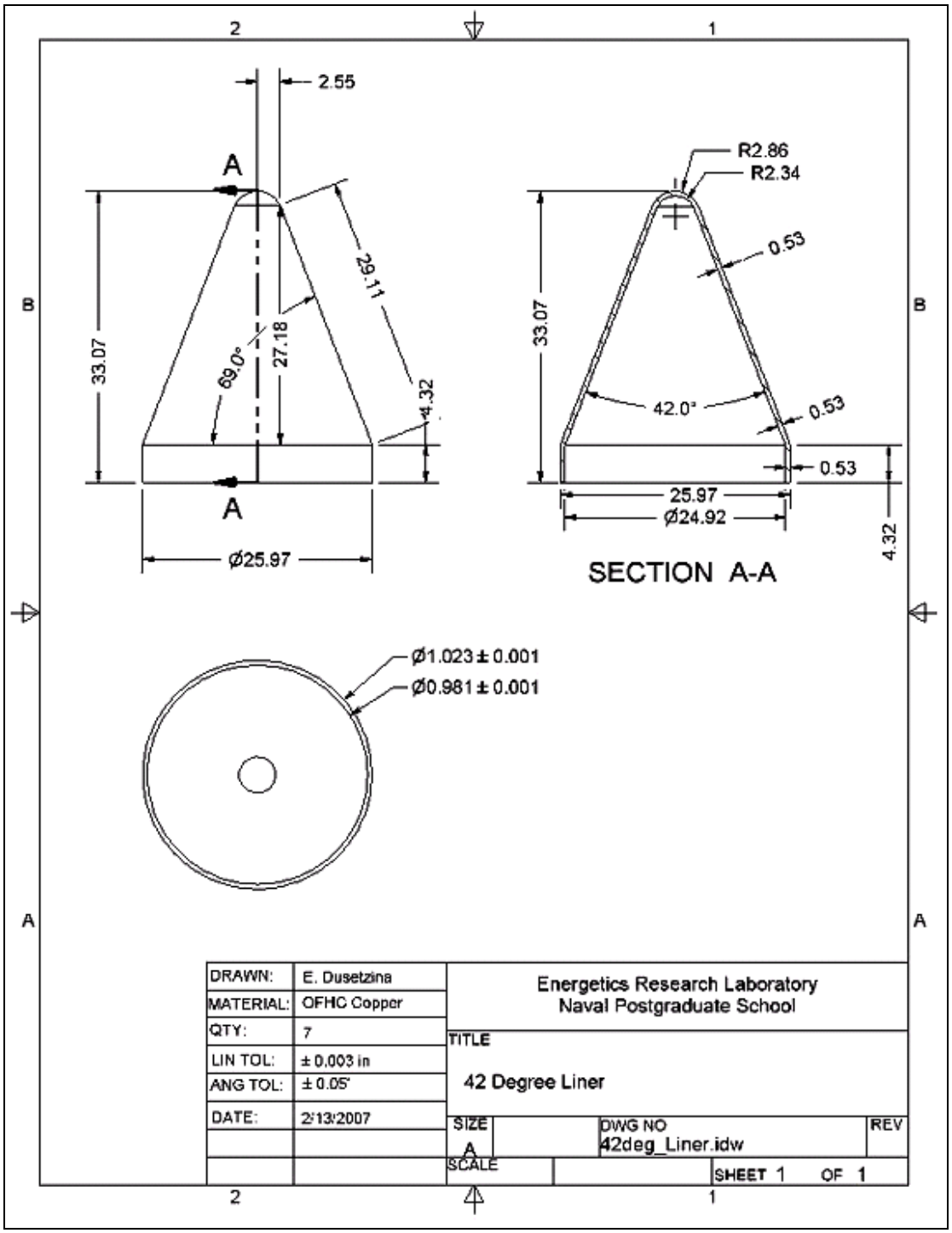

B. 42 DEGREE LINER COMPOSITE COPPER

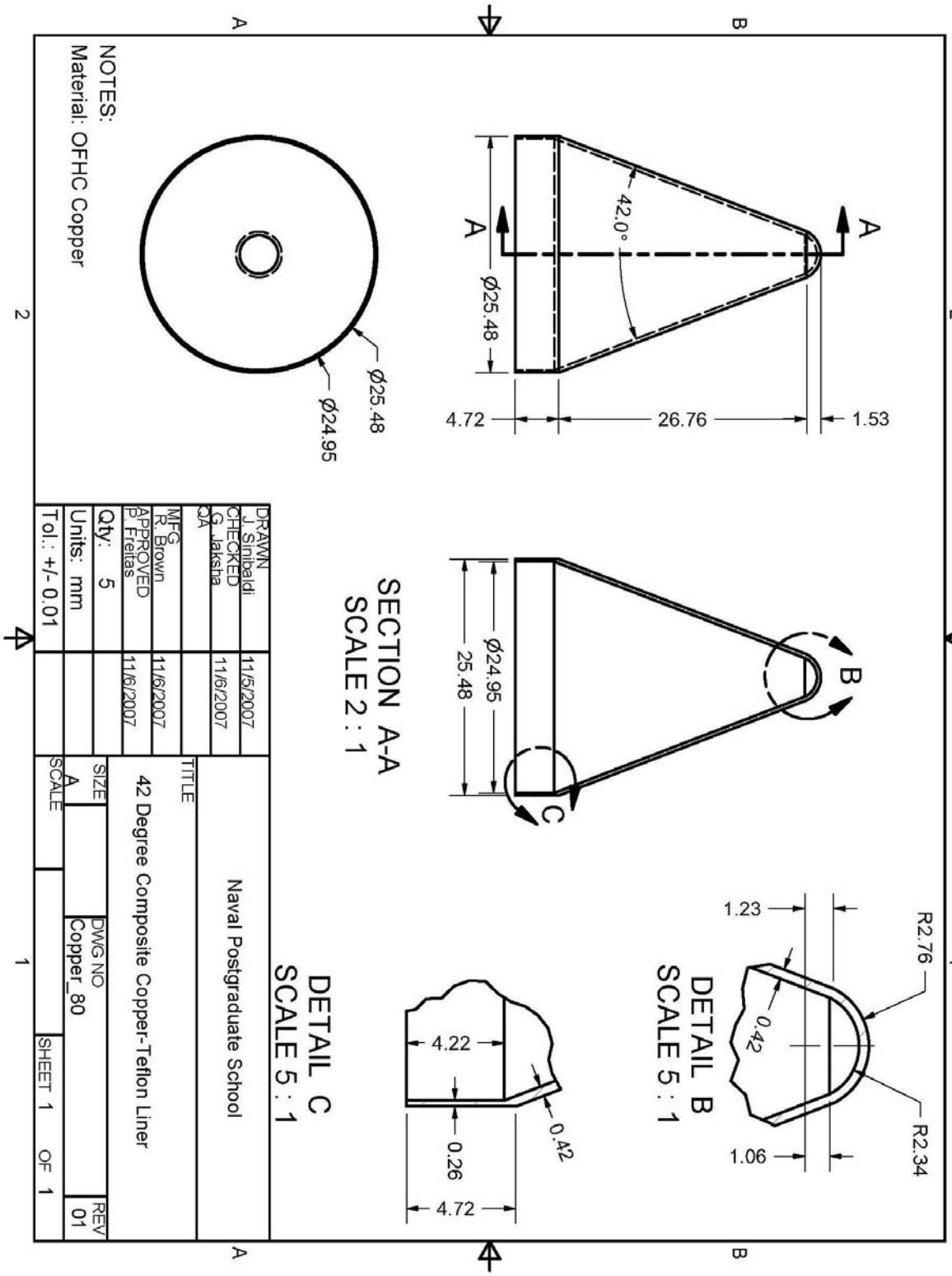

C. 42 DEGREE LINER COMPOSITE TEFLON

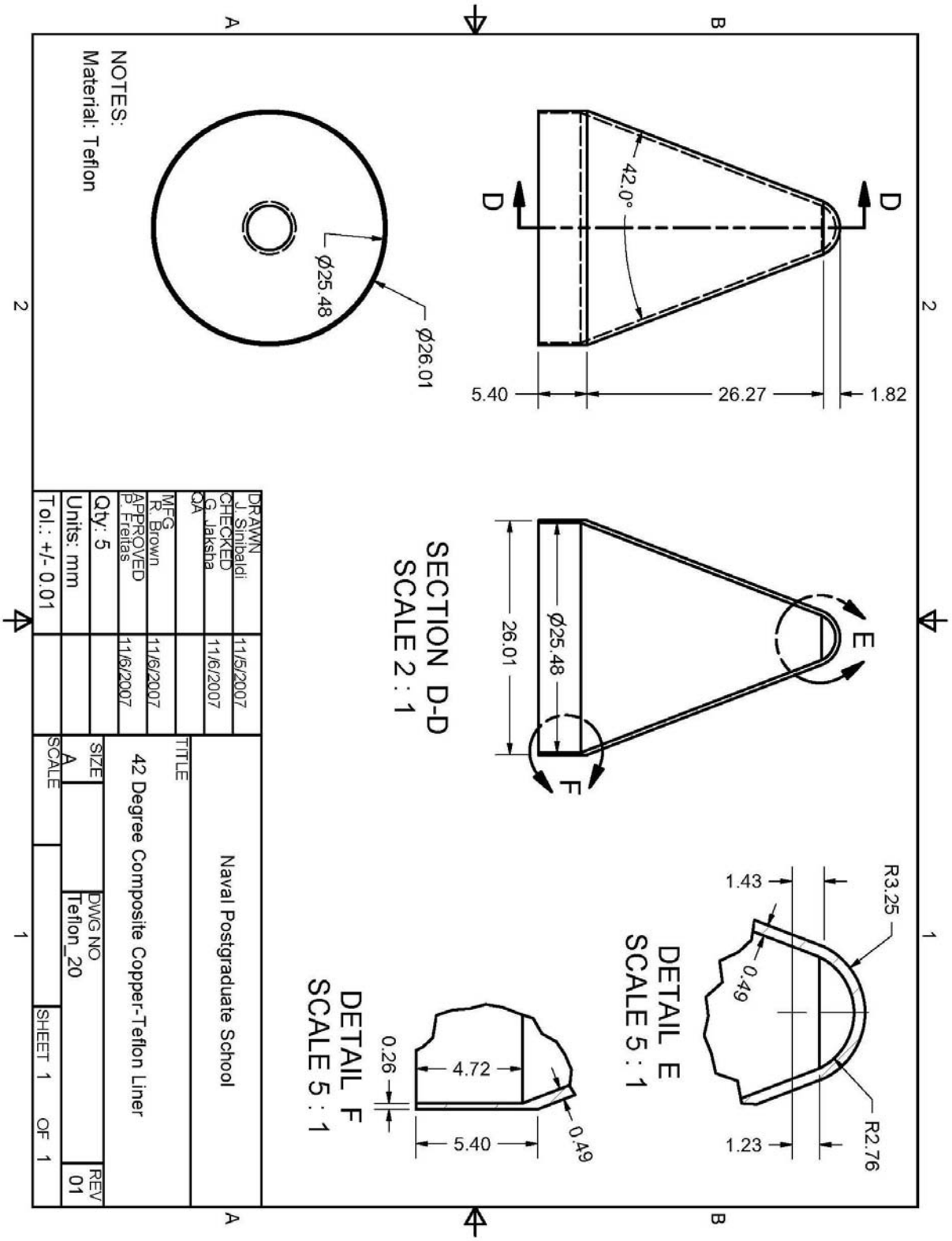

THIS PAGE INTENTIONALLY LEFT BLANK

APPENDIX E: SHAPED CHARGE DRAWINGS

A. SHAPED CHARGE MAIN BODY (TEFLON OR BRASS)

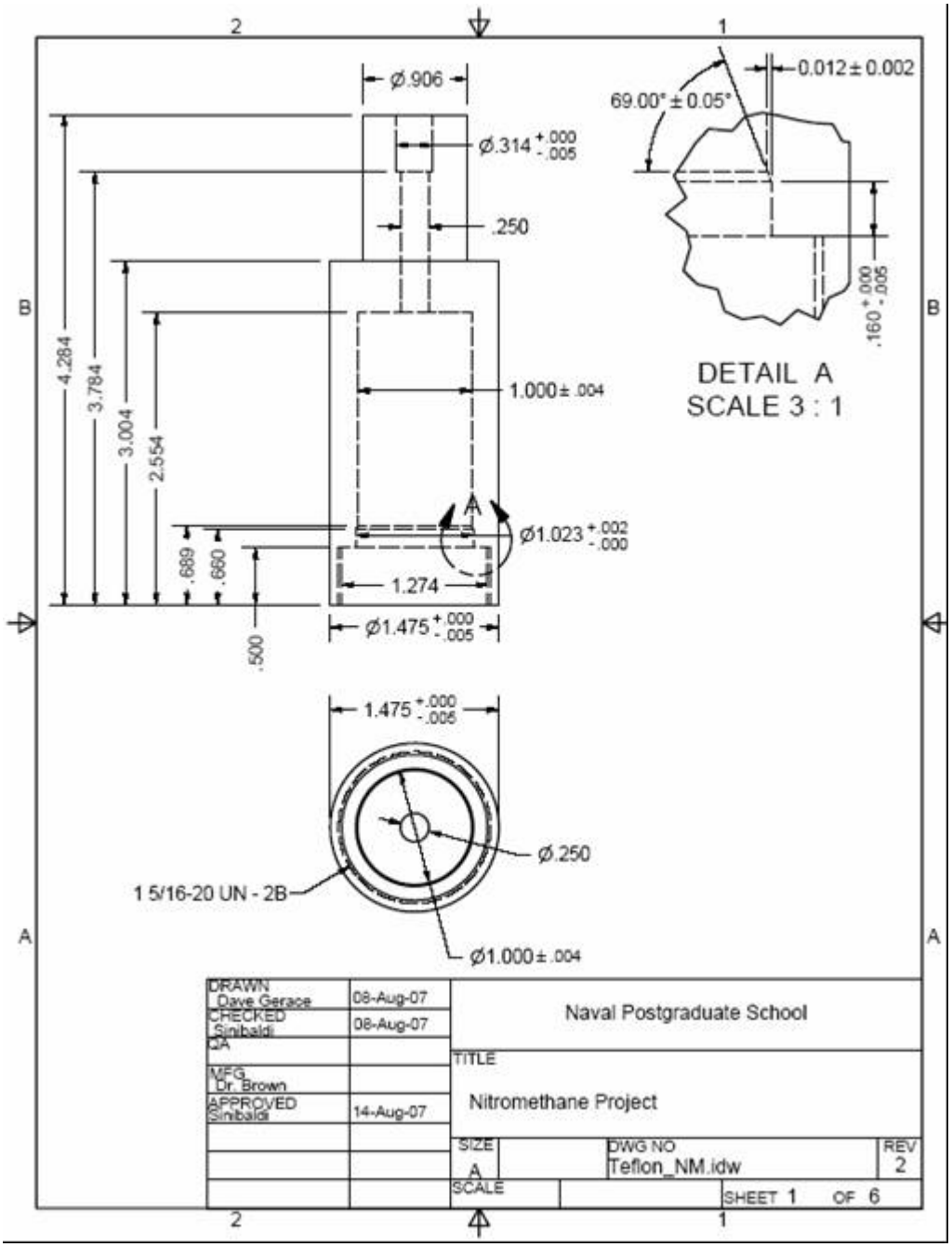

B. STANDOFFS

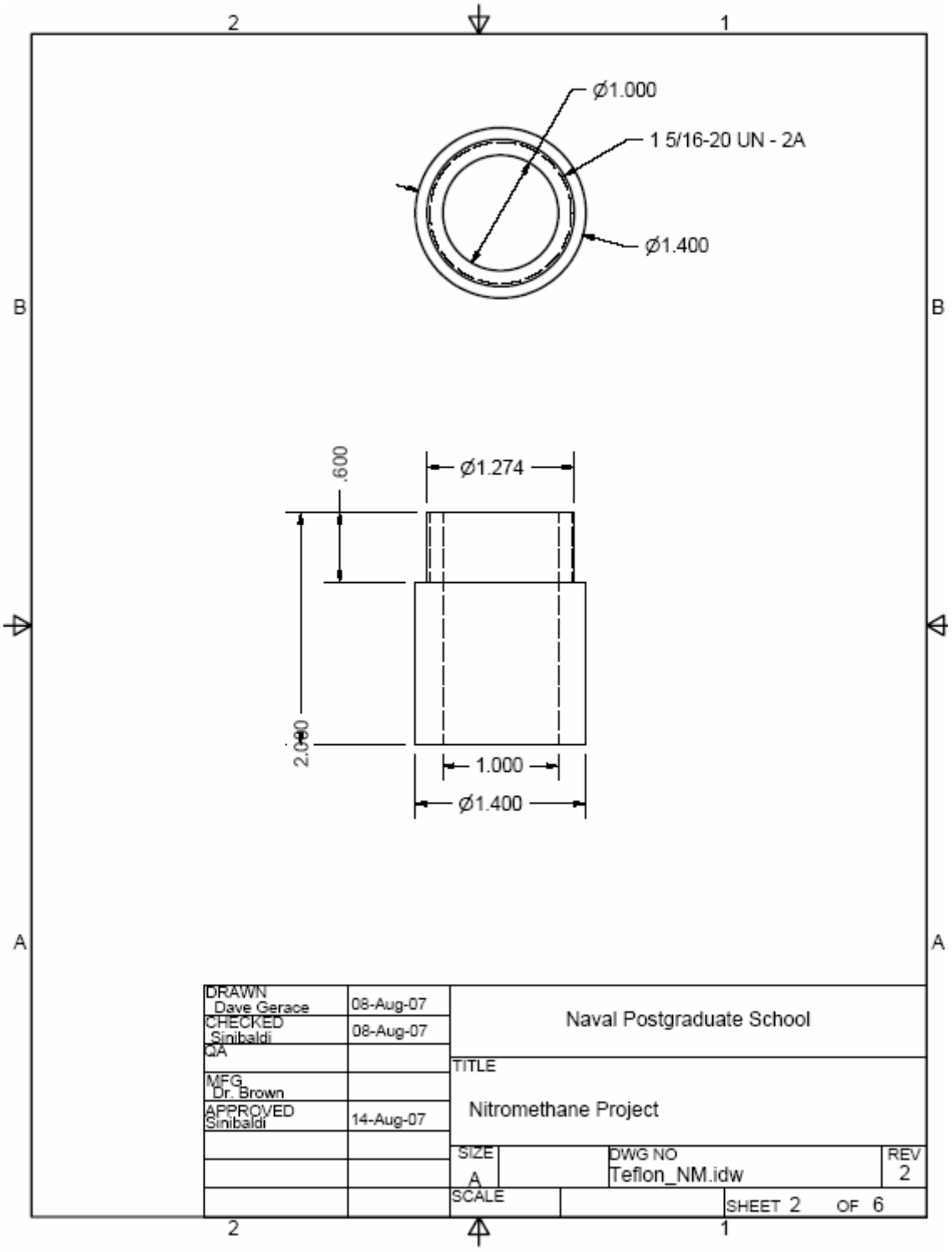
Ø1.000
1 5/16-20 UN - 2A
Ø1.400
.600
Ø1.274
2.000
1.000
Ø1.400
DRAWN Dave Gerace 08-Aug-07
CHECKED Sinibaldi 08-Aug-07
QA
MFG Dr. Brown
APPROVED Sinibaldi 14-Aug-07
Naval Postgraduate School
TITLE
Nitromethane Project
SIZE A
DWG NO Teflon_NM.idw
REV 2
SCALE
SHEET 2 OF 6

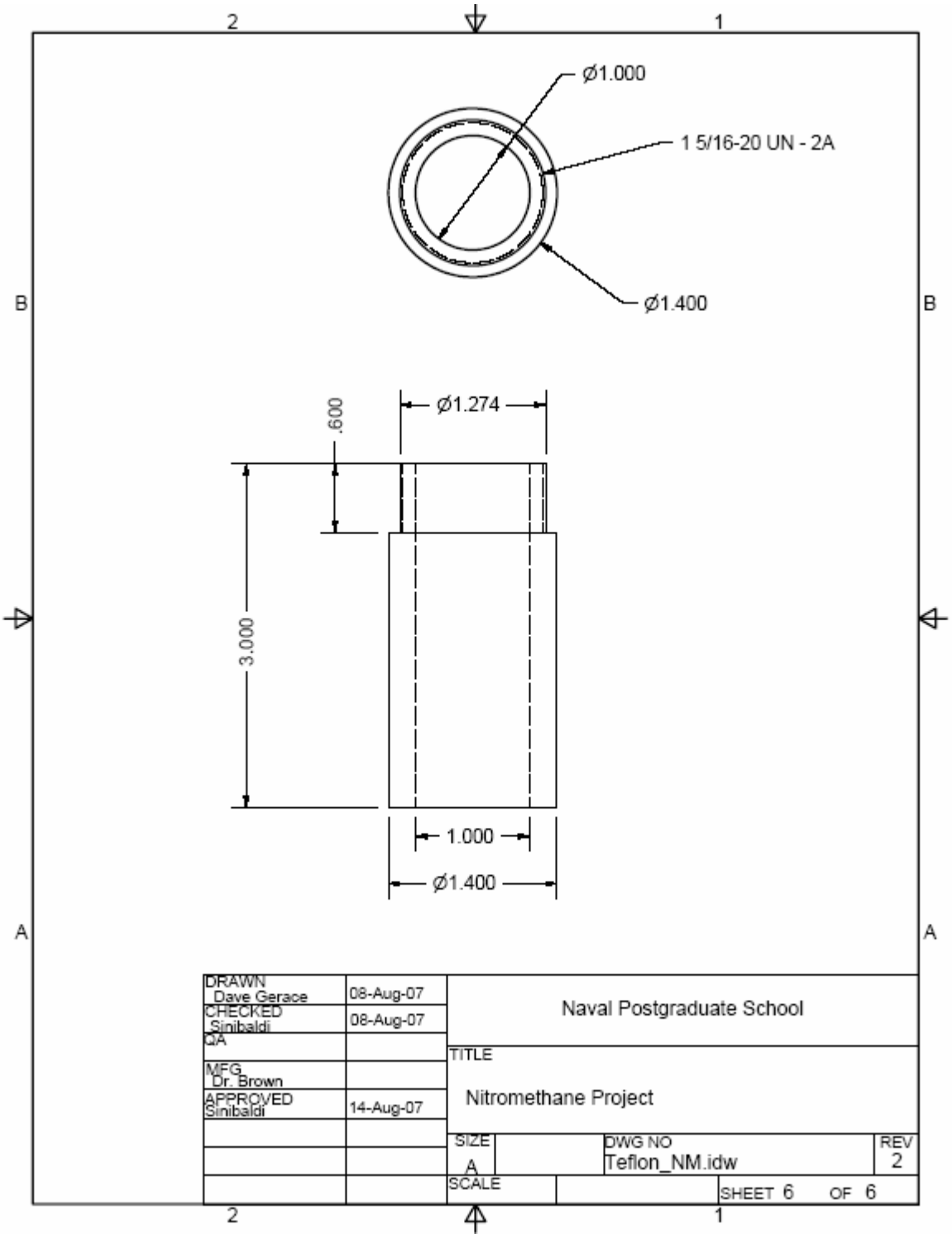
2
1
Ø1.000
1 5/16-20 UN - 2A
Ø1.400
B
B
.600
Ø1.274
3.000
1.000
Ø1.400
A
A
DRAWN
Dave Gerace
08-Aug-07
CHECKED
Sinibaldi
08-Aug-07
QA
MFG
Dr. Brown
APPROVED
Sinibaldi
14-Aug-07
Naval Postgraduate School
TITLE
Nitromethane Project
SIZE
A
DWG NO
Teflon_NM.idw
REV
2
SCALE
SHEET 6 OF 6
2
1

C. ULTEM CONFINEMENT

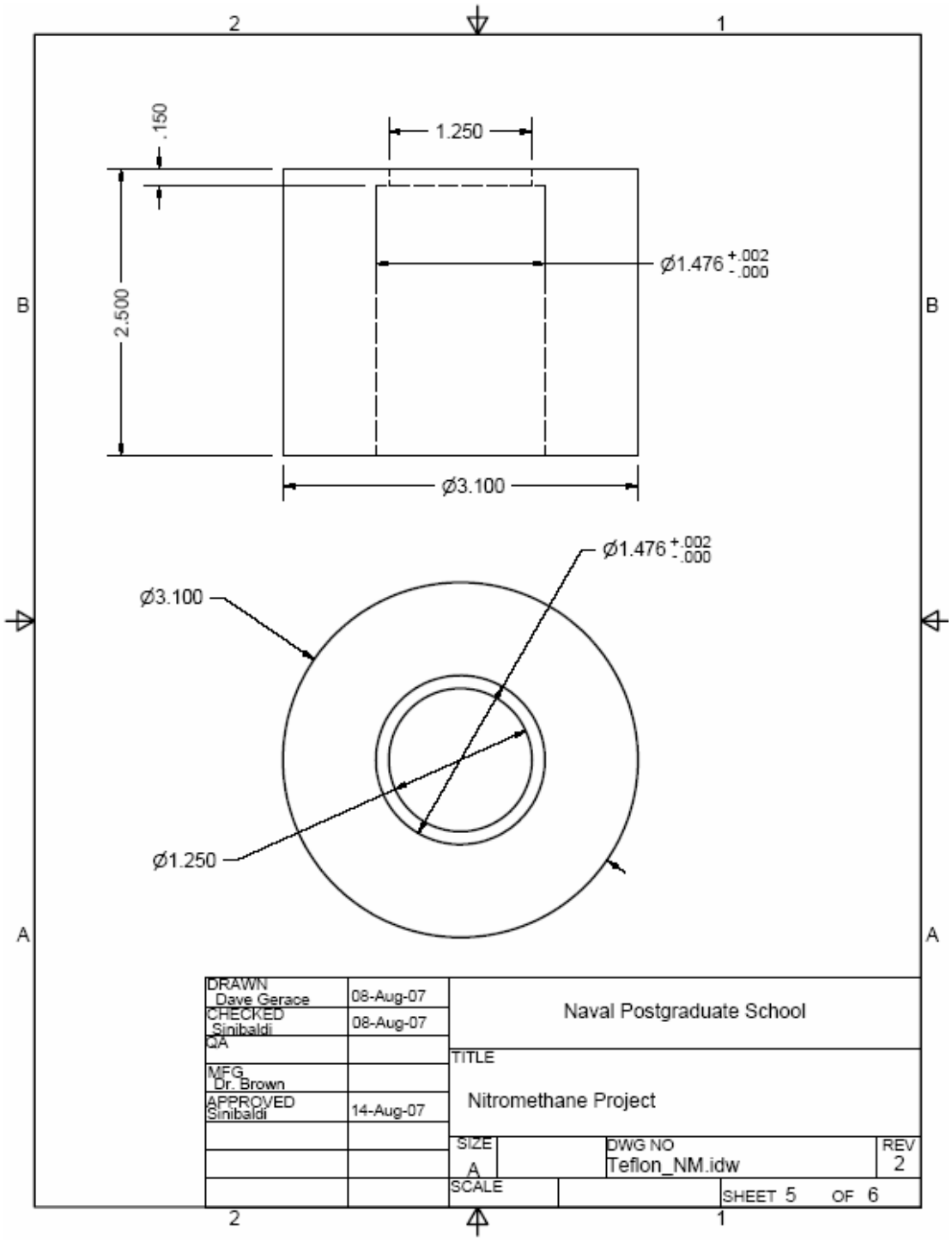

APPENDIX F. MATERIAL SPECIFICATION AND ACQUISITION LIST

Brass for shaped charge and stand-off:

Purchased from: www.nbmmetals.com CDA360 per ASTM B-16 H02 half-hard temper 1 in OD Round Solid x 144 in Long = 35lbs 1.5 in OD Round Solid x 144 in Long = 79 lbs

Teflon for shaped charge and stand-off and Ultem confinement:

Purchased from: www.polymerplastics.com

Metal Materials:

Purchased from: www.mcmaster.com [18]

Aluminum Target Plate Info:

Aluminum 6061 T6511 1ft thick, 4 in width, 6 ft length PART#8975K144

Aluminum 6061 T6511 4 ft thick, 4 in width, 36 in length PART#8975K243

Aluminum Alloy 6061 0.25 in thick, 4 in width, 6 ft length PART#:8975K29

Steel Target Plate Info:

Carbon Steel 1018 1 in thick, 4 in width, 6 ft length PART#8910K311

Carbon Steel 1018 ¼ in think, 4 in width, 6 ft length PART#8910K156

Steel Bracket Plates:

Carbon Steel 1018 3/8 in thick, 6 in width, 6 ft length PART# 6544K28

Flanges:

Butt-Weld Flange 1-1/4 in PART#68095K153

Nuts, Washers, Threaded Rods:

Fully threaded 36 in steel rod, 5/16 in -18 PART#98957A634

100 Hex nuts,steel, thread 5/16 in -18, 1/2 in width, 3/16 in height PART#90494A030

100 Round hole steel washers, 3/8 in ID, 7/8 in OD PART#90108A415

Epoxy, cable, and Packing Tape:

Purchased from: www.mcmaster.com

8265-S J-B Weld Epoxy 2 oz PART#7605A11

Polypropylene Strapping Tape Std Duty 2 in Wx60 yds L PART#7637A14

Polypropylene Strapping Tape Heavy Duty 2 in Wx60 yds L PART#7637A34

Flexible Shielded Cable 20 gge, 600VAC, 7 conductors PART#9936K53

APPENDIX G: BRACKET DRAWINGS

A. TOP BRACKET

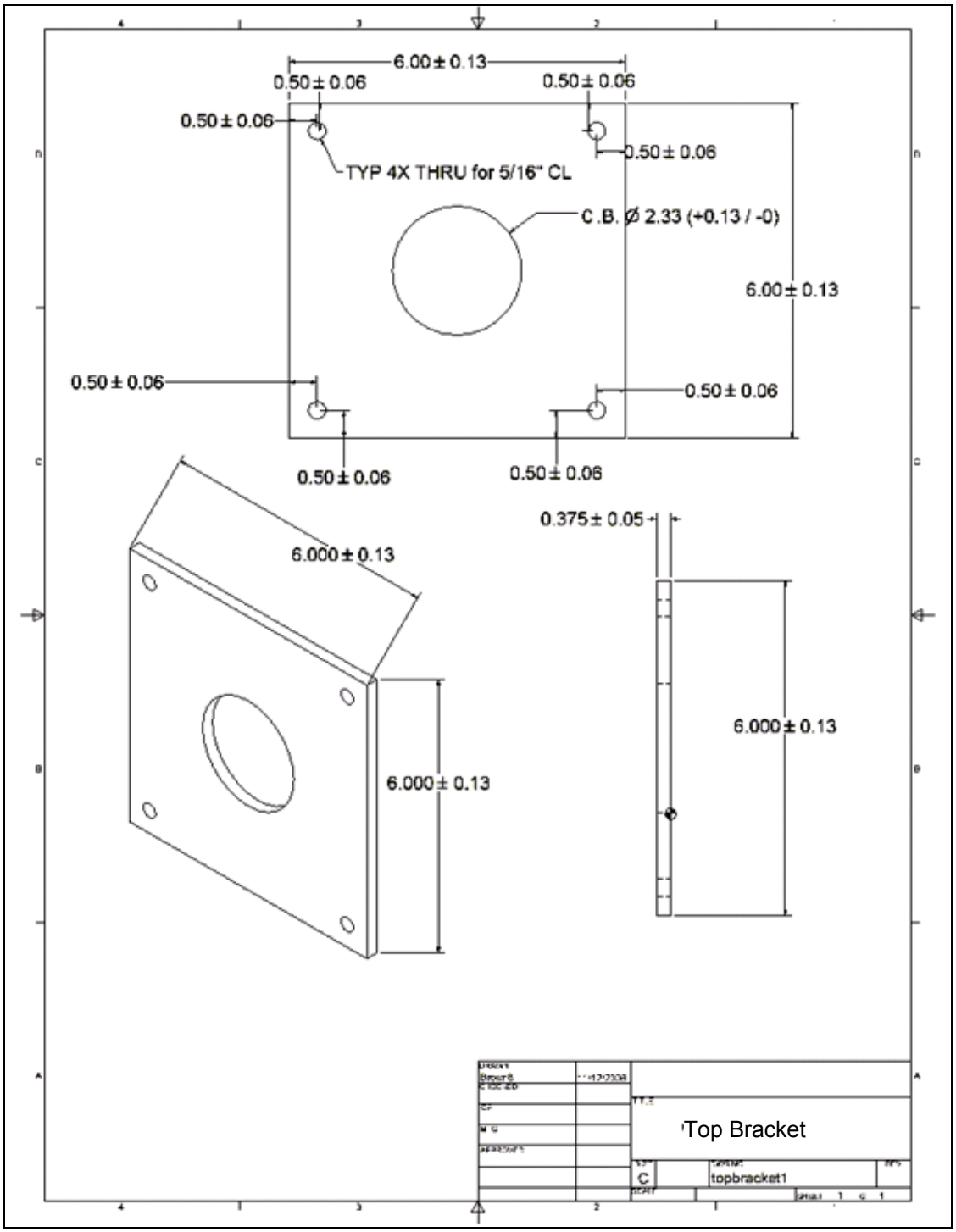

B. BOTTOM BRACKET

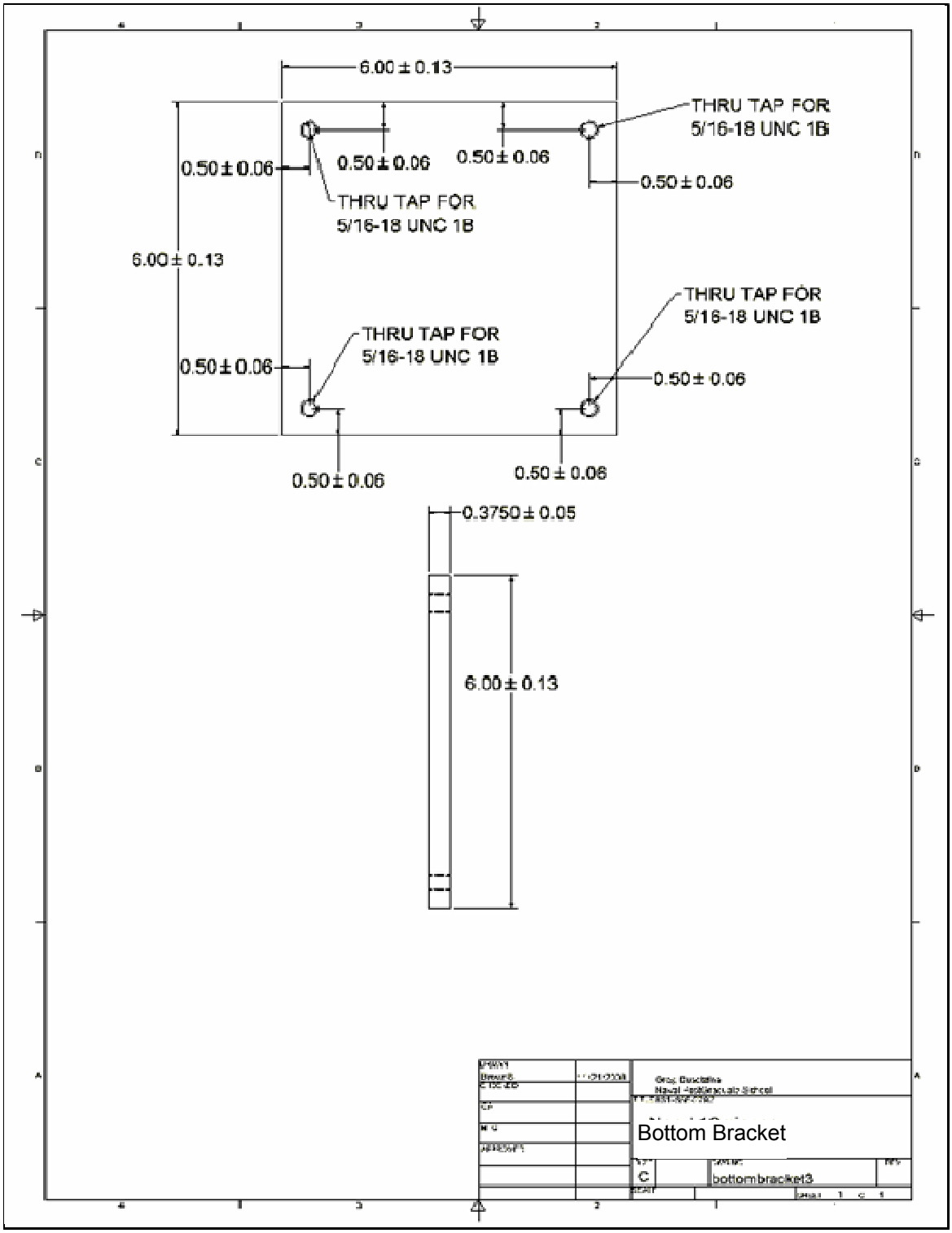

APPENDIX H: SENSORS

Equipment:

- Two inch wide packing tape made of tensile polypropylene film (without fiberglass filaments); this tape has high impact strength that allows elasticity without breaking. It will stretch before splitting and it snaps back to hold shifting loads. Ivory in color, the total tape thickness is .005 in.
- Heavy duty, kitchen grade Aluminum foil into 1.5 in wide and 4.25 in long pieces.
- Multi-conductor, shielded cable, cut into 3 ft lengths, with leads stripped about .25 to .5 inches.

Aluminum Sensor:

Heavy duty, kitchen grade aluminum foil was cut into 1.5 in wide and 4.25 in long pieces. A piece of foil was carefully laid onto a piece of the tape to avoid air bubbles from forming. The exposed cable leads were laid on top, making contact with the foil. A second piece of tape was placed on top, securing the wire to the foil. An additional piece of foil is placed on tape, which is then placed on top of the first tape and foil "sandwich", with another lead wire in contact with that piece of foil. The final result is a layered sensor with two aluminum conductors inside, electrically insulated from each other. An exposed lead wire is in contact with each piece of foil, yet remains separated from each other. Total thickness of the tape and aluminum sensor was 0.014 in [1].

THIS PAGE INTENTIONALLY LEFT BLANK

APPENDIX I: SIMULATION SET UP FOR SHAPED CHARGE

A. TRUMPET LINED SHAPED CHARGE:

- Size of Euler space depends on the length of the standoff distance (2CD, 3CD, etc).
- 8 zones across the thickness of the liner

  For finer zoning, ie. 16 cells/mm, use variable zoning
- Shaped charge dimensions are based on the actual design to accommodate approximately 20g NM.

SEQUENCE OF STEPS for Simulation:

Sequence	Options/Menu
1	Create new file
2	Select Symmetry
3	Select Units
4	Materials
5	Boundary Conditions
6	Parts
6a	Fill Parts (Copper Liner, Brass Body, NM)
6b	Gauges
6c	Set Boundaries
7	Detonation
8	Controls
9	Output
10	Run

MATERIAL SELECTION:

-The parameters for all materials are default values from AUTODYN

Material Name	Equation of State	Strength Model
Teflon	Shock	Von Mises
CU-OHFC	Shock	Steinberg Guinan
NM	JWL	None
AL 6061	Shock	Steinberg Guinan

MENU OPTIONS for SIMULATION:

Menu	Options
Symmetry	Axial
Units	mm, mg, ms
Materials	Teflon, CU-OHFC, NM Modify NM Cutoffs Min Density Factor to 1.0E-4
Boundaries	Outflow
Parts	SPACE, Euler
Detonation	Point (Origin X=0 Y=0)
Controls	CYCLE limit to 100000 TIME limit to 100000 Energy ref cycle 99999999 Global Cutoffs Max Vel=1E4 Transport INTERNAL Energy
Output	Save every 75 cycles
RUN	

Note about gauge placement: To determine velocity versus cumulative mass, place the gauges at the boundary. For penetrating targets, gauges are placed before the target and at least every 5 mm in the target.

SEQUENCE OF STEPS to generate Trumpet lined Shaped Charge:

1. Under Parts: Create Euler Space

For 2CD: (10cells/mm)		
X=0	DX=123	I=1230
Y=0	DY=60	J=600
Fill with VOID		
For 3CD:		
X=0	DX=147	I=1470
Y=0	DX=60	J=600

2. Fill by Geometrical Space, ELLIPSE

X-centre	37.48
Y-centre	58.41
X-semi axis	58.72
Y-semi axis	58.72
Fill with CU-OHFC	

3. Fill by Geometrical Space, ELLIPSE

X-centre	37.48
Y-centre	58.41
X-semi axis	57.96
Y-semi axis	57.96
Fill with NM	

4. Fill by Geometrical Space, RECTANGLE

X1	0
X2	54.92
Y1	0
Y2	60
Fill with NM	

5. Fill by Geometrical Space, ELLIPSE

X-centre	54.92
Y-centre	0
X-semi axis	3.01
Y-semi axis	3.01
Fill with CU-OHFC	

6. Fill by Geometrical Space, ELLIPSE

X-centre	54.92
Y-centre	0
X-semi axis	2.3
Y-semi axis	2.3
Fill with VOID	

7. Fill by Geometrical Space, RECTANGLE

X1	54.92
X2	59.81
Y1	0
Y2	2
Fill with VOID	

8. Fill by Geometrical Space, QUAD

X1	57.31	X3	54.92
Y1	0	Y3	2.3
X2	57.31	X4	54.92
Y2	3.1	Y4	0
Fill with VOID			

9. Fill by Geometrical Space, RECTANGLE

X1	73.4
X2	77.72
Y1	12.23
Y2	12.99
Fill with CU-OHFC	

10. Fill by Geometrical Space, RECTANGLE

X1	0
X2	120
Y1	12.99
Y2	60
Fill with VOID	

11. Fill by Geometrical Space, RECTANGLE

X1	0
X2	19.81
Y1	11.43
Y2	60
Fill with VOID	

12. Fill with Geometrical Space, RECTANGLE; fill with TEFLON

a.

X1	0
X2	19.81
Y2	3.94
Y2	11.43

b.

X1	19.81
X2	27.43
Y2	3.94
Y2	19.84

c.

X1	27.43
X2	72.41
Y1	12.22
Y2	19.84

d.

X1	72.41
X2	77.7
Y1	12.98
Y2	19.84

e. Stand-Off (TEFLON)

2CD:	
X1	77.7
X2	123
Y1	12.22
Y2	19.84
3CD:	
X1	77.7
X2	147
Y1	12.22
Y2	19.84
4CD:	
X1	77.7
X2	171
Y1	12.22
Y2	19.84
5CD:	
X1	77.7
X2	196
Y1	12.22
Y2	19.84

B. 42 DEGREE CONICAL LINED SHAPED CHARGE

Follow the same procedures detailed for trumpet lined shaped charge and use the dimensions outlined below:

1. Under Parts: Create Euler Space

For 2CD:		
X=0	DX=109	I=1090
Y=0	DY=60	J=600
Fill with VOID		
For 3CD:		
X=0	DX=134	I=1340
Y=0	DX=60	J=600

2. Fill by Geometrical Space, QUAD

X1	30.72	X3	11.43
Y1	2.55	Y3	12.7
X2	57.15	X4	11.43
Y2	12.7	Y4	2.55
Fill with NM			

3. Fill by Geometrical Space, RECTANGLE

X1	11.43
X2	30.72
Y1	0
Y2	2.55
Fill with NM	

4. Fill by Geometrical Space, ELLIPSE

X-centre	32.01
Y-centre	0
X-semi axis	2.86
Y-semi axis	2.86
Fill with Copper	

5. Fill by Geometrical Space, ELLIPSE

X-centre	32.01
Y-centre	0
X-semi axis	2.34
Y-semi axis	2.34
Fill with VOID	

6. . Fill by Geometrical Space, QUAD

X1	30.72	X3	57.9
Y1	2.02	Y3	12.99
X2	57.9	X4	30.72
Y2	12.46	Y4	2.55
Fill with Copper			

7. Fill by Geometrical Space, RECTANGLE

X1	33
X2	35
Y1	0
Y2	2.8
Fill with VOID	

8. Fill by Geometrical Space, RECTANGLE

X1	3.81
X2	11.43
Y1	3.99
Y2	20.32
Fill with BRASS	

9. Fill by Geometrical Space, RECTANGLE

X1	57.9
X2	62.22
Y1	12.46
Y2	12.99
Fill with Copper	

10. Fill by Geometrical Space, RECTANGLE

X1	0
X2	11.43
Y1	0
Y2	3.99
Fill with NM	

11. . Fill by Geometrical Space, RECTANGLE

X1	0
X2	3.81
Y1	3.99
Y2	7.69
Fill with BRASS	

12. .Fill by Geometrical Space, RECTANGLE

X1	11.43
X2	57.15
Y1	12.7
Y2	20.32
Fill with BRASS	

13. Fill by Geometrical Space, QUAD

X1	57.9	X3	57.15
Y1	12.99	Y3	20.32
X2	57.9	X4	57.15
Y2	20.32	Y4	12.7
Fill with BRASS			

14. Fill by Geometrical Space, RECTANGLE

X1	57.90
X2	62.22
Y1	12.99
Y2	20.32
Fill with BRASS	

15. STANDOFF

2CD:	
X1	62.22
X2	109
Y1	12.46
Y2	20.32
3CD:	
X1	62.22
X2	134
Y1	12.46
Y2	20.32

APPENDIX J: PHYSICAL CHARACTERISTICS OF ULTEM 1000

Ultem 1000 Technical Property Data

Ultem* l000 polyetherimide is an amorphous, high-performance polymer with exceptional flame and heat resistance. It performs continuously to 340°F (171°C), making it ideal for high strength/high heat applications, and those requiring consistent dielectric properties over a wide frequency range. It is hydrolysis resistant, highly resistant to acidic solutions and capable of withstanding multiple autoclaving cycles.

Ultem 100 is FDA and USP Class VI compliant. FDA compliant colors of Ultem are also available on a custom basis. Ultem commonly is machined into parts for reusable medical devices, analytical instrumentation, electrical/electronic insulators and a variety of structural components requiring high strength and rigidity at elevated temperatures.

Technical Data obtained from Reference [21].

Physical Properties	**Metric**	**English**	**Comments**
Density	1.28 g/cc	0.0462 lb/in³	ASTM D792
Water Absorption	0.25 %	0.25 %	24 hour immersion; ASTM D570
Moisture Absorption at Equilibrium	0.2 %	0.2 %	Water Vapor Regained
Water Absorption at Saturation	1.25 %	1.25 %	Immersion; ASTM D570
Outgassing - Total Mass Loss	0.4 %	0.4 %	
Collected Volatile Condensable Material	0 %	0 %	
Chemical Properties			
Ionic Impurities - Na (Sodium)	6.4 ppm	6.4 ppm	
Ionic Impurities - K (Potassium)	0.1 ppm	0.1 ppm	
Ionic Impurities - Fe (Iron)	0.7 ppm	0.7 ppm	
Mechanical Properties			
Hardness, Rockwell M	112	112	ASTM D785
Hardness, Rockwell R	125	125	ASTM D785

Hardness, Shore D	86	86	ASTM D2240
Tensile Strength, Ultimate	114 MPa	16500 psi	ASTM D638
Elongation at Break	80 %	80 %	ASTM D638
Tensile Modulus	3.45 GPa	500 ksi	ASTM D638
Flexural Modulus	3.45 GPa	500 ksi	ASTM D790
Flexural Yield Strength	138 MPa	20000 psi	ASTM D790
Compressive Yield Strength	152 MPa	22000 psi	10% Deflection; ASTM D695
Machinability	30 %	30 %	QEPP 10 to 100 scale
Shear Strength	103 MPa	15000 psi	ASTM D732
Compressive Modulus	3.31 GPa	480 ksi	ASTM D695
Coefficient of Friction	0.42	0.42	Dynamic; Dry vs. Steel; PTM55007
K (wear) Factor	2900	2900	10^{-10} in^3-min/lb-ft-hr; PTM55007
Limiting Pressure Velocity	0.0657 MPa-m/sec	1875 psi-ft/min	PTM55007
Izod Impact, Notched	0.267 J/cm	0.5 ft-lb/in	ASTM D256A

Electrical Properties

Surface Resistivity per Square	Min 1e+013 ohm	Min 1e+013 ohm	EOS/ESD S11.11
Dielectric Constant	3.15	3.15	1 MHz; ASTM D150(2)
Dielectric Strength	32.7 kV/mm	830 V/mil	Short Term; ASTM D149(2)
Dissipation Factor	0.0013	0.0013	1 MHz; ASTM D150(2)

Thermal Properties

CTE, linear 68°F	55.8 µm/m-°C	31 µin/in-°F	ASTM E831 (TMA)
Thermal Conductivity	0.122 W/m-K	0.85 BTU-in/hr-ft²-°F	
Maximum Service Temperature, Air	171 °C	340 °F	Continuous Service Without Load
Deflection Temperature at 1.8 MPa (264 psi)	204 °C	400 °F	ASTM D648
Glass Temperature	215 °C	419 °F	ASTM D3418

INITIAL DISTRIBUTION LIST

1. Defense Technical Information Center
   Ft. Belvoir, Virginia

2. Dudley Knox Library
   Naval Postgraduate School
   Monterey, California

3. Professor Ronald E. Brown
   Naval Postgraduate School
   Monterey, California

4. Professor Jose O. Sinibaldi
   Naval Postgraduate School
   Monterey, California

5. Dr. Ernest L. Baker
   US ARMY Armament Research, Development and Engineering Center
   Picatinny Arsenal, New Jersey

6. Mr. Jim Varosh
   TELEDYNE RISI, INC.
   Tracy, California

7. Mr. Jon H. Price
   TELEDYNE RISI, INC.
   Tracy, California

8. Professor Nicolas Glumac
   Mechanical Engineering Department, University of Illinois
   Urbana-Champagne, Illinois

9. Dr. Manfred Salk
   Institut Kurzzeitdynamik
   Ernst Mach Institut
   Freiburg, Germany

10. Mr. Brian Almquist
    Ocean Engineering and Marine Systems (3210E)
    Office of Naval Research
    Arlington, Virginia